MASTER THESIS

Titel der Masterarbeit/ Title of the Master's Thesis

„Influence of antioxidant rich diet especially equol on DNA damage, epigenetic regulation and gene expression of inflammatory mediators and DNA repair in obese mice C57BL/6J“

verfasst von / submitted by

Sylvia Christiana Roth, BSc

angestrebter akademischer Grad / in partial fulfilment of the requirements for the degree of

Master of Science (MSc)

Wien, 2016

Studienkennzahl lt. Studienblatt/ degree programme code as it appears on the student record sheet:	A 066 838
Studienrichtung lt. Studienblatt/ degree programme as it appears on the student record sheet:	Master Ernährungswissenschaften
Betreut von/ Supervisor:	Univ.-Doz.Dr. Alexander Haslberger

Ich erkläre hiermit, dass ich die vorliegende Masterarbeit selbstständig verfasst und keine anderen als die angegebenen Quellen und Hilfsmittel benützt habe.

_____

Sylvia Roth

I. Danksagung

An dieser Stelle möchte ich mich bei allen Personen bedanken, die mich während meines Studiums begleitet und in dieser Zeit immer unterstützt haben.

Allererst gilt mein Dank Univ.-Doz. Dr. Alexander Haslberger und Dr. Marlene Remely, die mich mit diesem Thema betraut und mich jederzeit bestmöglich unterstützt haben. Ein riesen Dank gilt meinen beiden Kolleginnen Sonja Sterneder und Tatjana Kepcija, ohne sie wäre ich an manchen Problemen verzweifelt und die Arbeit wäre nicht annähernd so schnell fertig geworden. Auf ihre Verlässlichkeit war immer Verlass und gemeinsam wuchsen wir zu einem hervorragenden Team.
Ein großes Dankeschön gilt auch allen Mitgliedern der Arbeitsgruppe, die uns mit ihrer Erfahrung bei Problemen weiterhalfen und für ein perfektes Arbeitsklima sorgten.

Ganz besonders möchte ich mich bei meinen Eltern bedanken, die mir das Studium ermöglicht und nie an mir und meinen Fähigkeiten gezweifelt haben. Vielen Dank an meinen Bruder Peter und meinen Freund Thomas die mit meinen Launen oft zu kämpfen hatten.

Herzlichen Dank an meine Freunde Astrid, Nina, Florence und Donna die mich in all der Zeit emotional unterstützten und mir immer wieder neuen Mut zusprachen.

VIELEN DANK!

II. Vorwort

Die Bearbeitung dieser Studie wurde von meinen Kolleginnen Tatjana Kepcija, Sonja Sterneder und mir, Sylvia Roth, durchgeführt, unter Anleitung von Univ.-Doz. Dr. Alexander Haslberger und Marlene Remely und unter der Vorarbeit von Irene Rebhahn und Martina Greunz.

Der Schwerpunkt der jeweiligen Masterarbeiten lag auf verschiedenen Antioxidantien und deren Wirkung auf unterschiedliche Gene.

Tatjana Kepcija konzentrierte sich auf die Wirkung von Vitamin E, Sonja Sterneder übernahm die Auswirkung von EGCG und ich fokussierte mich auf den Effekt von Equol auf die Gene DNA-Methyltransferase 1 (DNMT1), Interleukin-6 (IL-6) und MutL homolog 1 (MLH1).

III. Content

IV. List of figures

V. List of tables

VI. List of abbreviations

$CD4^+$	regulatory T-cells
$CD8^+$	effector T-cells
CRP	C-reactive Protein
DNMT	DNA methyltransferase
eNOS	endothelial NO synthase
ERα	Estrogen receptor α
ERβ	Estrogen receptor β
FFA	free fatty acids
HAT	Histone acetyltransferase
HDAC	Histone deacetylase
HDM	Histone demethylase
HMT	Histone methyltransferase
IFNγ	Interferon γ
IL10	Interleukin 10
IL13	Interleukin 13
IL4	Interleukin 4
IL6	Interleukin 6
iNOS	inducible NO synthase
NADPH	nicotinamide adenine dinucleotide phosphate
NF-Kb	Nuclear factor Kb
NOX	NADPH-oxidase
O-DMA	O-Desmethylangolensin
PAI-1	Plasminogen activator inhibitor 1
ROS	reactive oxygen species
SAM	S-adenosylmethionine
TH1	T-helper cells type 1
TH2	T-helper cells type 2
TNF-α	Tumor necrosis factor α

VII. Zusammenfassung

Übergewicht, in Kombination mit Dislipidämie, Hypertonie, Insulinresistenz und Glukoseintoleranz, ist einer der Hauptfaktoren für die Entstehung des metabolischen Syndroms. Übergewicht ist assoziiert mit schwacher, aber chronischer Entzündung, da das Fettgewebe Interleukin 6 (IL6) und C-reaktives Protein (CRP) freisetzt. Ein anderer negativer Effekt ist die Produktion von reaktiven Sauerstoffspezies (ROS) die aufgrund des hohen Anteils an freien Fettsäuren und Glukose gebildet werden. Diese Faktoren sind in der Lage das Epigenom über die DNA Methylierung zu verändern, welches zu abnormer Genexpression führt. Antioxidantien haben die Eigenschaft diese negativen Effekte von ROS zu minimieren.

Ziel dieser Arbeit war herauszufinden ob Equol Einfluss auf die Genexpression und Methylierung von DNMT1, MLH1 und IL6 in C57BL/6J Mäusen hat, welchen eine Kontrolldiät (CD) und eine Diät mit erhöhtem Fettanteil (HFD) gefüttert wurden, um eine mögliche Interaktion zwischen HFD und Equol auf Entzündung und ROS Produktion bei Übergewicht herauszufinden.

Equol, ein Isoflavon, welches zur Familie der nonsteroidalen Östrogenen gehört. Die Vorteile rühren von der antioxidativen Aktivität her, welche, die Stickstoffmonoxid (NO) Produktion und Verwertung beeinflusst und die Fähigkeit besitzt, die Bioverfügbarkeit von NO zu verlängern über herab Regulierung der O_2-• Produktion. Somit schützt es vor einer LDL-Modifikation in Richtung eines atherogenen Plaques.
DNA Methyltransferase 1 (DNMT1) katalysiert die Methylierung von Cytosin und ist beteiligt an der Aufrechterhaltung der DNA-Methylierung. MutL homolog 1 (MLH1) ist Teil des mismatch repair systems (MMR) und daher wichtig für die genomische Unversehrtheit.

Für die Arbeitsschritte der Genexpression und Methylierung wurden DNA und RNA gleichzeitig extrahiert. Genexpression von DNMT1, MLH1 und IL6 wurden

mittels reverser Transkiptase und Real-time PCR und die Methylierung mittels Bisulfitkonvertierung und anschließender Pyrosequenzierung durchgeführt.
Es gab einen signifikanten Unterschied in der Gewichtszunahme zwischen den CD und der HFD gefütterten Mäuse innerhalb der 20 Wochen. Wie zu erwarten war, nahmen die HFD Mäuse mehr Gewicht zu als die CD Mäuse, was an der höheren kalorischen Zufuhr aufgrund des erhöhten Fettanteils des Futters lag.
Die höhere Expression von DNMT1 in Mäusen, welche mit HFD+Q gefüttert wurden, könnte durch den positiven Effekt von Equol auf die Entzündung erklärt werden. Methylierung von DNMT1 in der Leber zeigt eine Erhöhung in HFD+Q verglichen mit HFD und CD.
Die MLH1 Genexpression war höher in HFD+Q als in CD+Q und HFD exprimiert, was wiederum die Hypothese unterstützt, dass sich Equol positiv auf die Reperaturmechanismen auswirkt. Allerdings zeigt die Methylierung von MLH1 eine Erhöhung in HFD und HFD+Q und eine Erniedrigung in CD+Q.

Es gibt Hinweise darauf, dass Equol einen Einfluss auf die Genexpression und die Methylierung in übergewichtigen Mäusen vor allem im Kolon haben könnte. Der Grund für die unterschiedlichen Ergebnisse in Leber und Kolon, könnte eventuell mit gewebespezischen Unterschieden im Metabolismus und dem enterohepatischen Kreislaufes zusammenhängen. Allerdings müssen in diese Richtung noch weitere Studien durchgeführt werden, um diesen Kreislauf, den Abbau und die Wirkung von Equol auf die DNA zu verstehen.

VIII. Summary

The increase of obesity is alarming, in combination with dyslipidemia, hypertension, insulin resistance and glucose intolerance, obesity is a major risk factor gaining metabolic syndrome. Obesity is also associated with low-grade inflammation because adipose tissue releases Interleukin 6 (IL6) and C-reactive protein (CRP). Another negative effect is the production of reactive oxygen species (ROS) due to the high amount of free fatty acids (FFA) and glucose. These factors are able to change the epigenome via DNA methylation and this again leads to an abnormal gene expression. Antioxidants seem to lower these negative effects of ROS.

Equol is an isoflavone which belongs to the family of nonsteroidal estrogens. The beneficial properties are believed to derive from the antioxidant activity. It affects NO production or utilization and has the skill to enhance the bioavailability of NO through downregulation of O_2-• production and helps to prevent LDL modification to an atherogenic particle.
DNA methyltransferase 1 (DNMT1) catalyzes the methylation of cytosine and is involved in the maintenance methylation. MutL homolog 1 (MLH1) is part of the mismatch repair system (MMR) and therefore important for the genomic integrity.

The aim of this thesis was to examine the effects of equol on gene expression and methylation of DNMT1, MLH1 and IL6 in C57BL/6J mice fed a control and a high fat diet, to comment a possible interaction between high fat diet and equol on inflammation and ROS production in obesity.

DNA and RNA were extracted simultaneously for further work with gene expression and methylation. The expression of DNMT1, MLH1 and IL6 were quantified with reverse-transcription real-time PCR and the methylation status were conducted by prior bisulfite conversion followed by pyrosequencing.

The higher expression of DNMT1 in HFD+equol mice could be explained through the positive effect of equol on inflammation. There was a higher methylation of DNMT1 in liver of HFD+Q compared to HFD and CD.
MLH1 was higher expressed in HFD+Q than in CD+Q as well as in HFD. What also brings back the hypothesis of the positive effect of equol on repair mechanisms. But the methylation patterns showed an increase of MLH1 in HFD and HFD+Q and a decrease in CD+Q.

There is evidence that equol may have an influence on gene expression and methylation in obese mice especially in colon. The reason for the different results in colon and liver may be due to the tissue specific metabolism and the enterohepatic pathway, but for better understanding, more researches in this direction have to be undertaken especially with focus on equol.

1. Introduction

1.1.1. Obesity and Metabolic Syndrome

Obesity is getting more and more a big problem in our society. The worldwide prevalence nearly doubled in the last three decades. Dependent on the country over 50% of men and women are overweight and around 23% of women and 20% of men are obese. The obesity problem starts now earlier than in the past, childhood obesity rises big concern about the future, because there is the risk that obese children before puberty remain overweight in early adulthood, which is strongly associated with type 2 diabetes, cardiovascular diseases, cancer and other noncommunicable diseases. (WHO, 2008).

The obesity rate increases in many countries and increases the fastest in low socioeconomic population groups. (WHO, 2014)

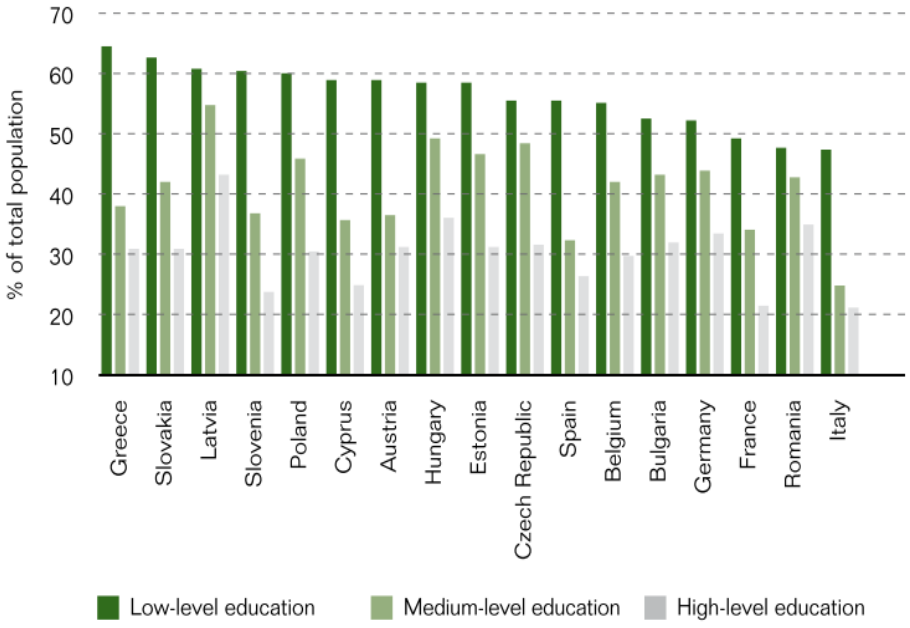

Figure 1: Overweight and obesity by educational level, WHO 2009

Obesity is also a risk factor for metabolic syndrome in combination with others like insulin resistance, glucose intolerance, dyslipidemia, non-alcoholic fatty liver disease and hypertension. Which all derives from a high food availability, physical inactivity but also genetic predispositions (Abete, Goyenechea, Zulet & Martinez,

2011). The cells of the adipose tissue, the adipocytes, generate a multitude of biologically active molecules like adipocytokines or adipokines involving plasminogen activator inhibitor-1 (PAI-1), TNF-α, resistin, leptin and adiponectin. A dysregulation of the adipokine production may result in an obesity-related metabolic syndrome. Also an insulin resistance in obese people could be derived from this dysregulation. Because an increased production of PAI-1, TNF-α and the activation of insulin-sensitizing and anti-atherogenic effects, due to adiponectin, may result in a lower plasma adiponectin level. (Furukawa, 2014)

1.1.2. Inflammation

There is a connection between low grade-inflammation response and metabolic diseases relating to obesity and type 2 diabetes. A higher level of C-reactive protein (CRP) in the blood occurs in obese individuals due to the excess adipose tissue. Together with its inducer Interleukin-6 (IL-6), CRP is referred to enhance the risk of type 2 diabetes. Besides, weight loss interventions lead to a reduction of CRP and IL-6. The secretory status of an adipose tissue depot can be diversified through changes in the cellular composition of the tissue, together with phenotype, alterations in the number and localization of immune, vascular and structural cells. The expression of adiponectin was lower in obese individuals but adiponectin protects against several metabolic and cardiovascular disorders which are associated with obesity. (Ouchi et al, 2011).

Adipose tissues are infiltrated by a large amount of macrophages and this recruitment is linked to systemic inflammation. The agglomeration of macrophages is corresponding to the grade of adiposity and it decreases with the amount of weight loss and results in a lower pro-inflammatory profile. (Wellen & Ho-tamisligil, 2003). There are different subsets of macrophages which have a diverse effect on the inflammatory process, they can be either pro- or anti-inflammatory. Macrophages in the tissue of obese mice expressed mainly M1 or “classically activated” macrophage phenotype in contrast to the lean mice they expressed M2 or “alternatively activated” macrophage phenotype. Stimulation with T helper cells (TH1)-type with cytokines and interferon-γ (IFNγ) induces the formation of

M1 macrophages which produce pro-inflammatory cytokines like TNFα and IL-6 and this increase the production of ROS. The M2 macrophages stimulate the production of anti-inflammatory cytokines like IL-10 in order to TH2-type cytokines (IL-4 and IL-13) and downregulate the accumulation of pro-inflammatory cytokines (Gordon, 2003) (Martin-Murphy, 2014) (Ouchi et al, 2011).

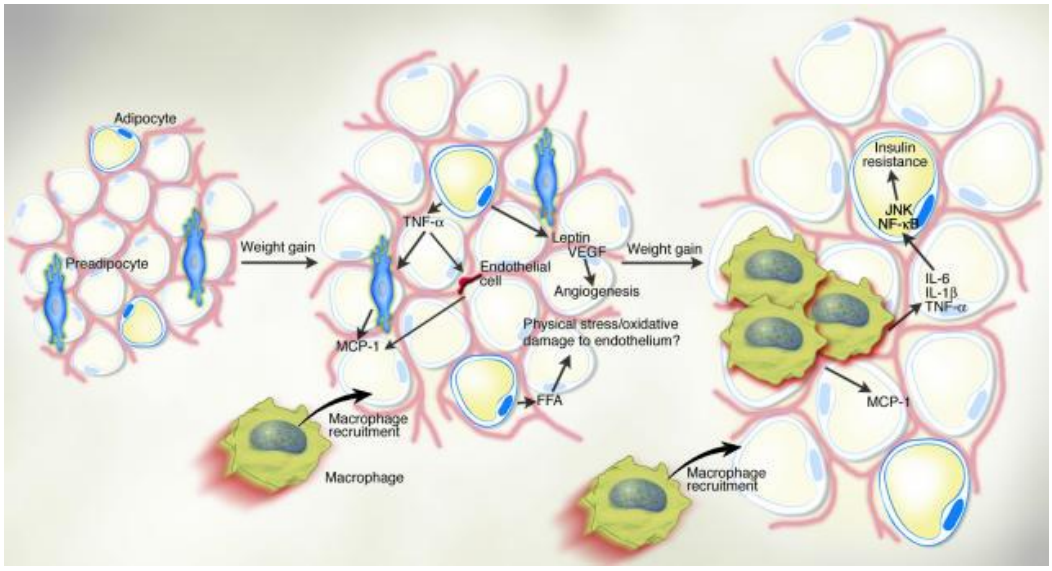

Figure 2: Obese adipose tissue is characterized by inflammation and the progressive infiltration of macrophages.

CD4+ regulatory T-cells appear in a higher amount in adipose tissue of lean mice and have protective effect against pro-inflammatory macrophages. CD8+ effector T-cells and TH1 cell-associated factors are able to induce the agglomeration and activation of macrophages and stimulate a pro-inflammatory process (Ouchi et al, 2011)

1.1.3. Reactive Oxygen Species (ROS)

The production of reactive oxygen species (ROS) plays a role in pathophysiology of obesity as well. High amounts of free fatty acids (FFAs) and glucose are carried to the adipose tissue where they cause local inflammation. This inflammation generates reactive oxygen species due to the accumulation of macrophages in response to chemotactic factors which are produced by adipocytes and that may

lead to insulin resistance. Adipocytes as well as macrophages release pro-inflammatory molecules which may lead to chronic low-grade inflammation and therefore to insulin resistance. ROS have been assumed to activate nuclear factor-κB (NfκB) through mediators of signal transduction pathways which results in an expression of the monocyte chemotactic factor genes, serum amyloid A3 and monocyte chemotactic protein-1. Quenching ROS with antioxidants inhibit such events (Chang Yeop Han, et al, 2012). NfκB plays very important roles in the regulation of cell survival, differentiation and proliferation. A dysfunction in NfκB leads to pathological processes like immune deficiency, autoimmune diseases, cancer, cardiovascular diseases and other inflammatory dependent diseases. Based on the inflammatory processes, NfκB is activated by pro-inflammatory cytokines like Interleukin-1 and TNF-α and the activation of NfκB results in a production of pro-inflammatory cytokines (McDonald, Geha, 2014). Another way of producing ROS is the β-oxidation of fatty acids, especially as a coproduct of peroxisomal acyl CoA oxidase activity. Together with the electron transport system in the mitochondria and the plasma membrane nicotinamide adenine dinucleotide phosphate (NADPH) oxidase, a higher production of ROS is obtained. NADPH oxidase is present in phagocytic cells where ROS play an important role of cellular defense. (Nakamura et al, 2009) The ROS production via NADPH oxidase (NOX) is directly proportional to accumulated body fat (Switzeny et al, 2012). NOX are enzyme complexes which are located in the membrane and transfer electrons from NADPH to oxygen whereat they produce superoxide and H_2O_2 predominantly by superoxide dismutase (Chang Yeop Han, et al, 2012).

It is not mandatory that it leads to harmful effects in healthy cells if this whole system is consistently regulated. However, when this system gets disrupted by an overrun of ROS and/or a lack of antioxidants it may lead to cytotoxic and genotoxic oxidative stress which results in DNA strand breaks. The deamination of cytosine to uracil (unmethylated cytosine) and 5-hydroxyuracil (methylated cytosine) is the outcome of this process. Uracil and 5-hydroxyuracil preferentially pair with adenine during DNA replication and this induces a G:C to A:T transition mutation. Guanine is acting in the same way it oxidizes to 8-oxo-7,8 dihydroguanosine via a vast of ROS and its mismatch with adenine would give rise to G:C to

T:A transversion mutation. Although the organism has its own defense mechanisms to keep up genomic integrity against continuous assaults on the genome and these mechanisms are known as DNA repair enzymes, like MLH1 (Hegde, Hazra, Mitra; 2008).

Its suggested that antioxidants are able to increase DNA repair enzyme activities (Switzeny et al, 2012).

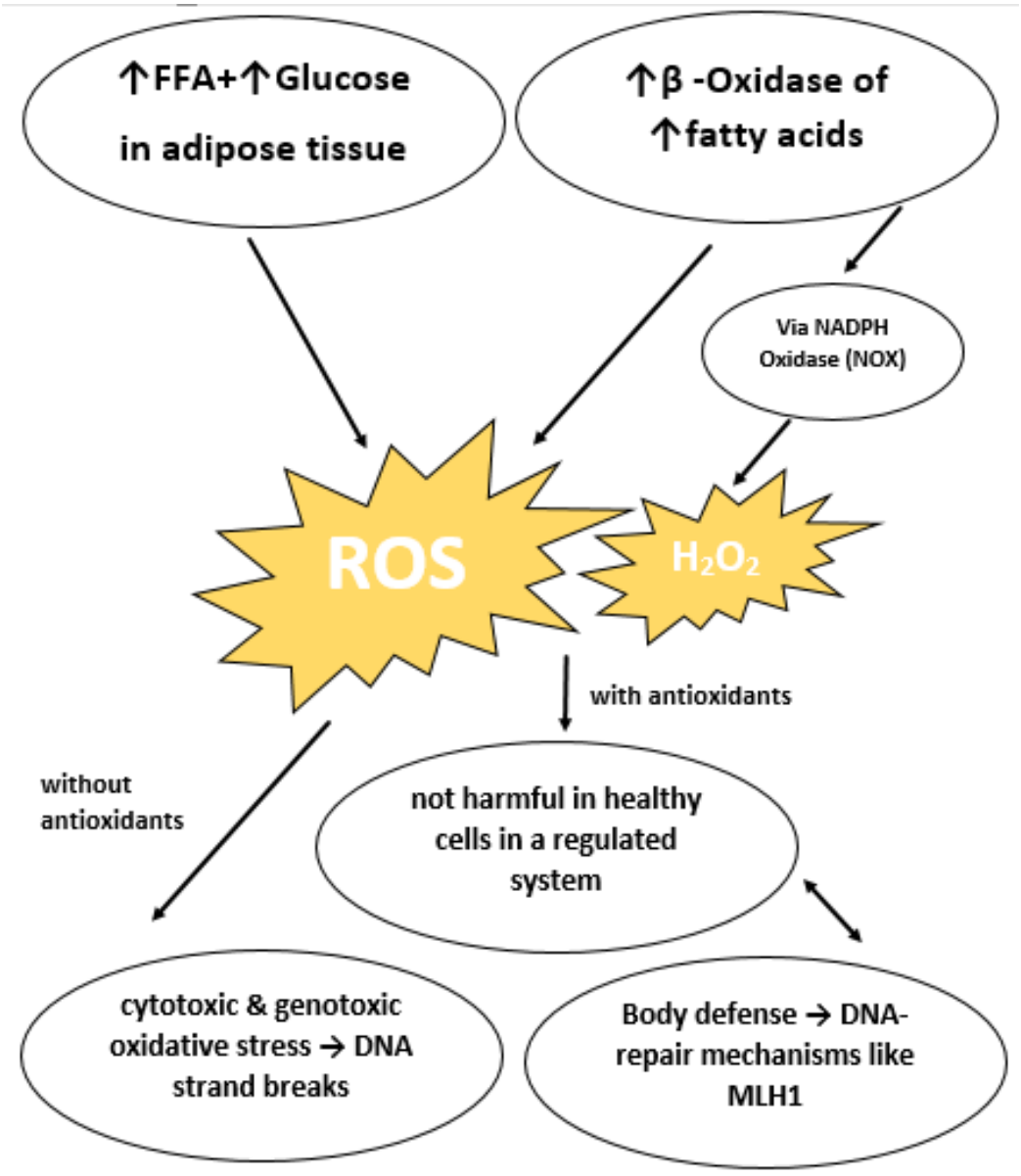

Figure 3: ROS production and impact on the system

2. Epigenetic

Epigenetic means the inherited modifications in gene function which occur independently of changes in the nucleotide sequence. The epigenome is very active and changes in response to ageing, physical exercise, nutrients, drugs, smoking, etc, what can cause many downstream effects including changes in metabolism and therefore a higher or lower disease risk. Many cells have almost the same nuclear genome but different cell types have their own epigenome what is important for the formation of cell specific phenotypes (Franks & Ling, 2010).
Epigenetic patterns include the changes in the genome like DNA methylation, histone modifications and microRNA gene regulation (Tammen, Friso & Choi, 2013).

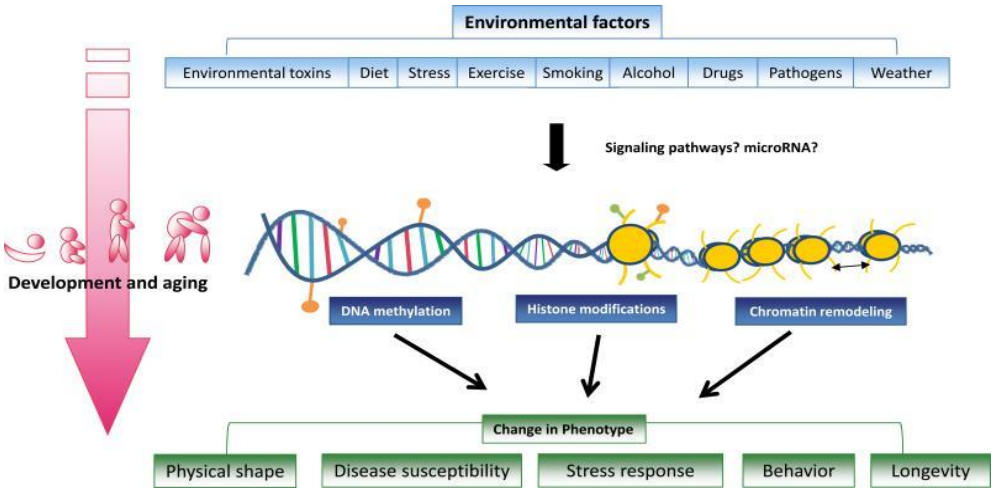

Figure 4: Epigenetic mechanisms between environmental factors and pheno-typical changes (Tammen, Friso & Choi, 2013)

2.1. DNA-Methylation

Methylation plays a role in the one-carbon metabolism pathway and needs a lot of cofactors like enzymes and micronutrients (e.g. folate, choline, betaine) to work with. The conversion from methionine to S-adenosylmethionine (SAM) is ATP dependent and SAM is a universal cellular methyl donor. The methyl groups from SAM are joining the carbon-5 position of the cytosine base with the aid of the DNA methyltransferases (DNMT) and they are generating 5-methylcytosine thus methylating DNA (Anderson, Sant & Dolinoy, 2012). In mammalians this process

happens at cytosin-phosphatidyl-guanin-(CpG) dinucleotides and can be catalyzed by three enzymes DNMT1, DNMT3a and DNMT3b (Eriksson, Taskinen and Leppä, 2006). There are two groups of sequences in the genome: CpG poor regions and CpG islands. CpG islands are longer than 500bp and their Guanin-Cytosin (GC) content is greater than 55%. These islands are often located in promoter regions and are located at the end of the 5' region. The CpG poor regions are the intergenic and the intronic regions (Takai & Jones, 2002). Under normal and healthy conditions, the CpG islands are hypomethylated and the CpG poor regions are methylated. At the carcinogenesis this system changes and the CpG islands become methylated and the CpG poor regions hypomethylated. These changes initiate alterations in the chromatin structure and this again induces a silencing of the tumor suppressor genes and instability of the genome (Jones & Baylin, 2002). However, the methylation of CpG islands and the genome are also important for regulating gene expression during the differentiation, development and the recruitment of repressive methyl-binding proteins.

DNA methylation is very important for silencing retroviral elements, genomic imprinting, regulating tissue specific gene expression and X-chromosome inactivation (Moore, Le & Fan, 2013).

There are two types of methylation: the de novo and the maintenance methylation. De novo methylation is important for the creation of methylation patterns in embryos, during development and carcinogenesis and is catalyzed by DNMT3a and DNMT3b. DNMT1 plays an important role for upkeep and care of this methylation patterns which are created by de novo methylation. (Eriksson, Taskinen and Leppä, 2006)

2.2. Histone modifications

Histone modifications combined with DNA methylation is an indispensable tool of the epigenetic machinery for regulating gene expression and chromatin architecture. Histones are proteins and around them ~147bp are tightly woven for making the DNA more compact and outcome of this is a DNA-protein complex what is called nucleosome. Every nucleosome owns an octamer of two copies of four core histones: H2A, H2B, H3 and H4. These histone proteins execute the coordination of the changes between tightly packed DNA (heterochromatin) which is unapproachable to transcription, and lightly packed DNA (euchromatin) where active transcription happens via binding of transcription factors. These changes appear in the tail of the histones. These tails contain a globular C-terminal domain and an unstructed N-terminal tail. N-terminal tail is the place for post-translational modifications like methylation, acetylation, phosphorylation, ubiquitination and biotinylation. The histone tails of lysine, arginin and serine are the major targets for these modifications and regulating therefore processes like transcription, replication and repair. The modifications of the histone can lead to activation but also to repression, it depends on the residues which are involved and what type of modification is present. Similar to DNA methylation the processes of histone modification are also reversible and these processes are done by the histone acetyltransferase (HAT), the histone methyltransferase (HMT), the histone deacetylase (HDAC) and the histone demethylase (HDM). The HATs and HMTs adding acetyl or methyl groups and causing a neutralization of lysine and therefore the interaction between DNA and the histone tail is degraded. The HDACs and HDMs working contrary, they are removing the acetyl or methyl groups from lysine what results in a status of positive charge again on the histone tail. (Link, Balaguer&Goel, 2010) (Tammen, Friso&Choi, 2013)(Lund&van Lohuizen, 2004).

2.3. MicroRNA – miRNA

MiRNAs also play a role in epigenetic gene regulation as a key factor. MiRNA consists of approximately 19-24 nucleotides in length. They are part of the non-coding RNA and support RNA splicing through performing catalytic functions and they are taking part in the post-transcriptional gene regulation. Translational inhibition or degradation is a result of sequence specific base pairing of miRNA with 3' untranslated regions of the target mRNA. MiRNAs are similar to normal cell physiology and are involved in cell proliferation, apoptosis and differentiation as well, that is why abnormal expression of non-coding RNA is linked to carcinogenesis. This expression can also be regulated by other epigenetic mechanisms like DNA methylation. For example, miRNA can change the expression of DNMT3A and DNMT3B due to DNA methylation and histone modification which again regulate the transcription of miRNA. In cancer cells the DNA methylation was responsible for an abnormal expression of miRNA. (Link, Balaguer & Goel, 2010) (Tammen, Friso & Choi, 2013).

There is also evidence that not only endogenous sources of miRNA can regulate the protein expression, exogenous miRNA may have influence as well. In the study of Zhang et al. 2011 exogenous miRNA out of rice were observed to pass through the GI tract where they pass the sera and is delivered to organs. Then they bound to their target mRNA sequence and reduce protein expressions. This miRNA was able to bind to human and mouse low density lipoprotein receptor adaptor protein 1 mRNA, which removes LDL from the plasma, and stopped its translation in murine liver (Zhang et al, 2011).

Thus there is great evidence that there is an association between our diet especially dietary components and gene expression.

3. Environmental influences and epigenetics

3.1. Equol

3.1.1. Chemistry

Equol [7-hydroxy-3-(49-hydroxyphenyl)-chroman] is an isoflavone which belongs to the family of compounds what are called nonsteroidal estrogens. Isoflavones in turn are part of a family called the flavonoids, which share a basic structure. They are build up of two benzene rings (A and B) which are linked by a heterocyclic pyrone C ring. Isoflavones differ in the position of the benzenoid B ring which is in the 3-position contrary to the 2-position in flavones. The molecular composition is $C_{15}H_{14}O_3$ and it contains two reactive hydroxyls in the heterocyclic structure and in the central furan ring it has one relatively inert and unreactive oxygen.

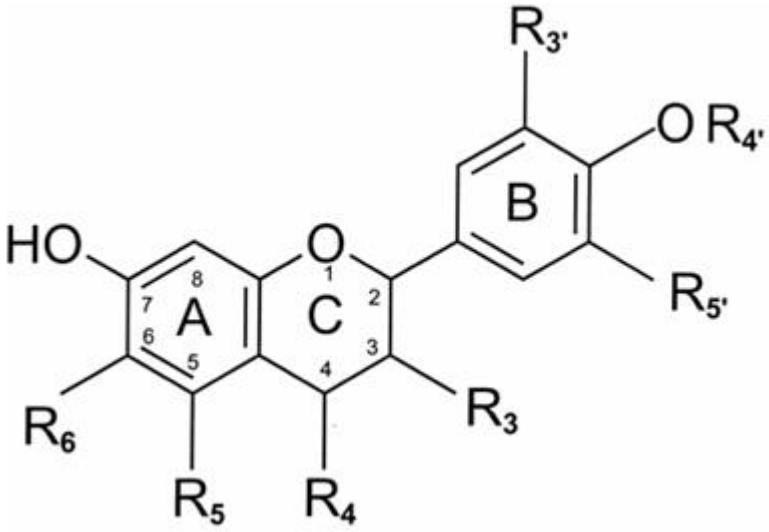

Figure 5: General structure of flavonoids

Because of the chiral carbon at the position C-3, equol occurs in two enantiomeric forms:
R-(+)equol and S-(-)equol. S-(-)equol is produced by intestinal bacteria in the intestine of humans or animals and is the natural diastereoisomer. The precursor of equol is daidzein and equol can be easily synthesized out of daidzein through catalytic hydrogenation but this way just results in a synthesis of R-(+)equol. S-(-

)equol is produced by a special bacterium in the intestine called *Lactococcus garvieae* in the presence of a daidzein-rich source e.g. soy. (Setchell & Clerici, 2010) (Yuan, Wang & Liu, 2007).

3.1.2. Metabolism

Many isoflavones exist as glycosides which are not that estrogenic as the aglycones in soy and unfermented soy products. The bioavailability is dependent on the conversion of glycosides to aglycones through intestinal β-glycosidase from bacteria in the gut which is important for the uptake in the circulation. After that uptake the soy isoflavones are partially hydrolyzed in the intestine, then the aglycones, genistein and daidzein, are getting released and the absorption by the gut epithelium is the result. The part of isoflavones which are not getting hydrolyzed or absorbed in the small intestine are remarkable and reach the colon together with the part of the isoflavones which are getting excreted into the small intestine via enterohepatic circulation. Bacterial enzymes deconjugate the glycosylated, sulfated and glucuronidated forms of daidzein in the colon and then get absorbed or undergo further metabolism by gut microbiota.

While genistein is converted to p-ethyl phenol and 4-hydroxy-phenyl-2-propionic acid, daidzein is reduced to O-Desmethylangolensin (O-DMA) or equol. This metabolism highly differs from person to person and is influenced by the diet and other micronutrients (Yuan, Wang & Liu, 2007). There exists a significant difference in biological activities between isoflavones and their bacterial metabolites. Equol as well as genistein and daidzein have a relatively strong affinity for estrogen receptors whereas O-DMA has a much weaker affinity and seems to be non-estrogenic. There is evidence that equol is able to initiate micronuclei in contrast to daidzein and 6-hydroxy-daidzein (Yuan, Wang & Liu, 2007).

Equol gets better absorbed through the colon than daidzein and also remains longer in plasma after intake of daidzein than daidzein alone or genistein. Equol reaches the top concentration 24h after the ingestion of the isoflavones, whereat the concentration after 4h is very, very low. Afterwards the concentration in plasma diminishes but stays higher than the baseline concentration after 48h. The plasma equol levels were higher after the intake of glycosides than the intake of aglycones over 48h (Zubik & Meydani, 2003).

This result may be possible due to passive absorption of the aglycone in the proximal small intestine whereas the glycoside is not taken to the enterocyte and

therefore not delivered to the distal small intestine and colon for further metabolism by bacteria. The glycoside remains longer in the intestine and has therefore more time to get subjected to both bacterial metabolism and intestinal glucosidase enzymes (Setchell et al., 2010). Another possibility that daidzein is very low in the plasma after the ingestion of glycosides, could be the bacterial metabolic conversion of daidzein to equol because of a longer transit time in the intestine for glycosides than of aglycones (Zubik & Meydani, 2003).

3.1.3. Individual differences in equol production

Many people are not able to produce equol out of soy or rather daidzein. In comparison to animals like rodents, humans produce very low levels of equol, that may be due to our shorter caecum and therefore less abundance of the gut microbiota. Also between humans the amount of conversion of isoflavones to equol is very diverging. In western countries only 25% to 30% of adults are able to produce equol in contrast to 50% to 60% of adults in Japan, China and Korea. The reason could be the different diets and dietary habits resulting in a diverging composition of the intestinal microbiota especially the consumption of soy food, because soy is rich in equol (Yuan, Wang & Liu, 2007) (He & Chen, 2013). Because of that difference in producing equol between Asian and Western countries the working group of Brown et al., 2014 examined the frequency of S-(-)equol production in 90 healthy infants who were fed breast milk, soy infant formula or cow's milk formula in their first year. The first 6 months to one year 3.8% and 6% of the formula-fed infants were equol producers in contrast to none of the breast fed infants. By the age of 3 25% of the breast fed infants were equol producers and 50% of the formula infants produced equol. That provides an indication that the production is developmentally regulated to diet composition and gives a possible explanation for the difference between Asians and Europeans. Not only the exposure to soy food in the first year also the exposition to it throughout the childhood is important for that difference. Antibiotics also have an influence on the stability of S-(-)equol production (Brown et al, 2014).

A different intestinal microbiota also requires a better conversion from daidzein to equol. Three strains of bacteria are identified as equol-producer *Bacteroides* ovatus spp., the gram-positive *Strepotococcus interme- dius* spp. and *Rumino-coccus productus* spp. Dietary changes may vary the bacterial profile of the gut and may lead to a different metabolism of isoflavones.

Dietary habits, food nutrients, composition of the microbiota, bacterial colonization, intestinal transit time and modifications in the redox level of the large intestine, all influencing the intestinal metabolism and bioavailability of isoflavones. The equol producer frequency is higher in vegetarians with 59% as in non-vegetarians with 25%, these results seem similar with the tendency of high soy consumption in Asian population in contrast to Caucasians. Suggesting that high consumption of dietary fiber, plant proteins, less fat and higher carbohydrate intake is strongly associated with equol producers. Higher carbohydrate intake involves a higher production of propionate and butyrate in turn stimulates the equol production, because they may be acting as an electron donor in the biotransformation of daidzein to equol.(Yuan, Wang & Liu, 2007).

However, several metabolic compounds like fatty acids, organic acids and H_2O_2 produced by lactic acid bacteria have antimicrobial effects. *Lactobacillus gasseri* is suggested to suppress the production of equol and decreases the plasma equol concentration and the total amount of equol in the cecal content. Therefore, a high amount of lactobacilli could influence the composition and/or metabolic activity (Tamura et al, 2004).

3.1.4. Antioxidant activities of equol

Equol is a nonsteroidal estrogen and is inimitable in having a lack of a double bond in the heterocyclic ring resulting in a chiral center and it occurs in two enantiomeric forms, S- and R-equol. Among all daidzein metabolites it has the strongest binding affinities and estrogenic activities especially for estrogen-receptor β. The difference between the two enantiomeric form is based on the different binding affinities to estrogen-receptor α (ERα) and estrogen-receptor β (ERβ). S-equol binds more effective on ERα and even better to ERβ than R-equol this

means that S-equol has nearly the same binding affinity than 17β-estradiol what means that S-equol is similar to genistein, the most estrogenic soy isoflavone (Yuan, Wang & Liu, 2007). Referred to equol non-producers the equol producers have a lower risk of breast cancer, less bone loss changes in postmenopausal women and tending to an improvement of plasma lipids including total cholesterol, LDL, LDL/HDL ratio, plasma triglycerides and lipoprotein A (Meyer et al, 2004).

The beneficial properties are believed to derive from the antioxidant activity. They are able to donate hydrogen/electron through hydroxyl groups and thus leading to the ability of acting as a free radical scavenger. Performing as a radical scavenger, the position of the hydroxyl groups and the position C-4 for hydroxyl substitution is very important. Due to the nonplanar structure of equol, which is important for its flexibility for conformational changes which facilitates the penetration into the interior of the membrane, it prevents protein or lipid structures of oxidative damage (Yuan, Wang & Liu, 2007).

Equol affects NO production or utilization and has the skill to enhance the bioavailability of NO through downregulation of O_2-• production and helps to prevent LDL modification to an atherogenic particle. This downregulation of O_2-• is, to a certain degree, the result of a reduced NOX activity. In cell culture equol reduced O_2-• production which resulted in an increase of free NO levels (Hwang et al, 2003). Equol induces the activation of endothelial NO synthase (eNOS) and enhances NO production at resting cystolic Ca^{2+} levels. NO has either atherogenic or vascular protective effects, the effect depends on the source and the amount of production. When NO is produced by the endothelial NO synthase (eNOS) then it ends up in a vasodilator function which has a positive and protective effect. When it is produced by the inducible nitric oxide synthase (iNOS) in macrophages in reaction to different stimuli it has the negative effect and may induce atherosclerosis (Joy et al, 2006). The inhibition of LPS-induced NO production and iNOS gene expression in macrophages through blocking the Akt activation and the following downregulation of NF-κB activity due to equol presents a potential mechanism for the antiatherosclerotic effect.

Nevertheless 3'-hydroxyequol with catechol structure is the major metabolite of equol which can undergo redox cycling after oxidation to semiquinones and form the corresponding quinones and ROS, both of them are able to damage cellular macromolecules and operate cytotoxic and genotoxic (Rannikko et al, 2006).
It has been observed that equol and daidzein also have the ability to invert the effects of NF-Kb signaling pathway and affect TNF-α on Jak/stat signaling cascade. In turn it may cause a downregulation of gene expression of several inflammatory cytokines, adhesion molecules and enzymes like iNOS (Pinent et al, 2011)

4. DNA methyltransferase 1 (DNMT1)

As was mentioned above methylation of genomic DNA is catalyzed by DNMTs. DNMT1 methylates newly biosynthesized DNA, has its origin at the replication fork and is supposed to be responsible for copying methylation patterns after DNA replication. A C-terminal catalytic portion and a large multi-domain N-terminal region of variable size are the two constituents of the DNMTs and provide regulatory functions. Between C5 DNMTs of eukaryotes and prokaryotes the C-terminal part is placed, this part consists out of 500 amino acids and in it lies the active center including amino acid motifs characteristic of the cytosine-C5 methyltransferases. The 621 amino acids out of which exists the N-terminal region is not crucial for DNMT1 activity but necessary for differentiation between unmethylated and hemi-methylated DNA. All DNMTs having the same core structure and this domain is involved in cofactor binding (motifs I and X) and substrate catalysis (motifs IV, VI and VIII). The non-conserved region lying between motif VIII and IX is considered to be the target recognition domain and part of DNA recognition and specificity. DNMT1 has a high precision in maintenance of methylation because of three sequences in the N-terminal region and enables the enzyme direct access to the nuclear replication site: the proliferating cell nuclear antigen (PCNA) binding domain, replication foci targeting sequence and the polybromo homology domain. Interactions between DNMT1 and PCNA are important for the newly synthesized daughter strands to get methylated and packaged into chromatin, this allows DNMT1 to bind newly and naked DNA (Subramaniam et al, 2014).

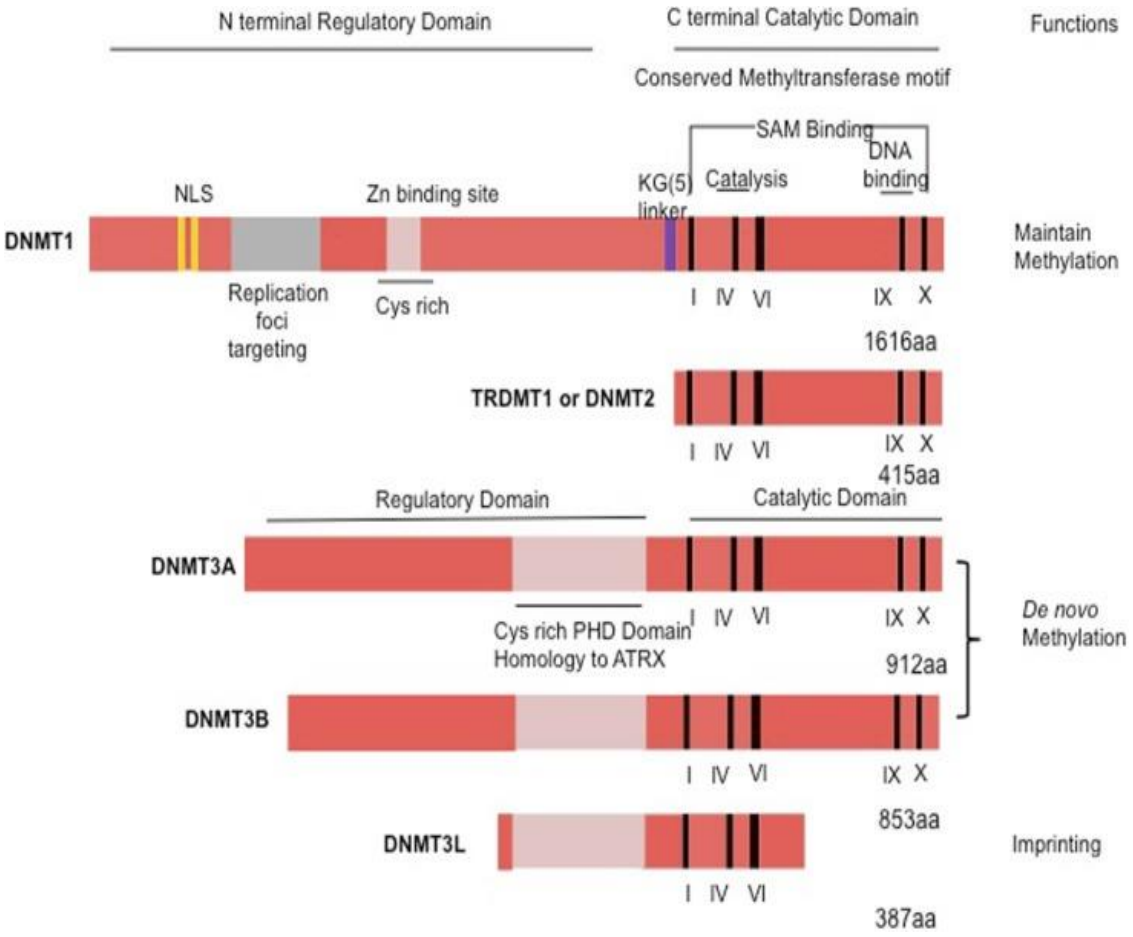

Figure 6:Scheme of the humans DNMTs (Subramaniam et al, 2014)

The binding of DNMT1 to unmethylated CpG DNA by the CXXC (C=cystein; X=any amino acid) domain results in a transcriptional gene silencing in a DNA methylation independent manner. Afterwards it can recruit histone H3 K9 methyltransferase G9a in order to lock the chromatin in a more repressed state. This cause a less reachable structure and transcription factors are inhibited to conduct their duties, which is observed during tumor suppressor gene repression in cancer cells. An effective cooperation of DNA and DNMT1 is very important for the transfer of the epigenetic information during proliferation. When targeting the CXXC/zinc-finger-like domain of DNMT1 through the help of small molecule inhibitors or stable unmethylated CpG this may induce an interference in DNA binding and an interruption of DNMT1 catalytic abilities (Pradhan et al, 2008).
Changes of DNMT1 may lead to either hypo- or hypermethylation, cause differences in mRNAs or proteins altogether impair health status.

Affected health status is partly referable to an obesity-induced lack of adiponectin expression what could be an outcome of a transcriptional regulation failure. It seems that DNA methylation is playing a major role in regulating adiponectin gene expression and adapting whole body-energy balance in obese individuals. In the promoter region of adiponectin, the R2, DNA methylation is conducted through DNMT1 and stimulates the subsequent formation of heterochromatin structure to lower adiponectin gene expression in obesity. But the inhibition of DNMT1 works against the downregulation of adiponectin resulting in improved metabolic parameters (Kim et al, 2015).

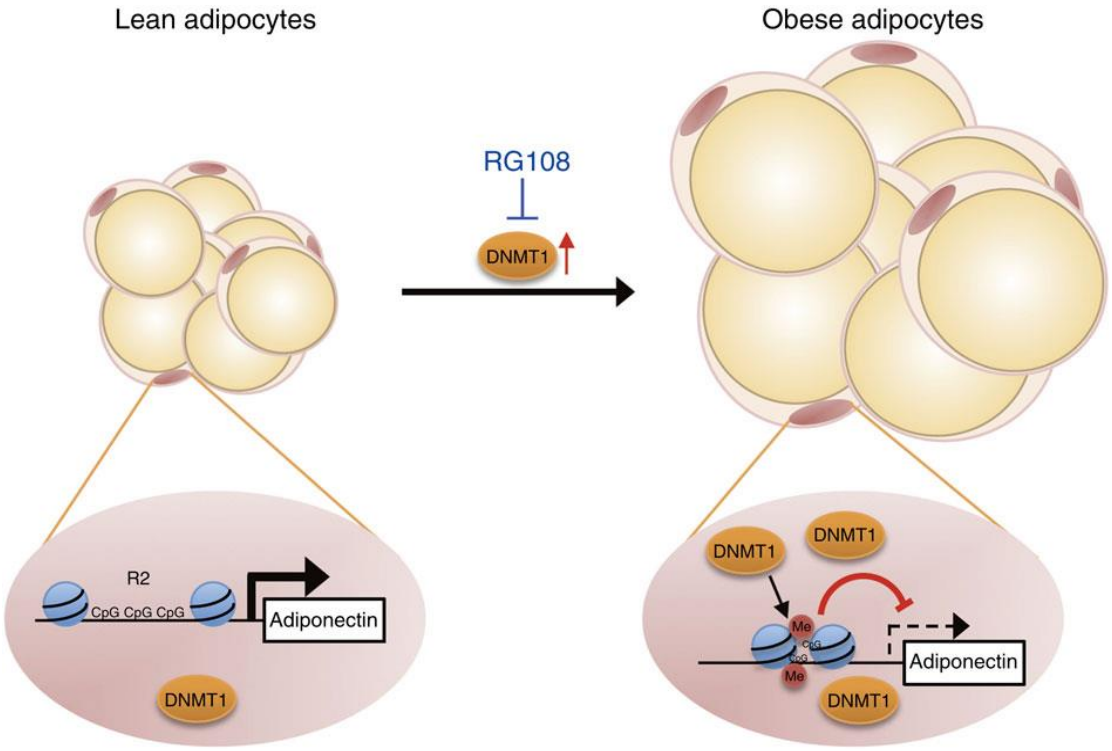

Figure 7: In obesity, higher DNMT1 levels induce DNA hypermethylation at the particular region (R2) of adiponectin promoter, leading to suppression of adiponectin gene expression in adipocytes (Kim et al, 2015)

5. MutL homolog 1 (MLH1)

MLH1 short for MutL homolog 1 is part of the DNA mismatch repair system and is responsible for sustaining genome stability by repairing mismatched base pairs. Such mismatched base pairs mostly arise due to replication errors. In the case of a replication error, this error is recognized and the affected DNA region is going to be removed. When that happens and this mismatch get recognized then the affected DNA region gets removed. The main factors of that system, such as proteins, have been highly conserved during the evolution from bacteria to mammalians, like MutL and MutS proteins have been also found in eukaryotes.

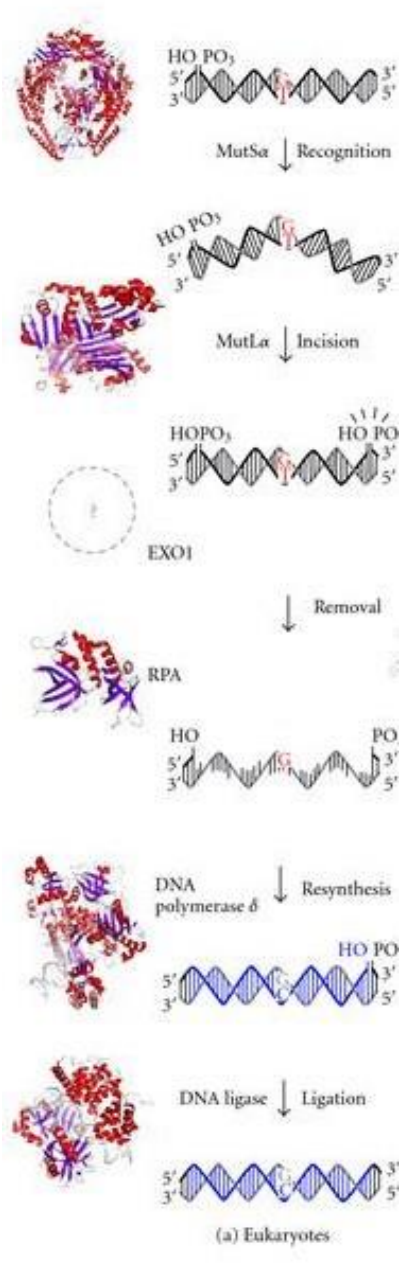

Figure 8: The MMR pathway (Fukui, 2010)

Appears a mismatched base then it gets recognized by a MutS homodimer and then MutL homodimer interacts with the MutS-DNA complex thereby MutL activates a MutH restriction endonuclease. This step allocates a signal by that the MMR system discriminates the error-containing-strand. MMR now exploits this situation of the absence of the methylation at the restriction site and tries to repair it. Helicases and exonucleases execute the removal of the error and the polymerase III and ligase synthesize a new strand.

Four different MutL homologs belong to the system in mammalian cells: PMS1, PMS2, MLH1 and MLH3. MLH1 interacts pairwise with the other three remaining MutL homologs and therefore it is the central MutL homolog. MutLα plays a major role in the MMR and is a heterodimer of MLH1 and PMS2.

MutL homologs contain a N-terminal ATPase/DNA-binding domain and a C-terminal dimerization/DNA-binding domain. Conformational changes of MutL homolog lead to interaction between the N- and the C-terminal domains and are therefore important to perform MMR reaction. MLH1 and PMS1 (MutLα) are bound by the C-terminal domain. The ATP induced dimerization of the N-terminal domain cause a condensation of the MutLα heterodimer. The endonuclease activity is thereby inactivated and this results in a binding to MutS heterodimers which starts the endonuclease activity due to the interaction of MutL and MutS induced ATP hydrolysis of MutLα (Fukui, 2010) (Harfe & Jinks-Robertson, 2000).

Mismatch base pairs not only occur because of replication errors but also from oxidative damage. ROS attack biomolecules such as proteins, lipids and DNAs. This assault on the DNA produces oxidized bases including 8-oxoguanine (8-OG) which is able to pair with cytosine as well as with adenine. As a result of the replication an 8-OG:A pair can be metabolized to a T:A pair, forming a G:C—T:A transversion mutation. MMR is able to recognize the 8-OG:A pair as a substrate and removes from the newly synthesized strand the mismatched adenine. O6-Methylguanine pairs with thymine what leads to G:C—A:T transition mutation again by replication. MMR now induces the apoptosis if the template strand is affected through crosstalk between MMR proteins and check point kinases (Fukui, 2010).

Some sorts of cancer are related to MMR defects, like a mutation in MLH1 is associated with hereditary non-polyposis colon cancer (HNPCC) or sporadic colorectal, endometrial and gastric carcinomas. It is not clear if the sporadic forms do have mutations in MLH1 as well but hypermethylation of the MLH1 promoter is involved goes along with a complete loss of protein expression (Harfe & Jinks-Robertson, 2000).

6. Interleukin 6 – IL-6

IL-6 is a pleiotropic cytokine which has an impact on various processes in immune homeostasis like inflammatory reactions, acute phase response, reproduction, ageing frailty, hematopoiesis and bone metabolism. There is a positive association between low grade inflammation and the metabolic syndrome, especially in combination with obesity. Too much adipose mass is responsible for a higher level of pro-inflammatory proteins like IL-6. The adipose tissue is likely to generate about one-third of total circulating IL-6. A reduction of these levels were seen in intervention studies with the aim of weight loss and thereby improving inflammation status. Because IL-6 has a major function in inflammatory processes it modulates the growth of many tumor cells and this is the consequence of abnormal IL-6 gene expression which has been associated with inflammatory disorders and ageing discomforts.

IL-6 is producing both pro- and anti-inflammatory effects and therefore it's unclear if a high serum level of IL-6 is a consequence of or a contributory cause to advanced tumor stage and if the inflammatory infiltrate hinders or helps tumors.

Expression and transcription is controlled at the level of its promoter which controls the immunological homeostasis as a biosensor for environmental stress. During stress like infections, traumas or ageing the usually low expressed IL-6 is getting higher due to the secretion of different cell types like endothelial cells, B- and T-cells, macrophages, dendritic cells and tumor cells. A possible way to downregulate IL-6 expressions are hormones through endocrinological feedback mechanisms and antioxidants.

IL-6's promoter region consists of 300bp upstream of the transcriptional initiation site and includes Nf-κB, API, CREB and C/EBP regulatory elements. This is necessary for IL-6 gene induction in combination with other stimuli usually combined with acute inflammatory or proliferative states (Dijsselbloem et al, 2004).

It also regulates several signalling pathways like Janus-activated kinase/signal transducer and activator of transcription 3b(JAK-STAT3), phosphoinositol-3 kinase (PI-3K) and mitogen-activated protein kinase pathways. It is able to induce

the expression and activity of DNMT1 due to epigenetic silencing and remethylation of p53, an important tumor suppressor gene and relevant in the cell cycle control and therefore it is supposed to have an effect on epigenetic mechanisms (Hodge et al, 2001,2005).

Equol lowers the secretion of IL-6 in inflamed adipocytes (Pinet, 2011).

7. Objectives

With this background on data and information relating to obesity, inflammation and oxidative stress, we hypothesized that dietary induced obesity may have an effect on inflammation, alters gene expression of genes and lead to adverse changes in DNA methylation and their repair mechanisms. Additionally, we hypothesized that equol with its antioxidative capacity would improve the gene expression status and DNA methylation caused by HFD. It has been observed that equol has the ability to invert the effects of NF-Kb signaling pathway and affect TNF-α on Jak/stat signaling cascade and in turn it may cause a downregulation of gene expression (Pinent et al, 2011).

For this study we examined the genes DNMT1, MLH1 and IL-6 which are playing an important role in methylation and repair system and through that influencing metabolic status. DNMT1 is involved in the maintenance methylation, catalyzes methylation of cytosine within CpG dinucleotides and is therefore indispensable for cell differentiation and has an impact on epigenetic mechanisms.

MLH1 is part of the MMR system, helps to repair mismatched base pairs and is important for genome stability.

IL-6 is a pleiotropic cytokine which has an impact on various processes in immune homeostasis like inflammatory reactions and acute phase response.

Aim of this study was to examine the effects of antioxidants, especially equol, on gene expression and methylation of DNMT1, MLH1 and IL-6 in C57BL/6J mice fed a control diet (CD) and a high fat diet (HFD). Colon and liver of the mice were investigated for differences in gene expression and methylation, to find a possible interaction between high fat diet and equol on inflammation and ROS production in obesity.

8. Materials and Methods

This animal experiment was authorized by the Ethical Committee of the Medical University of Vienna (BMWFW-66.009/0329-WF/V/3b/2014). The mice were kept at the animal laboratory at the Cancer Research Institute, Medical University of Vienna (Borschkegasse, Vienna) but all analyses were executed at the laboratory of AG Haselberger at the Department of Nutritonal Science.
60 C57BL/6J male mice at the age of six weeks (Janvier Labs, France) were used for this trial, because they are a relevant model for DIO. Under standard conditions (24 ± 1 °C, humidity 50 ± 5 %, 12 hours light/dark cycle) the mice were kept in plastic cages (Macrolon type III, Techniplast GmbH Germany) always three per cage and they had free access to water and food. After an acclimatization of 14 days with CD (EF R/M Control, 12 % fat, ssniff Spezialdiäten GmbH, Soest, Germany) they got divided into four groups. The four groups included as follows:

Control diet (CD)	11.4% energy fat and 12.6 kJ/g
Control diet plus equol (CD+Q)	Water was supplemented with Equol, 25mg/kg body weight (bw) per day
High fat diet (HFD)	58 % energy fat and 23.4 kJ/g (ssniff EF acc.D12492 (I) mod., ssniff Spezialdiäten GmbH, Soest, Germany
High fat diet plus equol (HFD+Q)	Water was supplemented with Equol, 25mg/kg body weight (bw) per day

Table 1: Dietary composition

Drinking Water was supplemented with 25mg/kg body weight of E-55-EQUOL® (CAS-No.: 94105-90-5, System Biologie AG). Body weights and food intake were measured weakly and water plus equol was changed every day.

Month		Water intake [ml]				Chow intake [g]				Weight [mg]			
		1	2	3	4	1	2	3	4	1	2	3	4
Intervention	**CD**	5.60 ± 0.99	5.36 ± 0.99	5.40 ± 0.91	5.05 ± 1.27	2.64 ± 0.17	2.11 ± 0.62	2.08 ± 0.61	1.99 ± 0.64	23.99 ± 1.50	25.92 ± 1.09	26.94 ± 1.42	27.88 ± 1.49
	CD+Q	5.38 ± 0.48	5.30 ± 0.47	5.29 ± 0.85	5.30 ± 1.22	2.65 ± 0.21	2.64 ± 0.22	2.65 ± 0.27	2.66 ± 0.34	23.83 ± 2.49	25.36 ± 2.45	26.48 ± 2.38	27.29 ± 2.34
	HFD	5.30 ± 0.43	5.13 ± 0.47	4.97 ± 0.54	5.07 ± 0.39	2.56 ± 0.10	2.59 ± 0.15	2.60 ± 0.13	2.56 ± 0.13	30.54 ± 3.43	37.62 ± 4.11	42.88 ± 4.58	45.99 ± 4.46
	HFD +Q	5.42 ± 0.59	4.94 ± 0.06	4.98 ± 0.08	4.58 ± 0.44	3.53 ± 4.43	2.61 ± 0.36	2.52 ± 0.18	2.20 ± 0.50	30.49 ± 2.99	37.47 ± 3.16	42.55 ± 3.89	45.24 ± 4.10

Table 2: Water, food intake and weight gain per mouse over a period of 4 months. Means of chow intake in gram, water intake in ml and body weight in gram divided into the different investigation groups (CD, CD+Q, HFD, HFD+Q); presented as mean ± SD. (CD= control diet, HFD= high fat diet, Q = equol)

8.1. Sample Collection

Animals were sacrificed by cervical dislocation after four months undertaken by a skilled person at the Institute of Cancer Research. After the tissue removal, the tissue was put in plastic tubes containing RNA-later solution (Qiagen, Germany) for stabilization. Afterwards they were stored immediately at -80°C for later extractions.

8.2. Gene expression analysis

8.2.1. DNA and RNA extraction

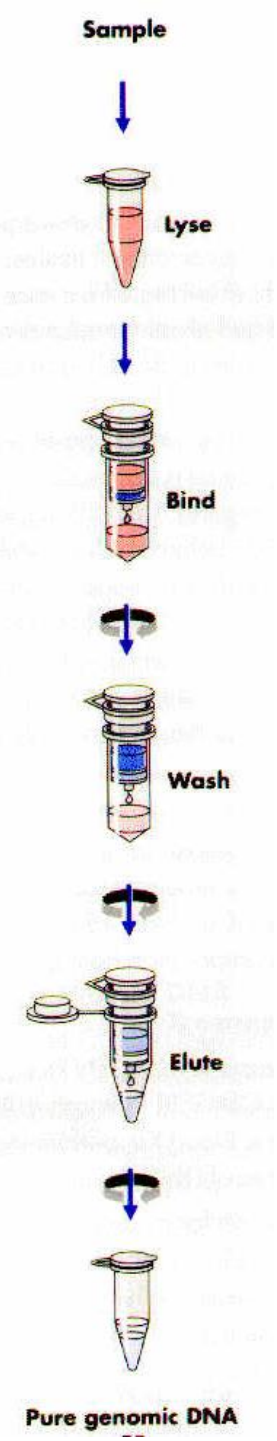

Figure 9: cDNA synthesis

RNA and DNA were isolated from colon and liver using the AllPrep DNA/RNA/miRNA/ Universal Kit (Qiagen, Germany) referred to the manufacturer's protocol (see Appendix).

There are four steps to get from the tissue to the pure DNA/RNA:

Lyse: an important step to release cell components like DNA and RNA

Bind: binding of DNA and RNA to membrane leads to separation of nucleic acids from other detergents

Wash: Removes all needless stuff like proteins, lipids, etc…

Elute: Elution of DNA and RNA in buffer or nuclease free water

8.2.2. Quantification

The concentration as well as the purity was measured with the Picodrop100 (Picodrop, UK). For the purity check they had to achieve a ratio ≥ 1,8 for DNA and ≥ 2 for RNA and was checked at the ratio 260/280.

8.2.3. Reverse transcription

The principle of reverse transcription is to get from mRNA the complementary DNA (cDNA). At the first step oligo-dT primers and random hexamers bind on RNA and then the activity of the RNA-dependent DNA polymerase induces a transcription of the RNA to a DNA hybrid. Afterwards the RNase H activity degrades the RNA from the RNA:DNA hybrid and the single stranded cDNA is the result.

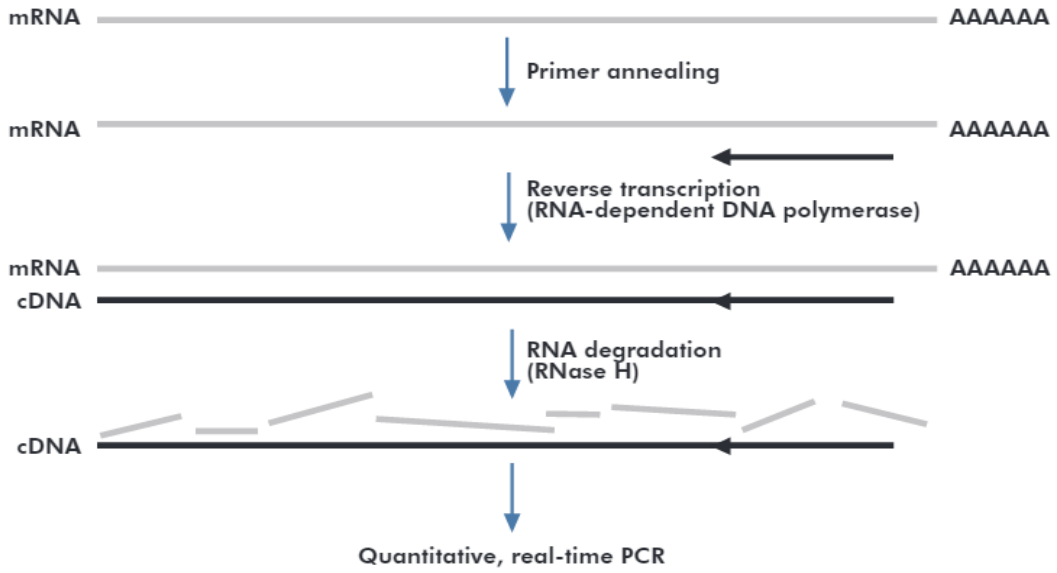

Figure 10: cDNA synthesis

To get the complementary DNA (cDNA) 1µg of total RNA was executed by reverse transcription using the RT2 First Strand Kit (Qiagen, Germany).
Therefore, 1µg of RNA was mixed with RNase-free water and Buffer GE in a sterile 8-strip 0.2ml PCR tube with single caps according to table 2. This mixture was incubated for 5 minutes at 42°C in a thermocycler (Biometra GmbH, Germany) and afterwards immediately put on ice for 1 minute.

Component	Volume per reaction
template RNA (25 ng–5 µg)	variable (max.8 µl)
RNase-free water	variable
Buffer GE	2 µl
Total volume	10 µl

Table 3: Genomic DNA elimination mix

The RT-mix was prepared according to the schema in table 3. For every step it was important to conduct a no reverse transcription control which served as a negative control in real-time RT PCR.

Component	Volume per reaction
5x Buffer BC3	4 µl
Control P2	1 µl
RE3 Reverse Transcriptase Mix	2 µl
RNase-free water	3 µl
Total volume	10 µl

Table 4: RT-Mix

10µl of the RT-mix was applied to each tube which contains the DNA elimination mix and was set 15 minutes at 42°C to start the RT. Incubation at 95°C for 5 minutes inactivates the RT-enzyme and the reaction stopped. Afterwards 91µl of RNase-free water was added to each tube and the template was ready to use in real-time PCR.

8.2.4. Real-time reverse transcription polymerase chain reaction

The principle of the real-time reverse transcription PCR is to copy a DNA region of interest and detect its amplification during the reaction. With real-time PCR the cDNA was analyzed by dint of qPCR Primer Assays (Qiagen, Germany) and RT2

SYBR Green Mastermix (Qiagen, Germany) according to the protocol (see Appendix).

The primers are binding to the target region and the DNA synthesis starts through DNA polymerase. The amplification is measured because of using fluorescent dyes which are able to bind at the synthesized double stranded DNA.

PCR conditions are as follows:

Initial step of 95°C for 10min, followed by 40 cycles of 95°C for 15 s and 60°C for 1min, finishing with melting curve analysis (gradient melting of the products was performed at 0.5°C/10 s from 65°C to 95°C).

Denaturation: To get single stranded DNA the bonds between the complementary bases are getting denatured due to the 90-95°C step.

Annealing: The primer anneals to the single stranded DNA at a primer specific temperature which depends on the sequence. If the temperature is too low the primer binds to unspecific sides if it is too high primer cannot anneal, usually 50-70°C.

Elongation: A new strand that is complementary to the DNA template is synthesized due to DNA polymerase which adds deoxyribonucleoside triphosphates (dNTP) at 72°C and starts at 3'-terminal end of the annealed primer.

Every cycle the DNA is doubled which leads to an exponential amplification. SYBR Green was used as an intercalating dye which fluoresces when it is attached to double stranded DNA: After each cycle this signal is measured and this represents the amount of copied DNA. Every sample was tested in duplicate, with normalization to the housekeeping gene GAPDH as an internal control. The housekeeping gene shows constant gene expression and is not affected with the intervention, its expression is calculated in all cDNA samples and therefore changes in the amount of cDNA can be adjusted.

The cycle threshold or CT value is used for quantification and defines the beginning of the exponential increase of DNA and is proportional to the amount of target DNA in the sample.

The CTs are normalized to GAPDH by calculating ΔCT. To get the difference between the control group and the intervention group ΔΔCT is measured by subtracting ΔCT of the control group from ΔCT value of the intervention group as shown in table 4. Relative changes between the intervention and the control group are determined by the 2-ΔΔCT equation.

ΔC_T	C_T gene of interest -- C_T housekeeping gene
$\Delta\Delta C_T$	ΔC_T intervention --ΔC_T control
Fold change	$2^{-\Delta\Delta CT}$

Table 5: Calculation of CT values

Meaning of fold change interpretation:
Fold change <1 = lower expression due to the intervention
Fold change >1 = higher expression due to the intervention

8.2.5. Execution of real-time PCR

Real-time RT PCR was executed by using RT² qPCR Primer Assay for Mouse GAPDH (NM_008084, Cat.no. PPM02946E), DNMT1 (NM_001199431, Cat.no. PPM03685E), MLH1 (NM_026810, Cat.no. PPM04973C) and IL6 (from Qiagen, Germany). Master mix for real-time RT PCR was prepared as following:

Component	Volume per reaction
RT² SYBR Green ROX™ qPCR Master Mix	12.5 µl
RT² qPCR Primer Assay (10 µM)	1 µl
RNase-free water	10.5 µl
cDNA template	1 µl

Table 6: Real-time PCR Master Mix

PCR was operated by an Applied Biosystem StepOnePlus real-cycler. Cycling conditions were 95°C for 10 minutes, 40 cycles of 95°C for 15 seconds and 60°C for 1 minute for every gene. A no template control (NTC) and a no reverse transcription control (NRT) had to be done to detect contamination. All of the samples

as well as the negative controls were determined in duplication and GAPDH were used as reference for ΔCT calculation afterwards.

8.3. Methylation analysis

8.3.1. Bisulfite conversion

To analyze the methylation status by pyrosequencing a bisulfite conversion is necessary. The aim is to get the complete conversion of unmethylated cytosines to uracil whereat the methylated cytosines remain unchanged. Therefore, the DNA is incubated in high sodium bisulfite concentrations at high temperature and low pH and then the PCR displaces uracil with thymine.
For this study the EpiTect Fast DNA Bisulfite Kit (Qiagen, Germany) was used according to the manufacturer's protocol (see Appendix). The input for every sample was 2µg ofs genomic DNA, afterwards single stranded DNA was measured again with Pico100 and stored at -20°C.

8.3.2. Pyrosequencing

Pyrosequencing is a good tool to get information about the methylation status of single CpGs in an investigated region.
Streptavidin beads are mixed with the PCR product and that forms a complex with the biotinylated end of the amplicon. In the vacuum tool this complex is denaturized and purified and leaves single-stranded biotin-tagged DNA aback. This single-stranded DNA is dissolved in buffer mix which contains the primer for the sequence of interest, DNA polymerase, ATP sulfurylase, luciferase, apyrase and the substrates adenosine 5' phosphosulfate (APS) and luciferin. In the Pyrosequencing reaction the first deoxyribonucleotide triphosphate (dNTP) is added and the addition of dNTP to sequencing primer is catalyzed due to the DNA polymerase. This happens only if its complementary to the base in the template strand. Every insertion step releases pyrophosphate (PPi) which is equal to the amount of inserted nucleotides. In the presence of APS PPi is converted to ATP due to

ATP sulfurylase. This ATP is responsible for the generated light because it converts luciferin to oxyluciferin, which is mediated by luciferase, what generates the visible light and that is proportional to the amount of ATP. This light is detected by sensors and is seen by a peak in the pyrogram. The height of the peak is proportional to the number of nucleotides inserted.

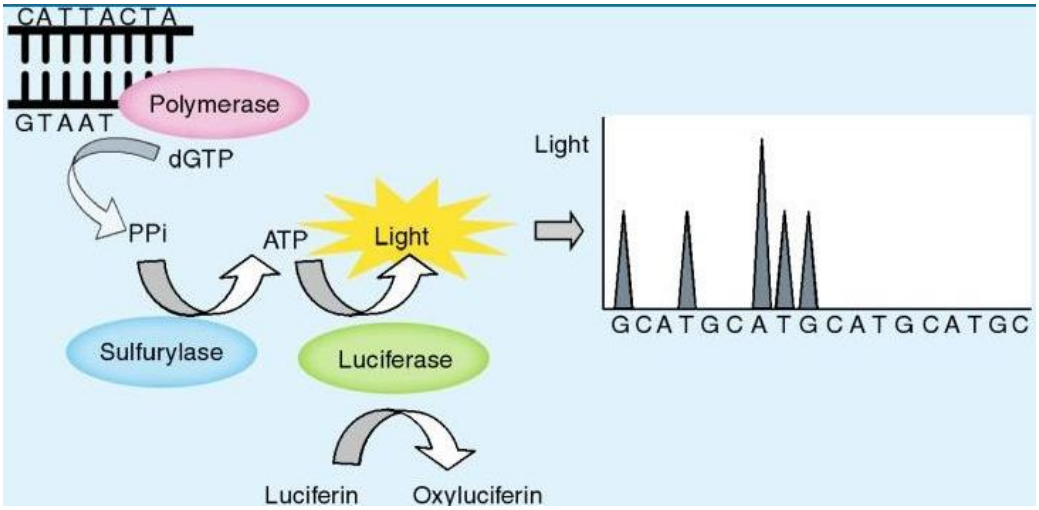

Figure 11: Principle of pyrosequencing (Expert Rev Mol Diagn © 2012 Expert Reviews Ltd)

A PCR amplification has to be done before pyrosequencing by using PyroMark PCR kit (Qiagen, Germany) according to manufacturer's instructions with primers for DNMT1 and MLH1 designed by PyroMark Assay Design SW 2.0 Software (Table 8).

15ng/µl of bisulfite converted DNA was used for DNMT1 and 10ng/µl template was used for MLH1. Concentration of primers and the preparation of the reaction mix as follows:

Component	**Volume per reaction**
RNase free water	9µl
Pyromark PCR Master Mix	15µl
Coral Load	3µl
Primer forward (10pmol/µl)	1µl
Primer reverse (10pmol/µl)	1µl
DNA template	1µl

Table 7: Reaction mix for PyroMark PCR for DNMT1

Component	Volume per reaction
RNase free water	9µl
Pyromark PCR Master Mix	15µl
Coral Load	3µl
Primer forward (7pmol/µl)	1µl
Primer reverse (7pmol/µl)	1µl
DNA template	1µl

Table 8: Reaction mix for PyroMark PCR for MLH1

Target	Primer	Sequence (5′->3′)
DNMT1	Forward	5'-GTA GGT TGT AGA MGA TAG AAT AGT TTT GA-3'-Biotin
	Reverse	5'-CCC ACT CTC TTA CCC TAT ATA ATA CAT-3'
	Sequencing	5'-CCC CTC CCA ATT AAT TTC-3'
Sequence to analyse	ACGAGACCCCGGCTTTTTCGCGCGCGCGGAAACCAATTGG-GAGGGGGCGGCGCAAGCG	
MLH1	Forward	5'-AGG GTA TTT TMG TTT TTA TTG GTT GGA GA-3'
	Reverse	5'-TTA CAC YTC AAT TCC TAA AAT CTC TAT CCC-3' – Biotin
	Sequencing	5'-TTT AGT TTT TAG AAA TGA GTT AAT A-3'
Sequence to analyse	GGAAGAGYGGATYGTGAATTTTGAYGYGTAAGYGYGTTGTTTTTTAG-TTTGGTGTYGGGTYGTTGTTTAGAGYGGGATAGAGATTTTAGG	

Table 9: Sequence to analyze and primers for CpG Methylation analysis

Methylation analyses were done by using a PyroMark Q24 System in combination with PyroMark Q24 Vacuum Workstation.

40µl PyroMark binding buffer, 1µl streptavidin sepharose beads (GE Healthcare, Austria) and 14µl nuclease free water were mixed with 25µl of PCR product, concentration depending on the gene. The vacuum tool sucked this mix and purified and denatured the DNA by using 70% ethanol, PyroMark denaturation solution and PyroMark wash buffer. The purified single stranded DNA was dispensed into

pyrosequencing plates which contained 24µl PyroMark annealing buffer combined with 1µl sequencing primer (5pmol/µl) and was heated up to 80°C on a heating block for two minutes.
Enzymes, substrates and nucleotides were filled into the cartridge and together with the plate it was inserted into the PyrosequencerTM.

8.4. Statistical analysis

All statistical analyses of gene expression and methylation were done using IBM SPSS Advanced Statistics 22.0 (SPSS, USA). All data are shown mean±SD. For testing the normalization of the data the Kolmogorov-Smirnov-Test was used and to determine the signification Mann-Whitney-U-Test was taken. For all comparisons: p-values ≤ 0.05 were considered as significant.
As mentioned above all ΔCT were calculated by normalization to the housekeeping gene GAPDH, the calculation is shown in table 4.

9. Results

Subsequent the results of relative gene expression and methylation percentage of DNMT1, MLH1 and IL6 are presented.

First of all, figure 12 gives a short overview over the weight gain within the 20 weeks. There is a clear difference between the CD and HFD fed mice, but the CD+Q fed mice don’t differ from the CD as well as the HFD+Q from the HFD. The chow intake of figure 11 shows that the CD and the HFD+Q ate a bit less than the other groups, but that didn’t affect the weight. The caloric intake of the HFD mice was higher (12,6 kJ/g CD, 24,4 kJ/g HFD) due to the fat content which results in a higher weight gain.

Figure 12: Weight gain: Mean body weight of the C57BL/6J mice of each intervention group (CD, HFD, CD+Q, HFD+Q) during the study period (in weeks), shown in grams. (CD= control diet, HFD= high fat diet, Q= equol**)**

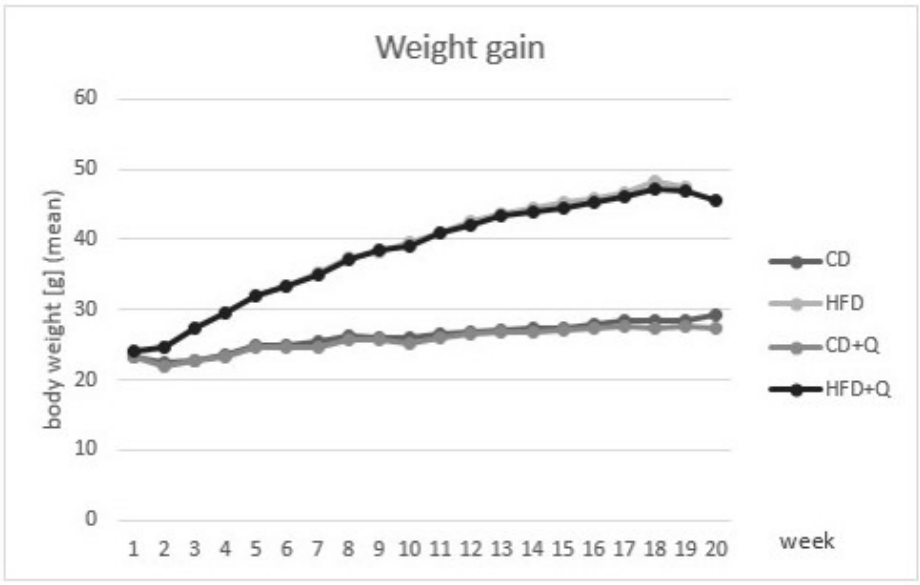

Figure 13: Chow intake: Mean chow intake of each intervention group (CD, HFD, CD+Q, HFD+Q) during the study period (in months), shown in grams. (CD= control diet, HFD= high fat diet, Q= equol)

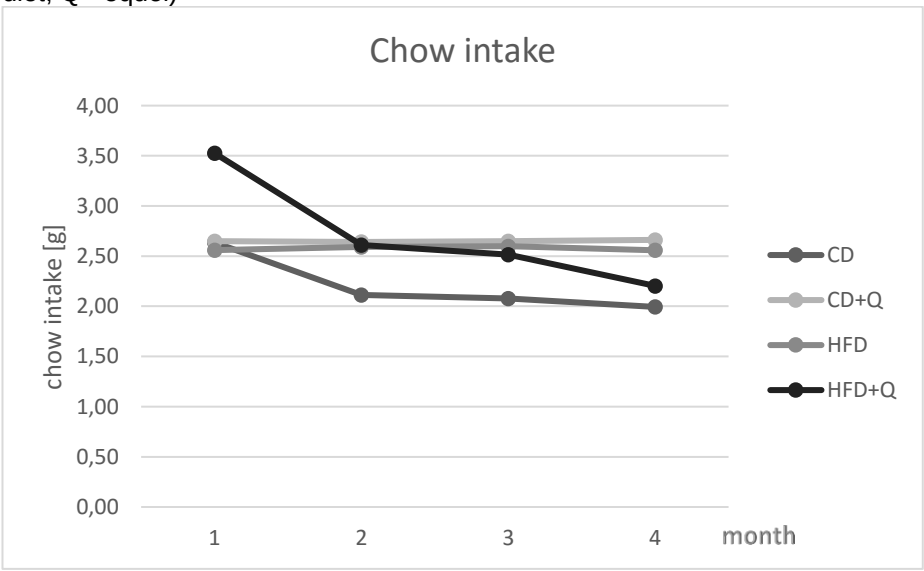

9.1. Relative gene Expression

As mentioned before gene expression levels were normalized to the housekeeping gene GAPDH. Due to some literature and previous researches there was evidence that GAPDH will fail as housekeeping gene for equol, because of estrogenic effects it may have an influence on the gene expression and interferes with GAPDH. It was shown that estrogen is able to either down or up regulate GAPDH depending on species and tissue. Possible mechanism could be that selective estrogen receptor ligands can induce different gene expression profiles. (Schroder, Pelch & Nagel, 2009). To test if the data with GAPDH is unreliable, test-runs were conducted with the housekeeping gene Rpl13a and Beta actin, which was obtained to be better of use in that case. But no significant differences between GAPDH, Rpl13a (p-value= 0,238) and Beta actin (p-value = 0,721) were seen that's why GAPDH remained as housekeeping gene.

figure 14: Difference between the HKGs relating to equol of MLH1 in liver

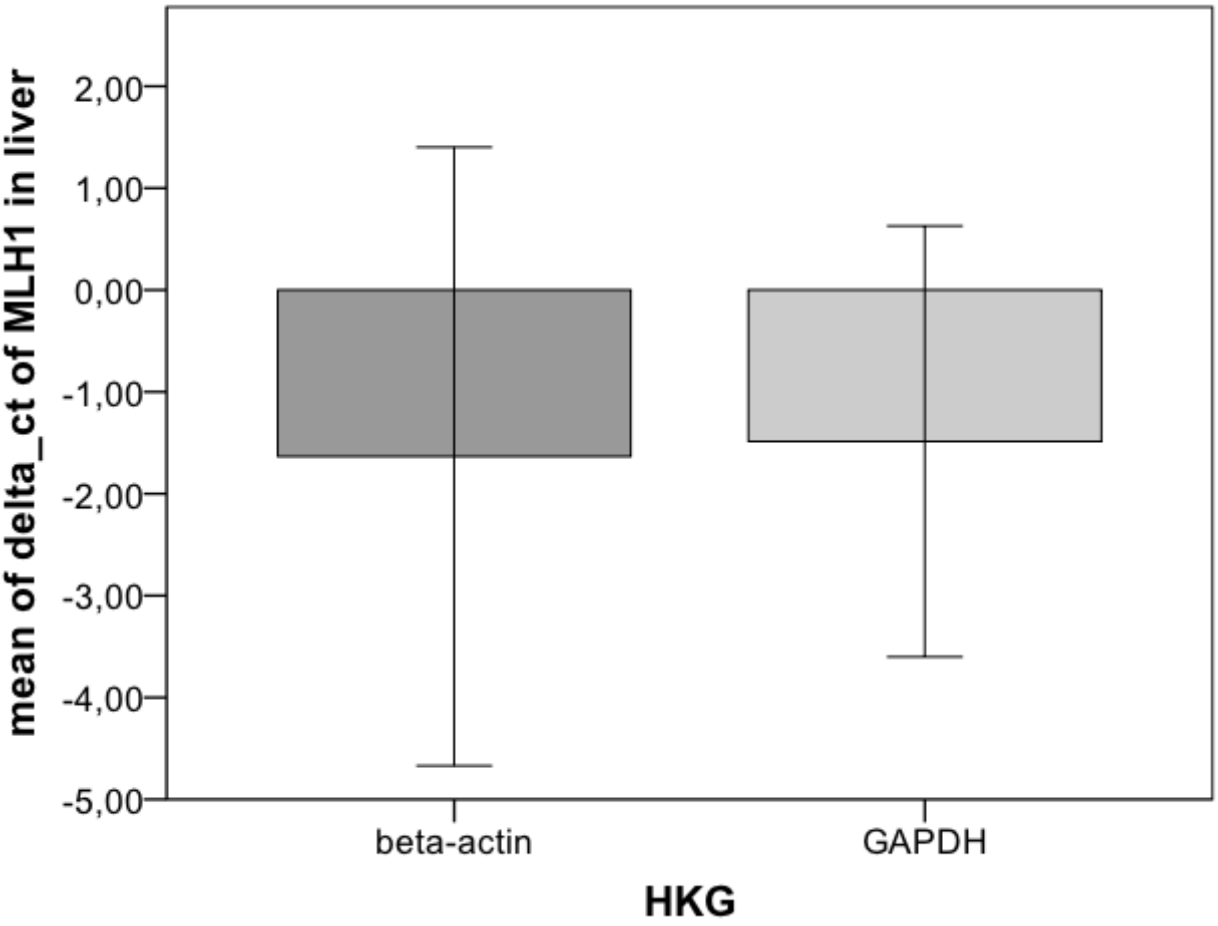

figure 15: difference between the two HKGs relating to equol of MLH1 in liver

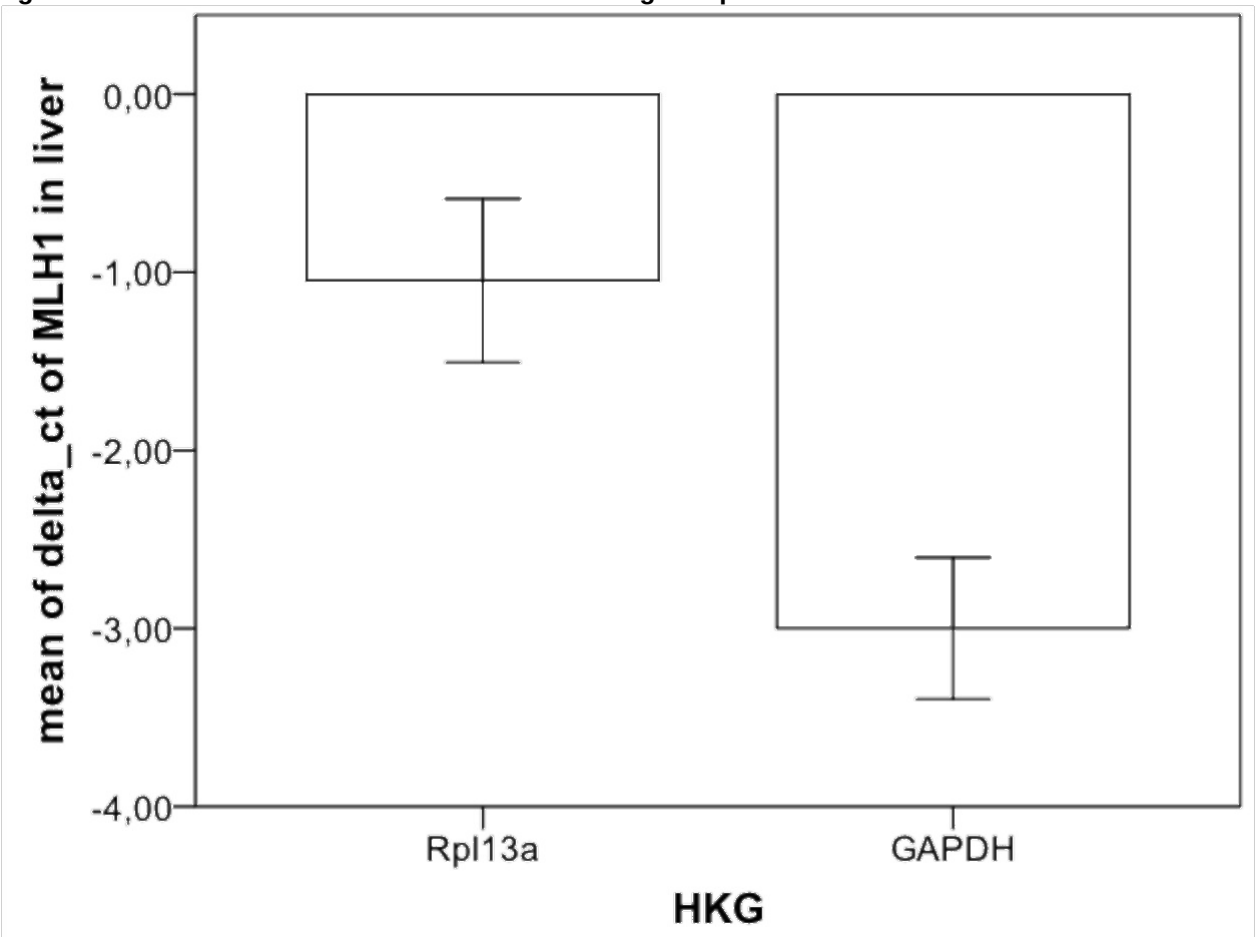

9.1.1. DNMT1

In general, there is a significant lower expression in all groups compared to the CD (p = 0,002) in liver. There is a significant lower expression of DNMT1 in liver in CD+Q (p = 0,002) than in CD and HFD. The HFD+Q (p = 0,002) has a significant higher expression than CD+Q. In colon DNMT1 is lower in HFD and CD+Q (p = 0,002) compared to CD.

Table 10: Relative expression of DNMT1 in CD+Equol intervention standardized to CD

Gene	N	Minimum	Maximum	Mean	Standard deviation	%-change of Relative expression standardized to CD

DNMT1_liver	6	.03	.13	.0757	.04491	-92.43
DNMT1_colon	6	.15	.43	.2603	.13387	-73.97

Table 11: Relative expression of DNMT1 in HFD+Equol intervention standardized to CD

Gene	N	Mini-mum	Maxi-mum	Mean	Standard deviation	%-change of Relative ex-pression standardized to CD
DNMT1_liver	6	.35	.47	.4020	.05679	-59.80
DNMT1_colon	6	.42	4.38	2.0393	1.85845	103.93

Figure 16: Relative gene expression of DNMT1 in colon of C57BL/6J male mice. All gene expression data are relative to CD and normalized to the housekeeping gene GAPDH. Error bar represents a 95% confidence interval. (Stars indicate significances: *p-value ≤ 0.05, **p-value ≤ 0.01, ***p-value ≤ 0.001) (CD= control diet, HFD= high fat diet, Q= equol)

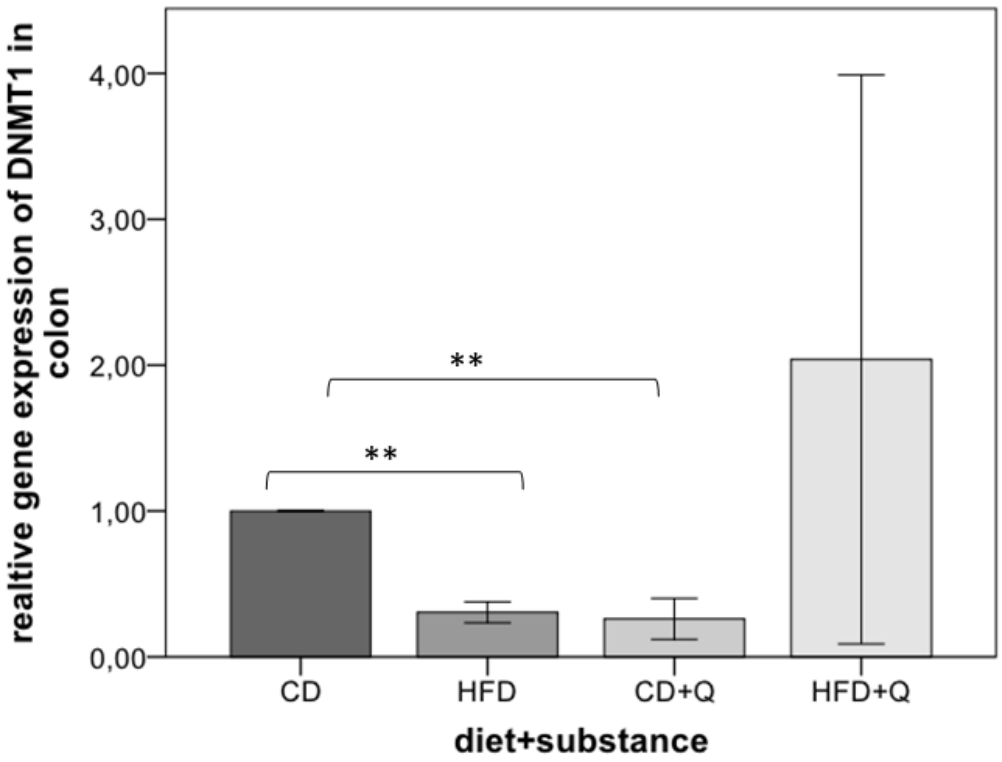

Figure 17: Relative gene expression of DNMT1 in liver of C57BL/6J male mice. All gene expression data are relative to CD and normalized to the housekeeping gene GAPDH. Error bar represents a 95% confidence interval. (Stars indicate significances: *p-value ≤ 0.05, **p-value ≤ 0.01, ***p-value ≤ 0.001) (CD= control diet, HFD= high fat diet, Q= equol)

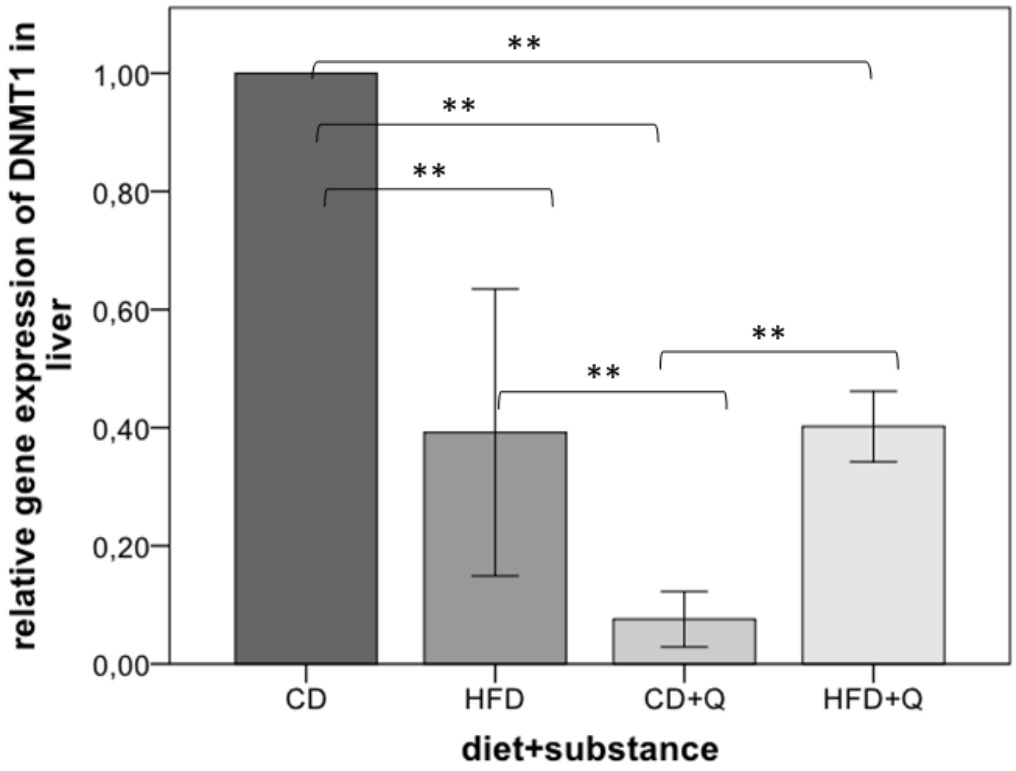

9.1.2. MLH1

In liver MLH1 is significant reduced in CD+Q and HFD+Q (p = 0,000) compared to the CD. Between the diets with equol intervention there is a higher expression in HFD+Q (p = 0,002) than in CD+Q, the expression also is higher between the HFD and HFD+Q (p = 0,002). In colon MLH1 tends to be higher in the equol supplemented diets but that is not significant.

Table 12: Relative gene expression of MLH1 in CD+Equol intervention standardized to CD

Gene	N	Minimum	Maximum	Mean	Standard deviation	%-change of Relative expression standardized to CD
MLH1_liver	6	.27	.42	.3597	.07271	-64.03
MLH1_colon	6	.70	2.44	1.6337	.78418	63.37

Table 13: Relative gene expression of MLH1 in HFD+Equol intervention standardized to CD

Gene	N	Mini-mum	Maxi-mum	Mean	Standard de-viation	%-change of Relative ex-pression standardized to CD
MLH1_liver	6	.70	.88	.7633	.08691	-23.67
MLH1_co-lon	6	.87	2.20	1.6097	.60945	60.97

Figure 18: relative gene expression of MLH1 in colon of C57BL/6J male mice. All gene expression data are relative to CD and normalized to the housekeeping gene GAPDH. Error bar represents a 95% confidence interval. (Stars indicate significances: *p-value ≤ 0.05, **p-value ≤ 0.01, ***p-value ≤ 0.001) (CD= control diet, HFD= high fat diet, Q= equol)

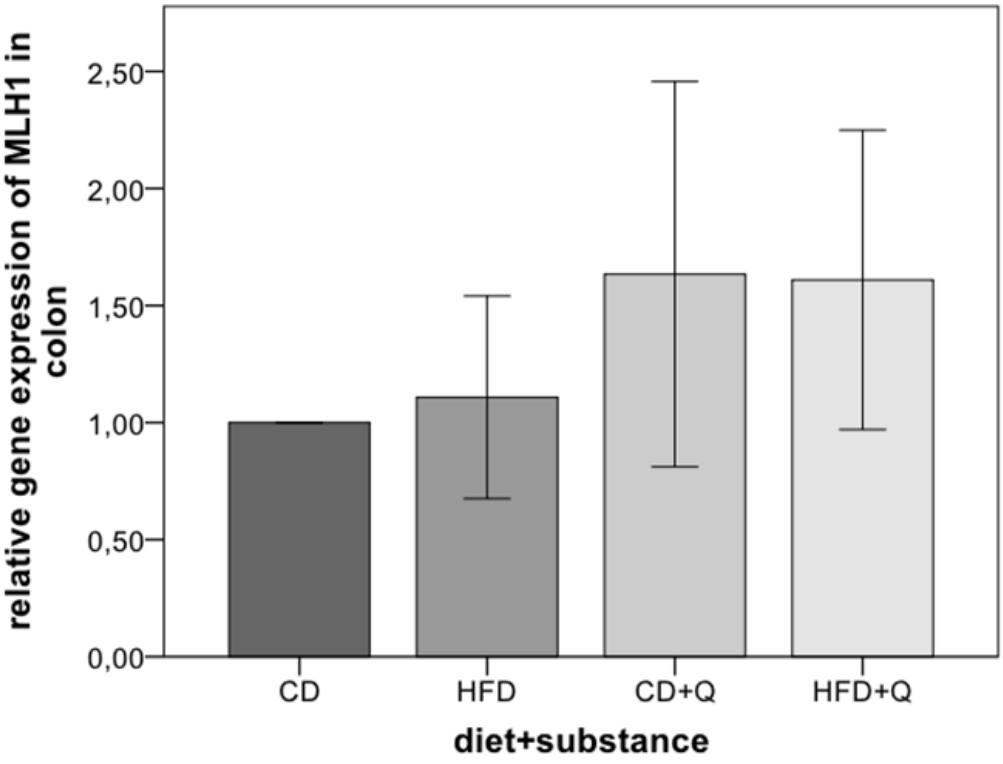

Figure 19: relative gene expression of MLH1 in liver of C57BL/6J male mice. All gene expression data are relative to CD and normalized to the housekeeping gene GAPDH. Error bar represents a 95% confidence interval. (Stars indicate significances: *p-value ≤ 0.05, **p-value ≤ 0.01, ***p-value ≤ 0.001) (CD= control diet, HFD= high fat diet, Q= equol)

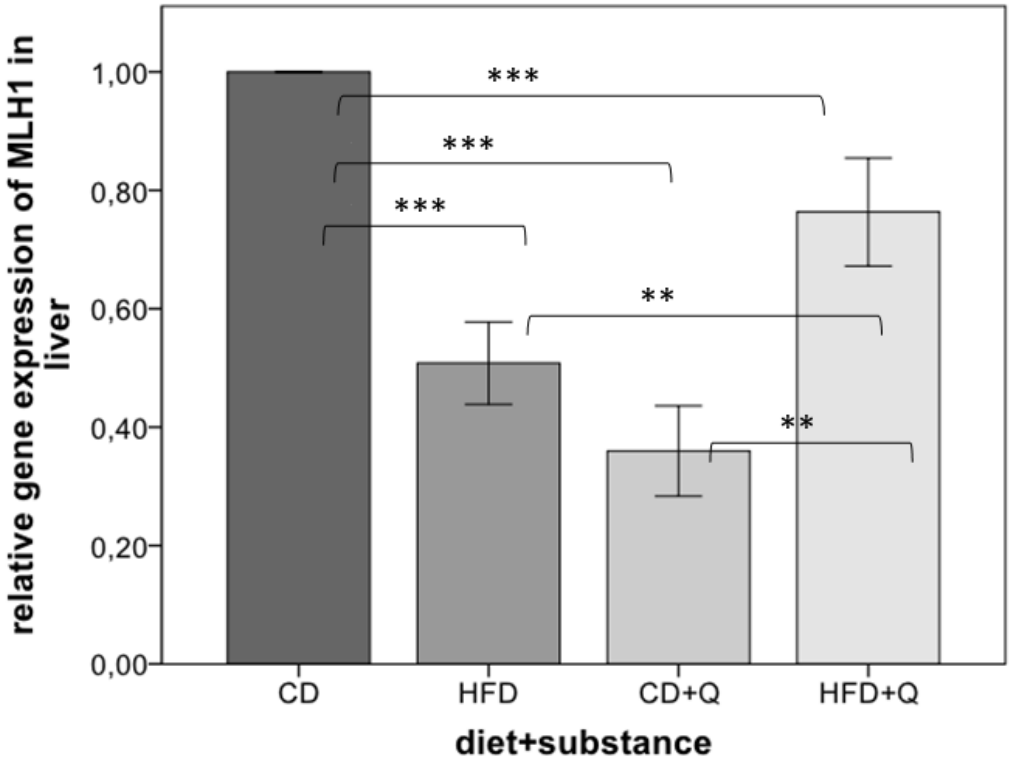

9.1.3. IL-6

There is a significant lower expression between CD and HFD (p = 0,000) and CD and HFD+Q (p = 0,000) in colon. In liver the measured values had been under the detection limit, thus no further measurements were done.

Table 14: Relative gene expression of IL-6 in CD+Equol intervention standardized to CD

Gene	N	Minimum	Maximum	Mean	Standard deviation	%-change of Relative expression standardized to CD
IL-6_colon	14	.05	4.18	.7740	1.45880	-22.60

Table 15: Relative gene expression of IL-6 in HFD+Equol intervention standardized to CD

Gene	N	Mini-mum	Maxi-mum	Mean	Standard de-viation	%-change of Relative ex-pression standardized to CD
IL-6_colon	14	.21	.52	.3321	.10089	-66.79

Figure 20: relative gene expression of IL-6 in colon of C57BL/6J male mice. All gene expression data are relative to CD and normalized to the housekeeping gene GAPDH. Error bar represents a 95% confidence interval. (Stars indicate significances: *p-value ≤ 0.05, **p-value ≤ 0.01, ***p-value ≤ 0.001) (CD= control diet, HFD= high fat diet, Q= equol)

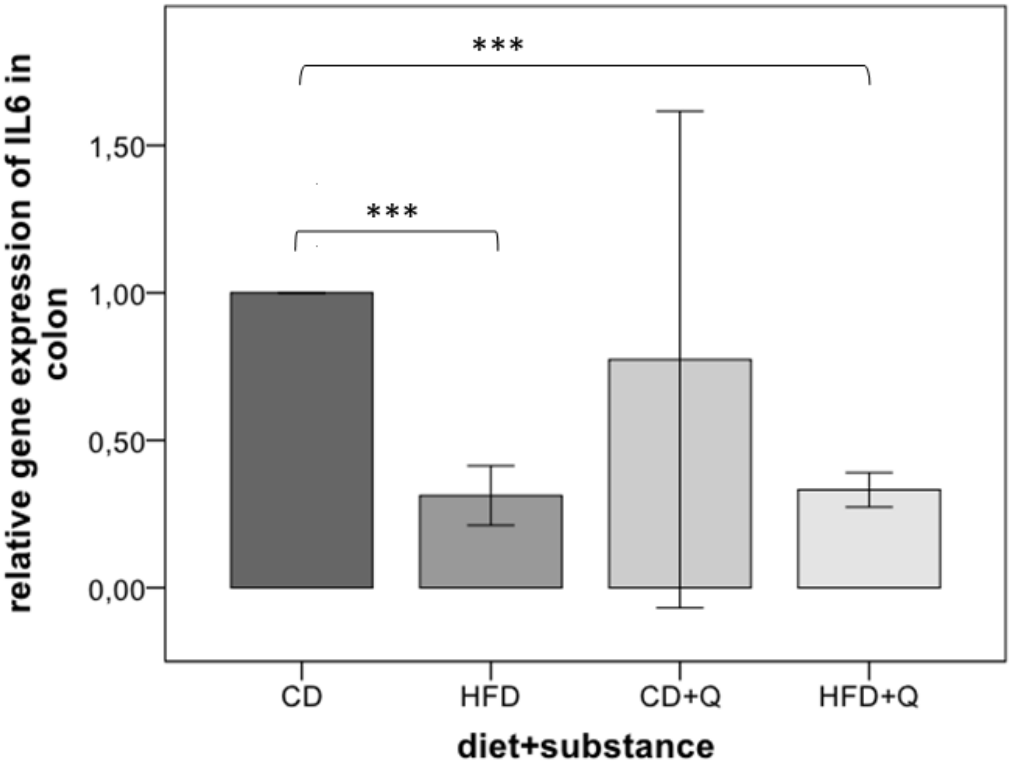

9.2. Methylation

DNA methylation of single CpGs was analyzed by pyrosequencing.

9.2.1. DNMT1

DNMT1 in liver shows at CpG 1 and 3 the most significant difference with higher methylation of HFD+Q compared to HFD at CpG1 (p = 0,026) and at CpG 3 higher methylation in HFD+Q compared to CD (p-value = 0,002) and CD+Q (p-value = 0,002). DNMT1 in colon did not show any significant methylation, it tends to be higher in CpG 1 and 2.

Table 16: Methylation of DNMT1 in liver standardized to CD - all CpGs

DNMT1 in liver - all CpGs				
Control diet + equol				
	CpG1	**CpG2**	**CpG3**	**CpG4**
N	6	6	6	6
Mean	1.3900	.8433	1.2067	.8933
Median	1.4100	.8500	1.2200	.8400
Standard deviation	.26877	.09852	.19704	.09048
Minimum	1.08	.73	.98	.83
Maximum	1.68	.95	1.42	1.01
%-change of methylation standardized to CD	39.00	-15.67	20.67	-10.67
p-value	0.026	0.589	0.132	0.818
High fat diet + equol				
	CpG1	**CpG2**	**CpG3**	**CpG4**
N	6	6	6	6
Mean	1.2467	.8200	1.4967	1.1267
Median	1.2500	.8000	1.5000	1.0400
Standard deviation	.07607	.14394	.02251	.32017

Minimum	1.16	.67	1.47	.82
Maximum	1.33	.99	1.52	1.52
%-change of methylation standardized to CD	24.67	-18.00	49.67	12.67
p-value	0.394	0.818	0.002	0.394

Table 17: Methylation of DNMT1 in colon - all CpGs

DNMT1 in colon - all CpGs				
Control diet + equol				
	CpG1	**CpG2**	**CpG3**	**CpG4**
N	6	6	6	6
Mean	1.2333	1.1867	.9933	1.1233
Median	1.3600	1.2500	.9400	.9100
Standard deviation	.26067	.37442	.08262	.41860
Minimum	.90	.74	.94	.80
Maximum	1.44	1.57	1.10	1.66
%-change of methylation standardized to CD	23.33	18.67	-0.67	12.33
p-value	0.132	0.818	0.818	0.818
High fat diet + equol				
	CpG1	**CpG2**	**CpG3**	**CpG4**
N	6	6	6	6
Mean	1.0033	1.1500	.9467	1.0833
Median	.9700	1.1400	.9100	1.1000
Standard deviation	.14542	.02366	.12404	.09480
Minimum	.86	1.13	.83	.97
Maximum	1.18	1.18	1.10	1.18
%-change of methylation standardized to CD	0.33	15.00	-5.33	8.33

p-value	0.818	0.394	0.394	0.818

Figure 21: relative CpG methylation status in promoter region of DNMT1 in colon of C57BL/6J male mice. Mean methylation data are shown relative to control diet. Error bar represents a 95% confidence interval. (Stars indicates significance: *p-value ≤ 0.05, **p-value ≤ 0.01, ***p-value ≤ 0.001) (CD= control diet, HFD= high fat diet, Q= equol**)**

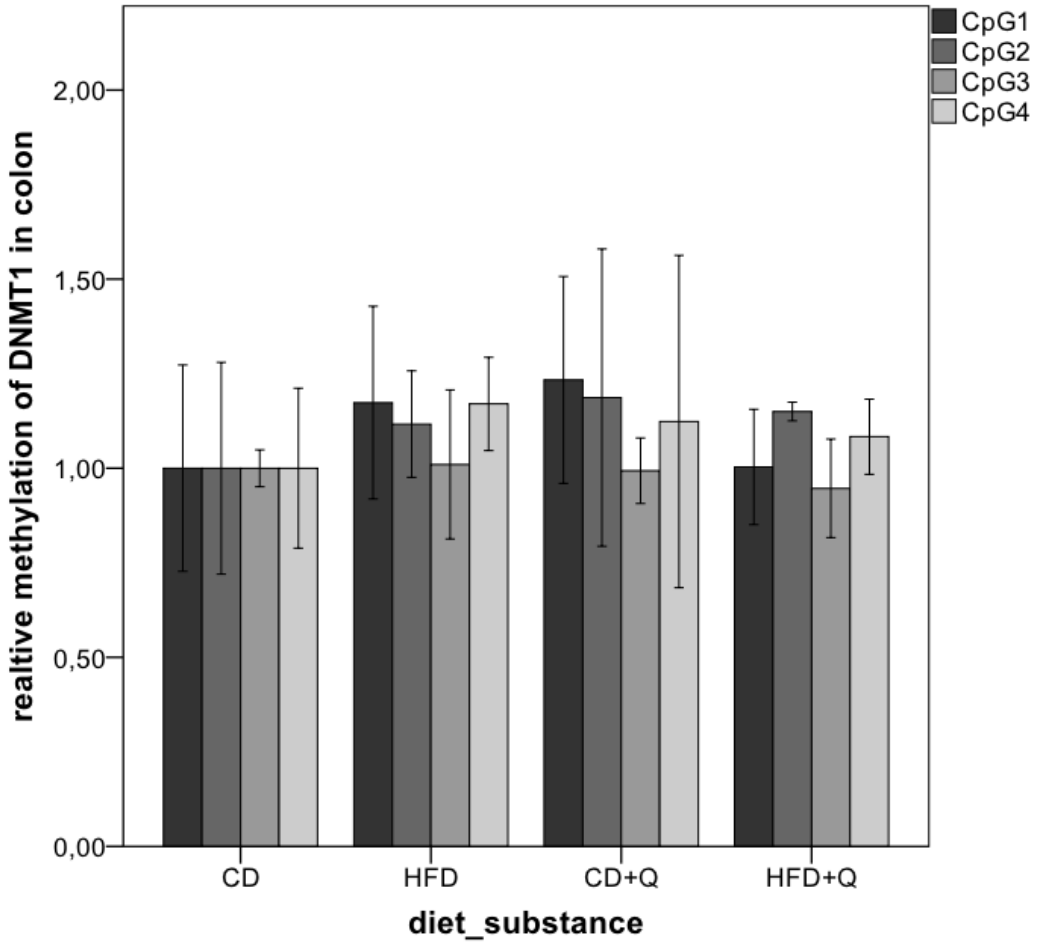

Figure 22: relative CpG methylation status in promoter region of DNMT1 in liver of C57BL/6J male mice. Mean methylation data are shown relative to control diet. Error bar represents a 95% confidence interval. (Stars indicates significance: *p-value ≤ 0.05, **p-value ≤ 0.01, ***p-value ≤ 0.001) (CD= control diet, HFD= high fat diet, Q= equol**)**

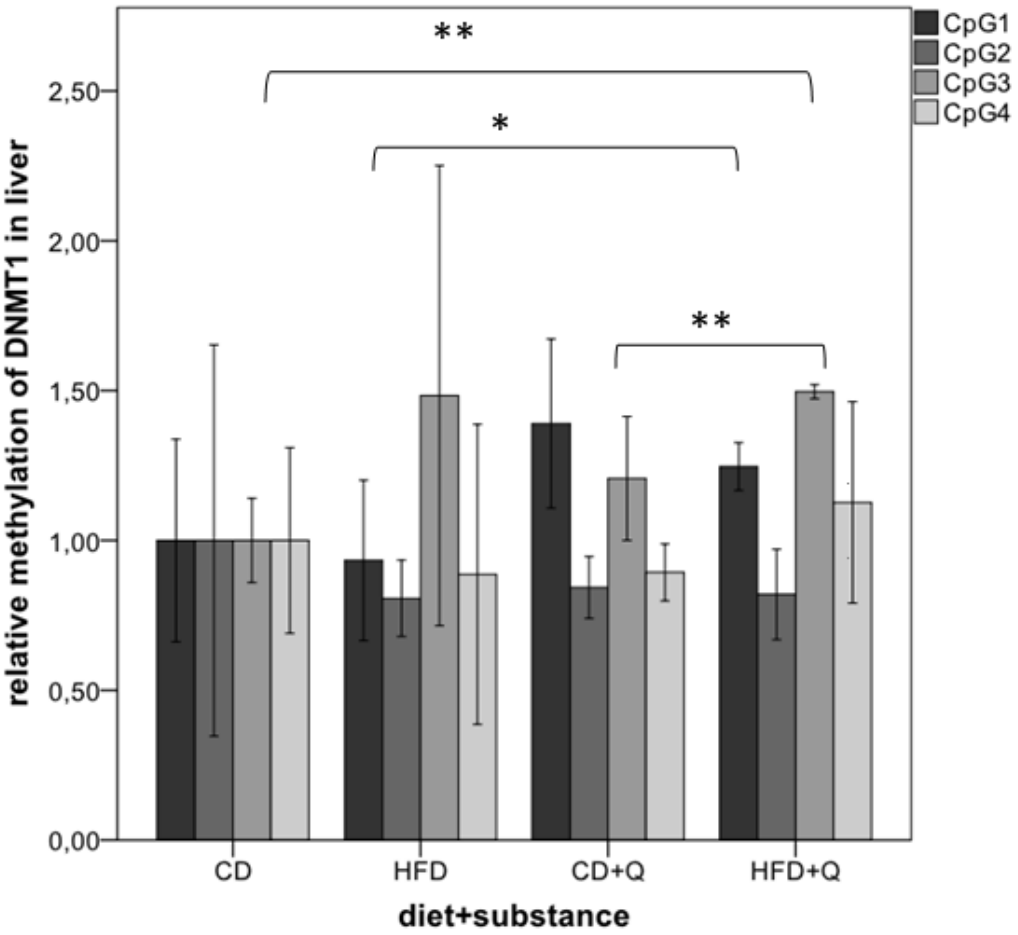

9.2.2. MLH1

MLH1 shows significant differences in methylation patterns in CpG 1, 2 and 3. In liver MLH1 is lower methylated at CpG1 in HFD (p-value = 0,002) and CD+Q (p-value = 0,026) compared to CD. At CpG2 and 3 CD+Q is significant lower than HFD+Q (p-value = 0,002).

In colon MLH1 is lower methylated in HFD (p-value = 0,002) and CD+Q (p-value = 0,002) at CpG2 compared to CD. At CpG4 HFD is significantly higher than CD (p-value = 0,002).

The methylation status was not well detectable at the CpGs 5 and 6, thus they are not included in this work.

Table 18: Methylation of MLH1 - all CpGs

MLH1 in liver – all CpGs						
Control diet + equol						
	CpG1	**CpG2**	**CpG3**	**CpG4**	**CpG5**	**CpG6**
N	6	6	6	6	6	6
Mean	.4740	1.5480	.5820	.9530	.9767	1.6770
Median	.2780	1.3980	.5460	.8610	.8510	1.6620
Standard de-viation	.31533	.24017	.22889	.16147	.25417	.61503
Minimum	.26	1.39	.35	.84	.78	1.00
Maximum	.88	1.86	.85	1.16	1.30	2.37
%-change of methylation standardized to CD	-52.6	54.80	-41.80	-4.70	-2.33	67.70
p-value	0.026	0.132	0.132	0.818	0.818	0.132
High fat diet + equol						
	CpG1	**CpG2**	**CpG3**	**CpG4**	**CpG5**	**CpG6**
N	6	6	6	6	6	6
Mean	.3250	1.1183	1.4527	1.0083	1.1957	1.4833

Median	.3070	1.0760	1.2310	1.0040	1.4880	1.8550
Standard deviation	.04175	.11866	.51387	.12035	.51448	.62284
Minimum	.29	1.01	1.02	.88	.53	.68
Maximum	.38	1.27	2.11	1.15	1.57	1.92
%-change of methylation standardized to CD	-67.50	11.83	45.27	0.83	19.57	48.33
p-value	0.002	0.818	0.394	0.818	0.394	0.132

Table 19: Methylation of MLH1 in colon - all CpGs

MLH1 in colon – all CpGs						
Control diet + equol						
	CpG1	**CpG2**	**CpG3**	**CpG4**	**CpG5**	**CpG6**
N	6	6	6	6	6	6
Mean	.4970	.3833	1.2873	.7770	.6977	.5903
Median	.5210	.4040	1.3290	.3790	.5480	.6090
Standard deviation	.13456	.04083	.15063	.65964	.31088	.19909
Minimum	.34	.33	1.10	.32	.45	.36
Maximum	.63	.42	1.43	1.63	1.10	.80
%-change of methylation standardized to CD	-50.30	-61.67	28.73	-22.30	-30.32	-40.97
p-value	0.002	0.002	0.026	0.394	0.132	0.132
High fat diet + equol						
	CpG1	**CpG2**	**CpG3**	**CpG4**	**CpG5**	**CpG6**
N	6	6	6	6	6	6
Mean	.4993	.5587	1.4350	.4950	.9830	.9037
Median	.5220	.6490	1.4110	.4900	1.1510	.8340

Standard deviation	.14773	.17104	.58346	.09176	.36561	.20102
Minimum	.32	.34	.80	.40	.52	.72
Maximum	.65	.69	2.10	.60	1.28	1.16
%-change of methylation standardized to CD	-50.07	-44.13	43.50	-50.50	-1.70	-9.63
p-value	0.026	0.002	0.132	0.002	0.394	0.818

Figure 23: relative CpG methylation status in promoter region of MLH1 in colon of C57BL/6J male mice. Mean methylation data are shown relative to control diet. Error bar represents a 95% confidence interval. (Stars indicates significance: *p-value ≤ 0.05, **p-value ≤ 0.01, ***p-value ≤ 0.001) (CD= control diet, HFD= high fat diet, Q= equol**)**

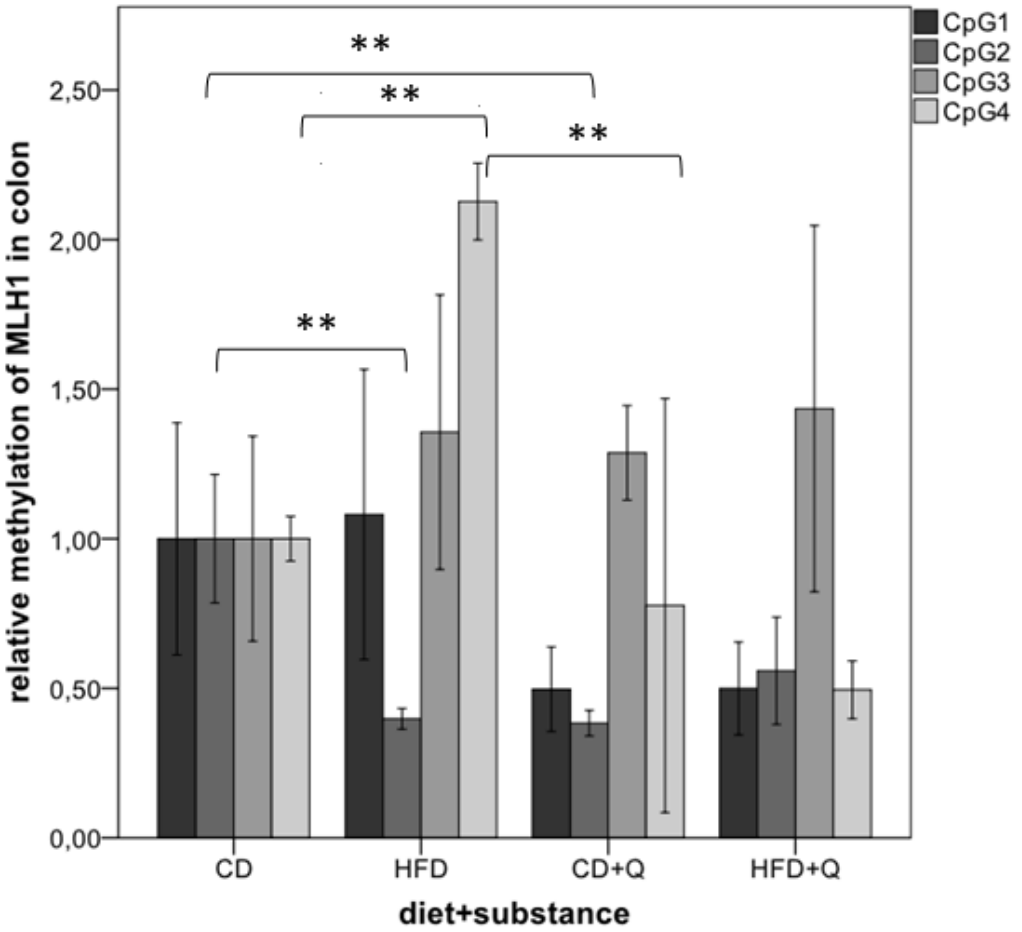

Figure 24: relative CpG methylation status in promoter region of MLH1 in liver of C57BL/6J male mice. Mean methylation data are shown relative to control diet. Error bar represents a 95% confidence interval. (Stars indicates significance: *p-value ≤ 0.05, **p-value ≤ 0.01, ***p-value ≤ 0.001) (CD= control diet, HFD= high fat diet, Q= equol**)**

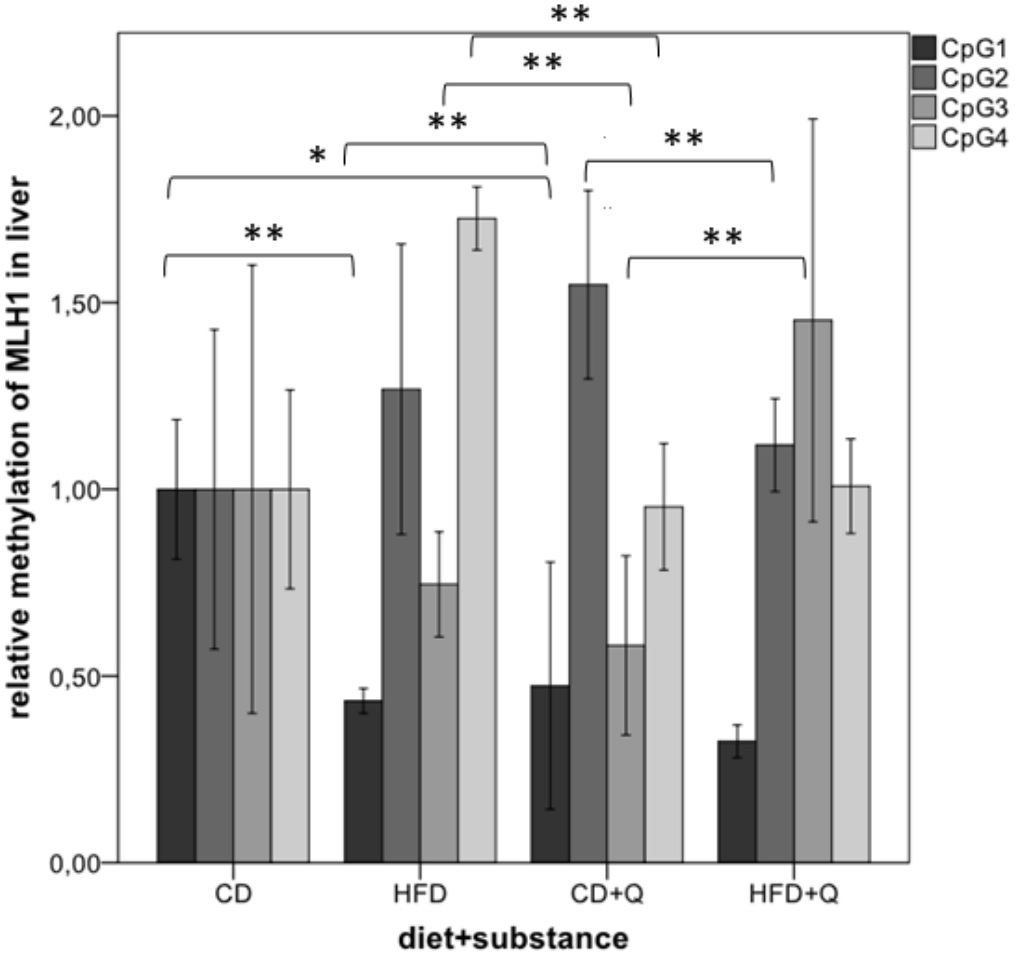

Figure 25: CpG methylation status at CpG2 of MLH11 in colon of C57BL/6J male mice. Mean methylation data are shown relative to control diet. Error bar represents a 95% confidence interval. (Stars indicates significance: *p-value ≤ 0.05, **p-value ≤ 0.01, ***p-value ≤ 0.001) (CD= control diet, HFD= high fat diet, Q= equol**)**

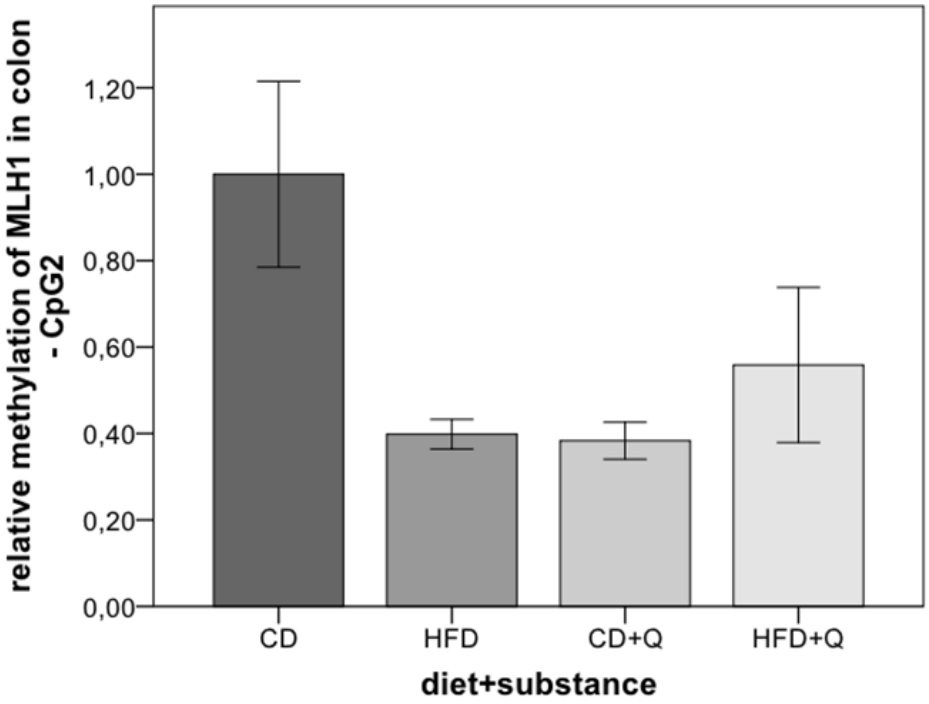

Table 20: Methylation of MLH1 in colon - CpG2

MLH1 in colon – CpG2

	CpG2
N	6
Mean	.3833
Median	.4040
Standard deviation	.04083
Minimum	.33
Maximum	.42
%-change of methylation standardized to CD	-61.67

10. Discussion

Obesity and the resulting formation of ROS is more and more assumed to have an influence on the genome and on epigenetic modifications. The underlying mechanisms are still unclear but it is suggested that inflammation and oxidative stress are playing a major role in its genesis and that antioxidants have a positive influence on the inhibition of inflammation via quenching ROS. Changes in the expression have an impact on the methylation patterns and vice versa. An elevated activity of IL-6 may be able to induce epigenetic gene silencing due to changes of DNMT1 expression patterns what may lead to a disruption of epigenetic programming (Hodge et at, 2005).

DNA methylation is mediated by DNMT1 and its expression is higher in adipocytes of obese patients. In obese mice a suppression of DNMT1 activity induced a stimulation of adiponectin expression and therefore inflammatory response and insulin sensitivity were increased (Kim et al, 2015).
In this study the expression of DNMT1 in colon was higher in HFD+Q mice than in the other groups. The methylation status of DNMT1 in colon didn't show any significance, but it tends to be higher in HFD and CD+Q compared to CD, in HFD+Q it's a bit inconsistent, at two CpGs its higher and at the other two a little bit lower. The higher expression of HFD+Q could be explained through the positive effect of equol on inflammation. Because equol acts as a radical scavenger due to its ability of donating hydrogen/electron through hydroxyl groups as well as the nonplanar structure of equol, which is important for its flexibility for conformational changes which facilitates the penetration into the interior of the membrane and therefor preventing protein or lipid structures of oxidative damage. Furthermore, equol has the skill to enhance the bioavailability of NO via downregulation of O_2-• production because of a reduced NOX activity thus helps to prevent LDL modification to an atherogenic particle (Yuan, Wang & Liu, 2007) (Hwang et al, 2003). The lower expression of the other groups could be deriving from the fact that the non-obese mice did not have any inflammation and therefore they did not use higher levels of DNMT1. In contrast the HFD fed mice without equol

also showed a lower expression and therefore the non-existence of equol could be the reason for this low expression level. Whereas in the liver the expression of DNMT1 were in all groups lower compared to CD.

MLH1 is part of the mismatch repair system and therefore very important for genome and DNA stability and integrity.
In colon the expression was not significant but it tends to be higher in all groups whereas in liver it was significant lower in all groups compared to CD. The methylation status shows similar results, in colon MLH1 was higher in HFD but degraded in CD+Q and HFD+Q compared to CD. In liver HFD and CD+Q showed lower methylation than CD and the methylation status in HFD+Q increased.
These results of a higher expression in colon maybe derived from a major need of repair systems in inflamed tissues what is caused by high fat intake and obesity. Equol could have a positive impact on the expression of MLH1 because CD+Q showed also a higher expression. Relating to the methylation status there is evidence that equol lowers the methylation compared to CD and HFD and there is evidence that a hypermethylation of MLH1 goes along with a complete loss of protein expression what may lead to colorectal carcinomas (Harfe & Jinks-Robertson, 2000).
In liver MLH1 was in all groups lower expressed compared to CD, but it was higher expressed in HFD+Q than in CD+Q as well as in HFD. What also supports the hypothesis of the positive effect of equol on repair mechanisms. Although the methylation patterns showed an increase in HFD and HFD+Q and a decrease in CD+Q.
There is evidence that under folate administration the DNA strand breaks and methylation status are connected in non-insulin dependent diabetes mellitus type 2 patients without affecting gene expression. Therefor antioxidants with their ability of ROS scavenging may alter DNA repair or reduce activity of DNA demethylating enzymes (Switzeny et al, 2012). The results in this thesis supports the hypothesis of induced DNA repair under equol mediation.

According to a study of McGarvey (2006) which indicated histone modifications, histone H3 lysine 9 (H3K9) and lysine 27 (H3K27) trimethylation and H3K9 dimethylation (H3K9me2), tend to be associated with MLH1 promoter hypermethylation. What lead to an absence of histone modifications in MLH1 hypomethylation status and a fully expression in euchromatic state (McGarvey et al, 2006). A Histone H3 lysine 9 (H3K9) silencing in MLH1 gene promoter and repressed expression in A549 cells due to chromate exposure and increased oxidative stress was seen in another study (Sun et al, 2009).
In this study there seems to be a higher expression and lower methylation status in colon what could be explained by that mechanism but these modifications may not directly affect MLH1 expression although could be a hint to epigenetic control of DNA methylation and gene expression.

IL-6 is involved in inflammatory processes, it modulates the growth of many tumor cells which is the result of abnormal IL-6 gene expression which has been associated with inflammatory disorders and ageing discomforts. A possible way to downregulate IL-6 expressions are hormones through endocrinological feedback mechanisms and antioxidants.
In this study IL-6 was not well detectable, that is why there are only results from colon, but these are as well inconsistent. According to Yeh et al (2016) a higher ERα expression decreased IL-6 in cancer associated fibroblasts and regulated macrophages activity to reduce secretion of IL-6 (Yeh et al, 2016). Equol has the ability to bind to ERα which could eventually change this process and maybe that is the reason for our vague IL-6 results.

Relating to the paper of Schroder, Pelch & Nagel (2009) estrogen is able to downregulate expression of GAPDH because it is playing a role in gene expression and cell proliferation. ERα and ERβ are connected with estrogen receptor elements and are situated in the promoter region regulating transcription (Schroder, Pelch & Nagel, 2009). With that background in combination with the knowledge of equol's estrogenic effect we hypothesized that GAPDH will fail as housekeeping gene. But with our results we can reject this hypothesis of GAPDH and that

equol doesn’t interfere with it. In this study there was no significant change in expression levels of GAPDH, Rpl13a and Beta actin.

11. Conclusion

Dietary induced obesity alters inflammation status which is related to metabolic diseases in combination with obesity and also may be able to induce epigenetic gene silencing.

Consolidated there is evidence that equol may have an influence on gene expression and methylation of obese mice especially in colon. The reason for the different results in colon and liver may be due to a different metabolism, the enterohepatic pathway and also the colonization of gut bacteria, but for better understanding more researches in this direction have to be undertaken. Just as well important is a better understanding in the metabolism of equol related to depletion and its estrogenic effect on liver or/and colon metabolism.

12. References

Abete I.; Goyeneche, E.; Zulet M. A.; Martinez J. A.; (2011), “Obesity and metabolic syndrome: Potential benefit from specific nutritional components”

Anderson Olivia S., Sant Karilyn E. and Dolinoy Dana C.; (2012); “Nutrition and epigenetics: An interplay of dietary methyl donors, one-carbon metabolism and DNA methylation”; Journal of Nutritional Biochemistry; Volume 23; Pages 853-859

Brown Nadine M., Galandi Stephanie L., Summer Suzanne S., Zhao Xueheng, Heubi James E., King Eileen C. and Setchell Kenneth D.R.; (2014); “S-(−)equol production is developmentally regulated and related to early diet com-position”; Volume 34; Pages 401-409

Chang Yeop Han, Tomio Umemoto, Mohamed Omer, Laura J. Den Hartigh, Tsuyoshi Chiba, Renee LeBoeuf, Carolyn L. Buller,¶ Ian R. Sweet, Subramaniam Pennathur, E. Dale Abel and Alan Chait; (2012) “NADPH Oxidase-derived Reactive Oxygen Species Increases Expression of Monocyte Chemo-tactic Factor Genes in Cultured Adipocytes”

Dijsselbloem Nathalie, Vanden Berghe Wim, Naeyer An De and Haegeman Guy; (2004); “Soy isoflavone phyto-pharmaceuticals in interleukin-6 affections Multipurpose nutraceuticals at the crossroad of hormone replacement, anti-cancer and anti-inflammatory therapy”; Biochemical Pharmacology; Volume: 68; Pages: 1171-1185

Eriksson Minna, Taskinen Minna and Leppä Sirpa; (2006); “Mitogen Activated Protein Kinase-Dependent Activation of c-Jun and c-Fos is required for Neu-ronal differentiation but not for Growth and Stress Reposne in PC12 cells”; Journal of cellular physiology; Volume 207; Pages 12-22

Franks Paul W. and Ling Charlotte; (2010); “Epigenetics and obesity: the devil is in the details”; BMC Medicine;

Fukui Kenji; (2010); “DNA Mismatch Repair in Eukaryotes and Bacteria”; Journal of Nucleic Acids; Volume 2010, Article ID 260512

Gordon Siamon; (2003) “Alternative activation of macrophages”; Nat.Rev.Immunol.; Volume 3; Pages 23-35;

Harfe Brian D and Jinks-Robertson Sue; (2000); “DNA mismatch repair and genetic instability”; Annu. Rev. Genet; Volume: 34; Pages: 359-399

He Fen-Jin and Chen Jin-Qiang; (2013); “Consumption of soybean, soy foods, soy isoflavones and breast cancer incidence: Differences between Chinese women and women in Western countries and possible mechanisms”; Volume 2; Pages 146-161

Hegde Muralidhar L, Hazra Tapas K, Mitra Sankar; (2008); “Early steps in the DNA base excision/single-strand interruption repair pathway in mammalian cells”; Cell research; Volume 18; Pages 27-47;

Hodge David R., Peng Benjamin, Cherry James C., Hurt Elaine M., Fox Ste-phen D., Kelley James A., Munroe David J. and Farrar William L.; (2005); “In-terleukin 6 supports the maintenance of p53 tumor suppressor gene promoter methylation”; Cancer Research; Volume: 65; Pages: 4673-4682;

Hodge David R., Xiao Weihua, Clausen Peter A., Heidecker Gisela, Szyf Moshe and Farrar William L.; (2001); “Interleukin-6 Regulation of the Human DNA Methyltransferase (HDNMT) Gene in Human Erythroleukemia Cells”; The journal of biology; Volume: 276; Pages: 39508-39511

Hwang J., Wang J., Morazzoni P., Hodis H. N., Sevanian A.; (2003); “The phytoestrogen equol increases nitric oxide availabil- ity by inhibiting superoxide production: An antioxidant mechanism for cell-mediated LDL modification”; Free Radic. Biol. Med.; Volume: 34; Pages: 1271–1282

Jones Peter A. and Baylin Stephen B.; (2002); “The fundamental role of epigenetic events in cancer”; Nature Reviews Genetics; Volume 3, Pages 415-428

Joy S., Siow R. C. M., Rowlands D. J., Becker M. et al.; (2006); “The isoflavone equol mediates rapid vascular relaxation-Ca2+-independent activation of endothelial nitric-oxide synthase/ Hsp90 involving ERK1/2 and Akt phosphoryla-tion in human endothelial cells”; J. Biol. Chem.; Volume: 281; Pages: 27335–27345

Link Alexander, Balaguer Francesc and Goel Ajay; (2010); “Cancer Chemoprevention by Dietary Polyphenols: Promising Role for Epigenetics”; Biochem Pharmacol.; Volume 80(12): Pages 1771–1792

Loring, Belinda, Robertson, Aileen (2014), WHO, “Obesity and inequities, Guidance for addressing inequities in overweight and obesity”

Lund Anders H, Van Lohuizen Maarten; (2004); “Epigenetics and cancer”; Genes & Dev.; Volume 18; Pages 2315-2335)

Martin-Murphy Brittany V., You Qiang, Wang Hong, De La Houssaye Becky A., Reilly Timothy P., Friedman Jacob E., Ju Cynthia; (2014); “Mice Lacking Natu-ral Killer T Cells Are More Susceptible to Metabolic Alterations following High Fat Diet Feeding”; PLoS ONE 9(1): e80949. doi:10.1371/journal.pone.0080949

McDonald Douglas R, Geha Raif S.; (2014); “Human Immunodeficiencies Resulting From Defective NF-κB Activation”; Stiehm's Immune Deficiencies; Pag-es 665-686

McGarvey, K.M., Fahrner, J.A., Greene, E., Martens, J., Jenuwein, T., Baylin, S.B., 2006. Silenced Tumor Suppressor Genes Reactivated by DNA Demethylation Do Not Return to a Fully Euchromatic Chromatin State. Cancer Res. 66

Meyer B. J., Larkin T. A., Owen A. J., Astheimer L. B. et al.; (2004); “Limited lipid-lowering effects of regular consumption of whole soybean foods”; Annu. Nutr. Metab.; Volume 48; Pages 67–78

Moore Lisa D, Le Thuc and Fan Guoping; (2013); “DNA methylation and its basic function”; Neuropsychopharmacology : official publication of the Ameri-can College of Neuropsychopharmacology; Volume 38; Pages 23-38

Ouchi Noriyuki, Parker Jennifer L., Lugus Jesse J. and Walsh Kenneth; (2011); “Adipokines in inflammation and metabolic disease”; National Institute of Health; Volume 11; Pages 85-97;

Pinent Montserrat, Espinel Alberto E., Delgado Marco Antonio, Baiges Isabel, Bladé Cinta and Arola, Lluís; (2011); “Isoflavones reduce inflammation in 3T3-L1 adipocytes”; Food Chemistry; Volume: 125; Pages: 513-520

Pradhan Mihika, Este`ve Pierre-Olivier, Chin Hang Gyeong, Samaranayke Mala, Kim Gun-Do and Pradhan Sriharsa; (2008); “CXXC Domain of Human DNMT1 Is Essential for Enzymatic Activity”; Biochemistry; Volume: 47; Pages: 10000–10009;

Rannikko A., Petas A., Raivio T., Jänne O. A.; (2006) “The effects of short-termoral phytoestrogen supple- mentation on the hypothalamic-pituitary-testicular axis in prostate cancer patients”; Prostate; Volume: 66, Pages: 1086–1091

Schroder Amy L., Pelch Katherine E. and Nagel Susan C; (2009); “Estrogen modulates expression of putative housekeeping genes in the mouse uterus”; Humana Press; Volume: 35; Pages: 211-219

Seiji Nakamura, Toshinari Takamura, Naoto Matsuzawa-Nagata, Hiroaki Takayama, Hirofumi Misu, Hiroyo Noda, Satoko Nabemoto, Seiichiro Kurita, Tsuguhito Ota, Hitoshi Ando, Ken-ichi Miyamoto and Shuichi Kaneko; (2009); “Palmitate Induces Insulin Resistance in H4IIEC3 Hepatocytes through Reac-tive Oxygen Species Produced by Mitochondria”; The Journal of Biological Chemistry;

Setchell Kenneth D R and Clerici Carlo; (2010); “Equol : History , Chemistry , and Formation”; the Journal of Nutrition; Volume 3; Pages 1355-1362

Subramaniam Dharmalingam, Thombre Ravi, Dhar Animesh and Anant Shrikant; (2014); “DNA Methyltransferases: A Novel Target for Prevention and Therapy”; Frontiers in oncology; Volume 4; Pages: 80

Sun, H., Zhou, X., Chen, H., Li, Q., Costa, M., 2009. Modulation of histone methylation and MLH1 gene silencing by hexavalent chromium. Toxicol. Appl. Pharmacol. 237, 258–66. doi:10.1016/j.taap.2009.04.008

Switzeny Olivier J, Müllner Elisabeth, Wagner Karl-Heinz, Brath Helmut, Au-müller Eva, Haslberger Alexander G.; (2012); “Vitamin and antioxidant rich diet increases MLH1 promoter DNA methylation in DMT2 subjects”; Clinical epigenetics

Takai Daiya and Jones Peter A.; (2002); “Comprehensive analysis of CpG islands in human chromosomes 21 and 22”; Proc Natl Acad Sci USA; Volume 99; Pages 3740–3745

Tammen Stephanie A., Friso Simonetta, and Choi Sang-Woon; (2013); “Epigenetics: the link between nature and nurture”; Molecular Aspects of Medicine

Tamura M., Ohnishi-Kameyama M. and Shinohara K.; (2004); “Lacto- bacillus gasseri, Effects on mouse intestinal flora enzyme activity and isoflavonoids in the caecum and plasma”; Br. J. Nutr., Volume 92; Pages: 771–776

Wellen Kathryn E. and Hotamisligil Gökhan S.; (2003); “Obesity-induced inflam-atory changes in adipose tissue”; J.Clin.Invest; Volume 112; Pages 1785-1788;

WHO, “The challenge of obesity – quick statistics”, (2008), [http://www.euro.who.int/en/health-topics/noncommunicable-diseases/obe-sity/data-and-statistics]

Yeh Chiuan-Ren, Slavin Spencer, Da Jun, Hsu Iawen, Luo Jie, Xiao Guang-Qian, Ding Jie, Chou Fu-Ju and Yeh Shuyuan; (2016); “Estrogen receptor α in cancer associated fibroblasts suppresses prostate cancer invasion via reducing CCL5, IL6 and macrophage infiltration in the tumor microenvironment.”; Molecular can-cer; Volume 15; Pages 7

Yuan Jian Ping, Wang Jiang Hai and Liu Xin; (2007); “Metabolism of dietary soy isoflavones to equol by human intestinal microflora - Implications for health”; Mo-lecular Nutrition and Food Research; Volume 51; Pages 765-781

Zhang Lin, Hou Dongxia, Chen Xi, Li Donghai, Zhu Lingyun, Zhang Yuijing, Li Jing, Bian Zhen, Liang Xiangying, Cai Xing, Yin Yuan, Wang Cheng, Zhang Tianfu, Dihan; (2011); “Exogenous plant MIR168a specifically targets mammalian LDLRAP1: evidence of cross-kingdom regulation by microRNA”; Cell Res.; Vol-ume 22(1); Pages 107–126

Zubik, L., Meydani, M.; (2003); “Bioavailability of soybean isofla- vones from agly-cone and glucoside forms in American women”; Am. J. Clin. Nutr.; Volume: 77; Pages 1459–1465

13. Appendix

13.1. AllPrep DNA/RNA/miRNA Kit Handbook

13.1.1. Adjusted protocol for tissue

Disruption and homogenisation

1. Maximum amount of 20 mg tissue stabilized in RNAlater.
2. **10 µl β-Mercaptoethanol** must be added per 1 ml Buffer RLT Plus before use. To reduce excessive foaming, **Reagent DX** can be added to Buffer RLT Plus at a final concentration of 0.5 %. Disrupt and homogenize the tissue in **600 µl Buffer RLT Plus** together with one stainless steel Bead (5 mm diameter) with Precellys 24-Dual homogenizer (5,000 rpm, 2x30 sec).
3. Centrifuge briefly to reduce foam (15 sec at full speed).
4. Transfer the lysate to an AllPrep DNA Mini spin column placed in a 2 ml collection tube and centrifuge it for 30 sec at full speed (max. 20,000 x g)
5. Place the AllPrep DNA Mini spin column to a new collection tube and store at room temperature (15-25 °C) or at 4 °C for later DNA purification (step 27).
6. Transfer flow through from the collection tube to a 2 ml tube for RNA purification
7. For lipid rich tissue (visceral fat and brain) **continue with step 8** from RNA purifi-cation. For other tissues **continue with step 11**.

Total RNA purification

8. Lipid-rich tissue: add **150 µl chloroform** to the flow through from step 6, vortex.
9. Centrifuge at 4°C for 3 min. at full speed to separate the phases.
10. Transfer the aqueous phase to a 2 ml tube.
11. Add **80 µl Proteinase K** to the flow-through from step 6 or the aqueous phase from step 3 lipid-rich RNA purification. Mix by pipetting
12. Add **350 µl 96 % ethanol** and mix well. Do not centrifuge! Mix by pipetting.
13. Incubate at room temperature for 10 minutes.
14. Add **750 µl 96 % ethanol** and mix well. Do not centrifuge!

15. Transfer **up to 700 µl** to RNeasy Mini spin column placed in a 2 ml collection tube and centrifuge. Discard the flow-through, reuse collection tube.
16. Repeat step 15 until the entire samples has passed through the RNeasy Mini spin column, reuse collection tube.
17. Add **500 µl Buffer RPE** to RNeasy Mini spin column. Centrifuge at full speed for 15 sec. Discard the flow-through, reuse collection tube.
18. Add **10 µl DNase I stock solution** to **70 µl Buffer RDD**. Mix by snipping fingers and centrifuge short.

- prepare DNase I Mix for numbers of samples + 1 surplus

19. Add **DNase I Mix (80 µl)** on RNeasy Mini spin column and place on the benchtop (20–30 °C) for 15 minutes.
20. Add **500 µl Buffer FRN** to RNeasy Mini spin column and centrifuge at full speed for 15 sec. **Save the flow-through!**
21. Place RNeasy Mini spin column in a new collection tube. **Apply the flow-through** from step 20 and centrifuge for 15 sec at full speed. Discard flow-through, reuse collection tube.
22. Add **500 µl Buffer RPE** to the RNeasy Mini spin column and centrifuge for 15 sec at full speed. Discard the flow-through, reuse collection tube.
23. Add **500 µl 96 % ethanol** to the RNeasy Mini spin column and centrifuge for 2 minutes at full speed to wash the spin column membrane.
24. Optional: centrifuge for another 2 minutes in a new collection tube. Discard the flow-through.
25. Place the RNeasy Mini spin column in a new **1.6 ml collection tube**. Add **30–50 µl RNase-free water** directly to the spin column and centrifuge for 1 minute at 10,000 rpm.
26. Repeat step 25 in the same tube and name it “UR RNA”. Aliquot 25 µl of the sam-ple and store it separately from the original sample.

Genomic DNA purification

27. Add **350 µl Buffer AW1** to AllPrep DNA Mini spin column from step 5 (9.1.1. Dis-ruption and homogenisation) and centrifuge for 15 sec at full speed. Discard the flow-through, reuse collection tube.

28. Add **20 µl Proteinase K** to **60 µl Buffer AW1**, mix gently by pipetting, and apply the mixture (80 µl) to the AllPrep DNA Mini spin column.

- prepare the mixture for numbers of samples + 1 surplus

29. Incubate for 5 minutes at room temperature.

30. Add **350 µl Buffer AW1** to the AllPrep DNA Mini spin column and centrifuge for 15 sec at max speed. Discard the flow-through, reuse collection tube.

31. Add **500 µl Buffer AW2** to the AllPrep DNA Mini spin column. Centrifuge for 2 minutes at full speed. Discard the flow-through.

32. Place the AllPrep DNA Mini spin column in a new **1.6 mL collection tube**. Add **100 µl Buffer EB** directly to spin column membrane and incubate for 1 minute at room temperature. Centrifuge for 1 minute at 10,000 rpm to elute "UR DNA". Ali-quot 25 µl of the sample and store it separately from the original.

33. Repeat step 32 in a new 1.6 ml tube and store the backup separately (DNA' = "DNA 2nd elution").

13.1.2. Adjusted protocol for whole blood

Erythrocyte lysis

1. Mix 1 volume (≥ 200 µl) of whole blood with **5 volume of Buffer EL**.

2. Incubate 10–15 minutes on ice. Mix by vortexing briefly 2 times during incubation.

3. Centrifuge at 400 x g for 10 minutes at 4°C. Discard supernatant.

4. Add **2 volume of Buffer EL** per volume of used whole blood to the cell pellet and resuspend by vortexing.

5. Centrifuge at 400 x g for 10 minutes at 4°C. Discard supernatant.

Nucleic acid purification

6. Add **350 µl Buffer RLT Plus** to pelleted leukocytes/cellular components (< 0.5 ml blood 350 µl Buffer; 0.5–1.5 ml blood 600 µl Buffer) and vortex.

7. Homogenise: 2 ml Tube, one stainless steel bead (5 mm diameter) with Precellys 24-Dual homogenizer (5,000 rpm, 2x15 sec)

8. Centrifuge briefly to reduce foam (15 sec at full speed)

9. Transfer the lysate lysate to an AllPrep DNA Mini spin column placed in a 2 ml collection tube and centrifuge at full speed for 30 sec.
10. Place the AllPrep DNA Mini spin column to a new collection tube store at room temperature (15-25 °C) or at 4 °C for later DNA purification (step 34).
11. Transfer flow-through from the collection tube to a 2 ml tube for RNA purification (put in Proteinase K before)

Total RNA purification for a volume of 200 µl whole blood

12. Add **50 µl Proteinase K** to the flow-through from step 11 and mix by pipetting
13. Add **200 µl 96 % ethanol** and mix well. Do not centrifuge!
14. Incubate at room temperature for 10 minutes.
15. Add **400 µl ethanol** and mix well. Do not centrifuge!
16. Transfer **up to 700 µl** to RNeasy Mini spin column placed in a 2 ml collection tube and centrifuge. Discard the flow-through, reuse collection tube.
17. Repeat step 16 until the entire samples has passed through the RNeasy Mini spin column, reuse collection tube.
18. Add **500 µl Buffer RPE** to RNeasy Mini spin column. Centrifuge at full speed for 15 sec. Discard the flow-through, reuse collection tube.
19. Add **10 µl DNase I stock solution** to **70 µl Buffer RDD**. Mix by snipping fingers and centrifuge short.

- prepare DNase I Mix for numbers of samples + 1 surplus

20. Add **DNase I Mix (80 µl)** on RNeasy Mini spin column and place on the benchtop (20–30 °C) for 15 minutes.
21. Add **500 µl Buffer FRN** to RNeasy Mini spin column and centrifuge at full speed for 15 sec. **Save the flow-through!**
22. Place RNeasy Mini spin column in a new collection tube. **Apply the flow-through** from step 21 and centrifuge for 15 sec at full speed. Discard flow-through, reuse collection tube.
23. Add **500 µl Buffer RPE** to the RNeasy Mini spin column and centrifuge for 15 sec at full speed. Discard the flow-through, reuse collection tube.
24. Add **500 µl 96 % ethanol** to the RNeasy Mini spin column and centrifuge for 2 minutes at full speed to wash the spin column membrane.

25. Optional: centrifuge for another 2 minutes in a new collection tube. Discard the flow-through.
26. Place the RNeasy Mini spin column in a new **1.6 ml collection tube**. Add **30 µl RNase-free water** directly to the spin column and centrifuge for 1 minute at 10,000 rpm.
27. Repeat step 26 in the same tube and name it “UR RNA”. Aliquot 25 µl of the sample and store it separately from the original sample.

Genomic DNA purification

34. Add **350 µl Buffer AW1** to AllPrep DNA Mini spin column from step 10 (9.1.2. Nu-cleic acid purification) and centrifuge for 15 sec at full speed. Discard the flow-through, reuse collection tube.
35. Add **20 µl Proteinase K** to **60 µl Buffer AW1**, mix gently by pipetting, and apply the mixture (**80 µl**) to the AllPrep DNA Mini spin column.

- prepare the mixture for numbers of samples + 1 surplus

36. Incubate for 5 minutes at room temperature.
37. Add **350 µl Buffer AW**1 to the AllPrep DNA Mini spin column and centrifuge for 15 sec at max speed. Discard the flow-through, reuse collection tube.
38. Add **500 µl Buffer AW2** to the AllPrep DNA Mini spin column. Centrifuge for 2 minutes at full speed. Discard the flow-through.
39. Place the AllPrep DNA Mini spin column in a new **1.6 ml collection tube**. Add **100 µl Buffer EB** directly to spin column membrane and incubate for 1 minute at room temperature. Centrifuge for 1 minute at 10,000 rpm to elute “UR DNA”. Aliquot 25 µl of the sample and store it separately from the original.
40. Repeat step 32 in a new 1.6 ml tube and store the backup separately (DNA’ = “DNA 2nd elution”).

13.2. Adjusted EpiTect Fast Bisulfite Protocol

Things to do before starting

- add 30 ml ethanol (96–100 %) to buffer BW
- add 27 ml ethanol to buffer BD (store at 2–8 °C)

- add 310 µl RNase-free water to lyophilized carrier RNA and dissolve by vortexing. If processing fewer samples, split dissolved carrier RNA into aliquots and store at -20 °C
- calculate volume of Buffer BL and dissolved carrier RNA required for number of samples:

Number of samples	1	4	8	16	24	48
Volume of Buffer BL*	350 µl	1,4 ml	2,8 ml	5,6 ml	8,4 ml	16,8 ml
Volume of carrier RNA solution	3,5 µl	14 µl	28 µl	56 µl	84 µl	168 µl

* The volumes given contain a 10% surplus for pipetting inaccuracies.

Bisulfite DNA conversion procedure

1. Thaw DNA, make sure Bisulfite Solution is completely dissolved (if necessary, heat solution to 60 °C and vortex until precipitates are dissolved).
2. Prepare bisulfite reaction in 200 µl PCR tubes according to list below (DNA solu-tion and RNase-free water must total 20 µl). Add each component in the order listed!

Component	Volume per reaction (µl)
DNA solution (1 ng–2 µg)	Variable (maximum 20 µl)
RNase-free water	Variable
Bisulfite Solution	85
DNA Protect Buffer	35
Total volume	140

3. Mix the bisulfite reaction by pipetting. DNA Protect Buffer should turn from green to blue after addition to DNA-Bisulfite Mix!
4. Program for thermal cycler:

Step	Time	Temperature
Denaturation	5 minutes	95°C
Incubation	10–20 minutes	60°C
Denaturation	5 minutes	95°C
Incubation	10–20 minutes	60°C
Hold	Indefinite	20°C

Clean-up of bisulfite converted DNA

5. Briefly centrifuge PCR tubes and transfer to clean 1.6 ml tubes.

6. Add **310 µl** freshly prepared **Buffer BL** containing 10 µg/ml carrier RNA. Mix by vortexing and centrifuge briefly. Carrier RNA is not necessary when using > 100 ng DNA.

7. Add **250 µl ethanol** (96–100%) to each sample. Mix by pulse vortexing for 15 seconds and centrifuge briefly.

8. Place EpiTect spin columns and collection tubes in suitable rack and transfer en-tire mixture from each tube on EpiTect spin column.

9. Centrifuge at maximum speed for 1 minute. Discard flow-through, reuse col-lection tube.

10. Add **500 µl Buffer BW** and centrifuge at max. speed for 1 minute. Discard flow-through, reuse collection tube

11. Add **500 µl Buffer BD** and incubate for **15 minutes** at room temperature.

12. Centrifuge spin columns at max. speed for 1 min. Discard flow-through, reuse col-lection tube.

13. Add **500 µl Buffer BW** and centrifuge at max. speed for 1 minute. Discard flow-through, reuse collection tube.

14. Repeat step 13.

15. Add **250 µl ethanol** (96–100%) to each spin column and centrifuge for 1 mi-nute.

16. Place spin column into new 2 ml collection tubes. Centrifuge at max. speed for 1 minute to remove any residual liquid.

17. Optional: Incubate spin columns with open lids in a heating block set to 60 °C for 5 minutes to evaporate remaining liquid.
18. Place spin columns into clean 1.6 ml tubes. Add **15 µl Buffer EB** directly onto the centre of each membrane.
19. Incubate the spin columns at room temperature for 1 minute. Elute DNA by cen-trifugation for **1 minute at 12,000 rpm**
20. Store bisulfite converted DNA up to 24 hours at 2–8 °C, for longer at -20 °C

13.3. Kits and Reagents

DNA Extraction

AllPrep DNA/RNA/mi RNA kit	Qiagen, Germany (Cat. no. 80224)
RNAlater	Qiagen, Germany (Cat. no. 76106)
β-Mercaptoethanol	Merck, Germany
Na2EDTA	on stock
Isopropanol	Merck, Germany
Chloroform	VWR Chemicals, USA
Buffer EL	Qiagen, Germany (Cat. no. 79217)
5 mm stainless steel beads	Qiagen, Germany (Cat. no. 69989)
Reagent DX	Qiagen, Germany (Cat. no. 19088)

Gene expression analysis

RT2 First Strand Kit	Qiagen, Germany (Cat. no. 330404)
RT2 qPCR Primer Assay *GAPDH* mouse	Qiagen, Germany (Cat. no. PPM02946E)
RT2 qPCR Primer Assay *DNMT1* mouse	Qiagen, Germany (Cat. no. PPM03685E)
RT2 qPCR Primer Assay *MLH1* mouse	Qiagen, Germany (Cat. no. PPM04973C)

RT2 SYBR Green ROX qPCR Master Mix	Qiagen, Germany (Cat. no. 330520)

Methylation analysis

EpiTect Fast DNA Bisulfite Kit	Qiagen, Germany (Cat. no. 59826)
Primer (*DNMT1*, *MLH1*)	Biomers.net GmbH, Germany
EpiTect HRM PCR Kit	Qiagen, Germany (Cat. no. 59445)
PyroMark PCR Kit	Qiagen, Germany (Cat. no. 978703)
PyroMark Q24 Gold Reagents	Qiagen, Germany (Cat. no. 971802)
PyroMark binding buffer	Qiagen, Germany (Cat. no. 979009)
PyroMark annealing buffer	Qiagen, Germany (Cat. no. 979006
PyroMark denaturation solution	Qiagen, Germany (Cat. no. 979007)
PyroMark wash buffer	Qiagen, Germany (Cat. no. 979008)
Streptavidin-coated sepharose beads	GE Healthcare, Austria (Cat. no. 17-5113-01
peq Green	VWR Chemicals, USA
QIAmp DNA Mini Kit	Qiagen, Germany (Cat. no. 51306)

Further laboratory materials

2 ml reaction tubes	Biozym Scienfific, Germany
1.6 ml reaction tubes	Biozym Scientific, Germany
0.2 ml PCR strip tubes and caps	Applied Biosystems, United Kingdom
0.1 ml strip tubes and caps	Qiagen, Germany
96-well plates	Applied Biosystems, United Kingdom
Plastic seal	BioRad Laboratories, USA
Nuclease free water	Qiagen, Germany
Ethanol 96 %	VWR Chemicals, USA

Working Equipment

Precellys 24-Dual homogeniser	Bertin Technologies, France
Pico100	Picodrop Limited, United Kingdom
TProfessional Basic Thermocycler	Biometra, Germany

StepOnePlus	Applied Biosystems, United Kingdom
PyroMark Q24	Qiagen, Germany
PyroMark Q24 Vacuum Workstation	Qiagen, Germany

Software

StepOne Software v2.1	Applied Biosystems, United Kingdom
PyroMark Assay Design 2.0	Qiagen, Germany
PyroMark Q24	Qiagen, Germany
IBM SPSS Statistics Version 22	IBM, USA

14. Publication draft

14.1 Equol induces *DNMT1*, *MLH1* and *IL-6* gene expression and DNA methylation, reverses gut microbiota aberrancies in C57BL/6J male mice fed a high-fat diet

Remely Marlene[1a], Ferk Franziska[2b], Roth Sylvia[1c], Setayesh Tahereh[2d], Sterneder Sonja[1f], Tatjana Kepcija[1e], Rahil Noorizadeh [2g], Rebhan Irene[1h], Greunz Martina[1i], Beckmann Johanna[1j], Wagner Karl-Heinz[1k], Knasmüller Siegfried[2l], Haslberger Alexander[1*]

[1] Department of Nutritional Sciences, University Vienna, Vienna, Austria

[2] Institute of Cancer Research, Department of Medicine I, Medical University of Vienna, Vienna, Austria

[a] marlene.remely@univie.ac.at

[c] rothsylvia@gmail.com

[e] sonja.sterneder@gmail.com

[f] tatjana.kepcija@gmail.com

[h] irene.rebhan@gmx.at

[i] martina.greunz@gmx.at

j Johanna.beckmann@gmx.de

k karl-heinz.wagner@univie.ac.at

b franziska.ferk@meduniwien.ac.at

d n1249216@students.meduniwien.ac.at

g a0922767@unet.univie.ac.at

l siegfried.knasmueller@meduniwien.ac.at

[*]Althanstraße 14, 1090 Vienna, Tel 0043 4277 54997, alexander.haslberger@univie.ac.at

1. Abstract

Overweight and obesity, especially excess of visceral adipose tissue often correlated with an aberrant gut microbial composition, are associated with a chronic state of low-grade inflammation and increased oxidative stress. Both factors can alter the epigenome of an organism by affecting DNA methylation status, in turn cellular regulation of gene expression. Thus, mechanisms of antioxidative /epigenetically active substances, e.g. equol, in obesity are of great interest.

We investigated gut microbiota composition using PCR, DNA damage using SCGE assays, DNA methylation and gene expression of IL-6, DNMT1 and MLH1 with qPCR and pyrosequencing in C57BL/6J male mice fed a high fat diet or a control diet supplemented with equol (25 mg/kg body weight).

Gut microbial composition differs between dietary feeding: lower total bacterial abundance, lower microbial diversity, higher *Firmicutes/Bacteroidetes* ratio, lower abundance of *F. prausnitzii,* and *Akkermansia,* reduced incidence of *butyryl CoA: acetate CoA-transferase* gene and *butyrate kinase* gene due to high fat diet. Equol partially reversed high fat diet induced aberrancies in gut microbiota composition by improving the *Firmicutes/Bacteroidetes* ratio, *Bacteroidetes*, *F. prausnitzii* and *Lactobacilli* abundance.

High fat feeding resulted in a higher inflammatory status which in turn induced a higher DNA repair. Equol in turn decreased DNMT1 gene expression reflected by a higher methylation status in the promoter region. Either the methylation status in MLH1 promoter region decreased whereas gene expression increased.

DNA damage

According to changes in GI microbiota and their anti-inflammatory effects equol might be suggested for the potential use for the prevention or in the therapy of obesity-related and oxidative stress-induced health risks through antioxidative and epigenetic activities. However, different effects between microbial derived equol and supplementation on epigenetic/ antioxidative mechanisms need to be explored.

2. Abbrevations

BMI body mass index
CD control diet
CD+Q control diet with Equol supplementation
DGGE denaturing gradient gel electrophoresis
DNMT1 DNA methyltransferase 1
GAPDH glycerinaldehyd-3-phosphat-dehydrogenase
HAT histone acetyl transferase
HDAC1 histone deacetylase 1
HFD high fat diet
HFD+Q high fat diet with equol
IL-6 Interleukin-6
iNOS inducible nitric oxide synthase
LDL low-density lipoprotein
MCP-1 monocyte chemotactic protein-1
MLH1 MutL homologue 1
ODMA O-desmethylangolensin
PAI-1 plasminogen activator inhibitor-1
PCR polymerase chain reaction

qPCR real-time polymerase chain reaction
Rb retinoblastoma (
ROS reactive oxygen species
SCGE single cell gel electrophoresis
SD standard deviation
TNF-α tumor necrosis factor-α

3. Introduction

Obesity is associated with a positive energy balance, an abnormal increase of adipose tissue and weight gain. Genetic factors, like single nucleotide polymorphisms in related genes, the environment, social surroundings, dietary behavior, metabolism, microbiota, and physical activity have an influence on the development of obesity (WHO Consultation on Obesity., 2000). Apart from overweight and elevated levels of body mass index (BMI) the distribution of accumulated adipose tissue has a huge impact on the development of obesity associated diseases (Ness-Abramof and Apovian, n.d.). The cells of the adipose tissue, the adipocytes, generate a multitude of biologically active molecules like adipocytokines or adipokines involving plasminogen activator inhibitor-1 (PAI-1), tumor necrosis factor-α (TNF-α), resistin, leptin and adiponectin (Furukawa et al., 2004). DNA methylation is playing a major role in regulating adiponectin gene expression and adapting whole body-energy balance in obese individuals. In the promoter region of adiponectin, the R2,

DNA hypermethylation maintained by DNA methyltransferase 1 (DNMT1) stimulates the subsequent formation of heterochromatin structure to lower adiponectin gene expression in obesity (Kim et al., 2015). Interleukin-6 (IL-6) in turn is able to induce the expression and activity of DNMT1 due to epigenetic silencing and remethylation of p53, an important tumor suppressor gene and relevant in the cell cycle control and therefore it is supposed to have an effect on epigenetic mechanisms (Hodge, 2005; Hodge et al., 2001). Additionally the adipose tissues are infiltrated by a large amount of macrophages (Wellen and Hotamisligil, 2005). Adipocytes as well as macrophages release pro-inflammatory molecules which may lead to chronic low grade inflammation and therefore to insulin resistance. Reactive oxygen species (ROS) have been assumed to activate nuclear factor-κB (Nf-κB) through mediators of signal transduction pathways and lead to an expression of the monocyte chemotactic factor genes, serum amyloid A3 and monocyte chemotactic protein-1(MCP-1). The cytotoxic and genotoxic oxidative stress results in a break of DNA strands. The deamination of cytosine to uracil (unmethylated cytosine) and 5-hydroxyuracil (methylated cytosine) is the result of this process. Uracil and 5-hydroxyuracil preferentially pair with adenine during DNA replication and this induces a G:C to A:T transition mutation. Guanine is acting in the same way it oxidizes to 8-oxo-7,8 dihydroguanosine via a vast of ROS and its mismatch with adenine would give rise to G:C to T:A transversion mutation. DNA repair enzymes, e.g. MutL homologue 1 (MLH1), maintain genomic integrity against continuous assaults. However, quenching ROS with antioxidants inhibits DNA strand breaks (Han et al., 2012) and increases DNA repair enzyme activities (Olivier J Switzeny et al., 2012).

Diets rich in epigenetically active antioxidants are recommend to reduce oxidative stress, inflammation in obesity (Boqué et al., 2013). Equol [7-hydroxy-3-(49-hydroxyphenyl)-chroman], which can be also produce by gut microbiota, belongs to the family of nonsteroidal estrogens with relatively strong affinity for estrogen receptors. Because of the chiral carbon at the position C-3, equol occurs in two enantiomeric forms: R-(+)equol and S-(-)equol. S-(-)equol is produced by intestinal bacteria from daidzein in the human intestine or animals and is the natural diastereoisomer (Setchell and Clerici, 2010; J. P. Yuan et al., 2007). The beneficial properties are believed to derive from the antioxidant activity as radical scavenger (J. P. Yuan et al., 2007). Equol affects nitric oxide (NO) production or utilization and has the skill to enhance the bioavailability of NO through downregulation of O2-• production and helps to prevent low-density lipoprotein (LDL) modification to an atherogenic particle (Hwang et al., 2003). It has been also observed that equol and daidzein have the ability to invert the effects of Nf-κB signaling pathway and effects of TNF-α on Jak/stat signaling cascade. In turn may induce a down-regulation of the gene expression of several inflammatory cytokines, adhesion molecules and enzymes like inducible nitric oxide synthase (iNOS) (Pinent et al., 2011). Equol lowers the secretion of IL-6 in inflamed adipocytes (Pinent et al., 2011).

In the present study, we focused on the consequences of diet induced obesity and the effect of an antioxidant supplementation, equol, in physiologically applicable doses. Therefore we investigated the gut microbiota composition and diversity with PCR (polymerase chain reaction) to imply

gut microbial equol production, DNA damage using SCGE assays, DNA methylation with a pyrosequencer and gene expression by qPCR (real-time polymerase chain reaction) of inflammatory mediators: IL-6; DNMT1, and DNA repair: MLH1 in liver and colon of C57BL/6J mice.

4. Materials and Methods

This animal experiment was authorized by the Ethical Committee of the Medical University of Vienna (BMWFW-66.009/0329-WF/V/3b/2014). 60 C57BL/6J male mice at the age of six weeks (Janvier Labs, France) were kept under standard conditions (24 ± 1 °C, humidity 50 ± 5 %, 12 hours light/dark cycle) in plastic cages (Macrolon type III, Techniplast GmbH Germany) three per cage with free access to water and food.

After an acclimatization of 14 days fed with a control diet (CD; EF R/M Control, 12 % fat, ssniff Spezialdiäten GmbH, Soest, Germany) mice were divided into four groups: 1) CD group (EF R/M Control, 11 kJ % fat, ssniff Spezialdiäten GmbH, Soest, Germany), 2) CD with Equol group (CD+Q), 3) high-fat diet (HFD) group (54 kJ % fat ssniff EF acc.D12492 (I) mod., ssniff Spezialdiäten GmbH, Soest, Germany) and 4) a HFD with Equol group (HFD+Q). Drinking water was supplemented with 25mg/kg body weight of E-55-EQUOL® (CAS-No.: 94105-90-5, System Biologie AG). Body weights and food intake were measured weakly and water and equol were changed daily (Table 1).

4.1. Gut microbiota analysis

Before intervention and continuously after 1 month until the end of the study period stool was collected and stored at -20 °C until microbial DNA extraction by using the QIAamp® Fast DNA Mini Kit (Qiagen, Germany) following the manufacturer‘s protocol including two steps of 45 sec beadbeating at 4000 rpm with a 60 sec break in-between to increase the DNA yield. DNA concentration and purification was verified with a Pico100 (Picodrop Ltd., Cambridge UK).

The abundance of gut microbial subgroups were analyzed according to Remely et al. (2013) [26]. The diversity of gut microbiota was analyzed using denaturing gradient gel electrophoresis (DGGE) [26].

4.2. Gene expression analysis

Liver and colon samples were stored at -80 °C until RNA and DNA isolation using the AllPrep DNA/RNA/miRNA Universal Kit (Qiagen, Germany) and reverse transcripted using RT2 First Strand Kit (Qiagen, Germany) according to the manufacturer's protocol. Concentration respectively purity were verified with a Picodrop100 (Picodrop, UK). cDNA was analyzed in real-time PCR using qPCR Primer Assays (Qiagen, Germany) and RT2 SYBR Green Mastermix (Qiagen, Germany) according to manufacturer’s protocol: initial step of 95°C for 10 min, followed by 40 cycles of 95°C for 15 s and 60°C for 1 min, ending with melting curve analysis (gradient melting of the products was performed at 0.5°C/10 s from 65°C to 95°C). Each sample was analyzed in duplicate, with normalization to the housekeeping gene GAPDH (glycerinaldehyd-3-phosphat-dehydrogenase).

4.3. Methylation analysis

Genomic DNA was bisulfite converted with EpiTect® Fast Bisulfite Conversion kit (Qiagen, Germany) and amplified by PCR using the PyroMark PCR Kit (Qiagen, Germany) according to manufacturer's protocol with primers for *DNMT1* and *MLH1* designed by PyroMark Assay Design SW 2.0 Software (Table 2).

The PCR was carried out in a total reaction volume of 25.0 µL, containing 12.5 µL Pyromark 2X PCR master mix, 10 pmol (*DNMT1*) or 7 pmol (*MLH1*) of each primer, 2.5 µL Coralload Concentrate 10X (Qiagen, Germany), and 10.0 ng (*DNMT1*) or 15.0 ng (*MLH1*) bisulfite converted DNA. Thermocycling condition were as follows: initial denaturation at 95 C for 15 min, followed by 45 cycles at 94°C for 30 s, 55.5°C for 45 s, 72°C for 45 s and a final extension at 72°C for 10 min. After an agarose gel-electrophoresis CpG methylation analysis were performed in a Pyromark Q24 MDx (Qiagen, Germany).

4.4. SCGE (single cell gel electrophoresis) assay

4.5. Statistical analysis

For SCGE assays statistical analyses GraphPad Prism 5.02 (GraphPad Software, USA) was used. The means and standard deviation (SD) of % DNA in the comet tails of the nuclei from the different treatment groups were calculated. Comparisons of groups were done by student´s t-test based on the means of three slides/animal.

All statistical analyses of gut microbiota, gene expression and methylation analysis were performed using IBM SPSS Advanced Statistics 20.0 (SPSS, USA). All data are shown mean±SD. ΔCT values were normalized to GAPDH (ΔCT = CT-Target – CT-GAPDH). The ΔΔCT value shows the difference between the two groups. (ΔΔCT = ΔCT+EGCG - ΔCT-Control). Relative changes in gene expression between the intervention and control group are determined by the 2-ΔΔCT equation (fold change = 2-ΔΔCT). Normalization of the data was approved by Kolmogorov-Smirnov-Test. The Mann-Whitney-U Test was used to examine significant relationships. For all comparisons p-values ≤ 0.05 were considered as statistical significant.

5. Results

5.1. Body weight, food intake and equol uptake

According to Table 1 food intake and total water consumption did not differ between the groups (Table 1). Mean equol uptake was about 0.68 mg in the CD group and of 1.13 mg in the HFD group of each mouse per day. HFD fed mice increased significantly more body weight (T1: 30.54 ± 3.43g; T4: 45.99 ± 4,46g) as well as mice fed HFD+Q (T1: 30.49 ± 3.16 g; T4: 45.24 ± 4.10g) in comparison to CD fed mice (T1: 23.99 ± 1.50g; T4: 27.88 ± 1.49g) and CD+Q (T1: 23.83 ± 2.49g; T4: 27.29 ± 2.34g; Figure 1). The body weight increase over study period was significant in all groups ($p \leq 0.01$).

5.2. Gut microbiota composition and diversity

Differences in total bacterial abundance were shown between CD and HFD ($p \leq 0.01$) as well as between CD+Q and HFD+Q ($p \leq 0.01$) but also between HFD and HFD+Q ($p = 0.04$, Figure 2B). High-fat feeding caused a significant lower bacterial abundance in both HFD groups resulting in

a lower microbial diversity compared to CD (HFD bands= 21.4 ± 5.08, HFD+Q bands = 18.6 ± 2.51, CD bands= 20.4 ± 4.62, CD+Q bands=21.4 ± 3.58).

The *Firmicutes/Bacteroidetes* ratio is significantly higher in both HFD groups compared to CD groups ($p \leq 0.01$). Equol treatment induced a lower ratio in HFD+Q compared to HFD ($p = 0.851$, Figure 2B) and a significantly lower ratio in CD+Q compared to CD ($p \leq 0.01$). *Lactobacilli* abundance showed an increase with equol intervention. Both clostridial clusters (*Clostridium cluster IV, Clostridium cluster XIVa*) were significantly lower in HFD groups compare to CD groups ($p \leq 0.01$). *Clostridium cluster IV* significantly increased in HFD+Q compared to HFD ($p = 0.04$). *Clostidium cluster XIVa* increased in CD+Q compared to CD ($p = 0.851$) and were significantly higher abundant in comparison to HFD+Q ($p \leq 0.01$). In turn, *F. prausnitzii* is less abundant in HFD groups compared to CD groups ($p \leq 0.01$). An increasing effect on *F. prausnitzii* abundance of equol is seen in CD+Q group compared to CD, whereas HFD+Q lowers the abundance (HFD: HFD+Q $p = 0.04$; CD: CD+Q: $p= 0.574$; CD+Q: HFD+Q: $p \leq 0.01$; Figure 2C). *Bacteroidetes* were significantly lower abundant in HFD compared to CD ($p \leq 0.01$) but significantly increase in HFD with equol intervention (HFD: HFD+Q $p \leq 0.01$). An increase was shown in CD mice due to equol treatment as well ($p = 0.09$).

Akkermansia showed a lower abundance in HFD fed mice compared to CD ($p = 0.09$). Equol treatment resulted in lower abundance in CD+Q and in HFD+Q groups compared to each reference group CD and HFD ($p = 0.9$).

In HFD mice *butyryl CoA: acetate CoA-transferase* gene was significantly lower in comparison to CD mice ($p \leq 0.01$). Intervention with equol in CD group resulted in a significant decrease ($p \leq 0.01$) whereas in HFD no significant effect was seen. Results of the *butyrate kinase* gene showed similar results whereas HFD+Q group showed a significant increase (CD: CD+Q $p = 0.02$; HFD: HFD+Q $p \leq 0.01$).

5.3. Relative gene expression and DNA methylation in liver and colon cells

On the basis of some evidences in literature of biased GAPDH gene expression as house keeping gene due to equol treatment based on the estrogenic effects, we also analyzed beta actin and Rpl13a additionally (Schroder et al., 2009). No significant differences were shown between GAPDH, Rpl13a ($p = 0.238$) and beta actin ($p = 0.721$) gene expression thus further gene expression evaluations were done with GAPDH as housekeeping gene.

5.3.1. Relative gene expression and CpG methylation of DNMT1 in colon and liver cells

In colon cells the relative expression of DNMT1 in HFD is decreased compared to CD (61 %; $p \leq 0.01$). The equol supplemented group was lower expressed in CD+Q compared to CD (74 %; $p \leq 0.01$). The relative gene expression of DNMT1 in HFD+Q showed no significant difference compared to CD ($p = 0.394$) as well as HFD compared with CD+Q ($p = 0.394$, Figure 3A). Between HFD+Q and CD+Q no differences were shown. In liver, there is a significant lower gene expression of DNMT1 in all groups compared to the CD ($p \leq 0.02$, Figure 3B). DNMT1 relative gene expression in the liver is significantly lower in CD+Q than in CD (92 %; $p \leq 0.02$) and HFD

($p \leq 0.01$). The HFD+Q was lower expressed compared to CD (60 %; $p \leq 0.01$). There is no significant difference between HFD and HFD+Q ($p \leq 0.394$).

For the methylation status four different CpGs were analyzed in the promoter region of DNMT1 in colon and liver. DNMT1 in colon did not show any significant differences in methylation status between all groups (Figure 4). Whereas in liver the DNMT1 methylational status shows a significant difference at CpG 1 and 3 with a higher methylation in HFD+Q compared to HFD at CpG1 ($p \leq 0.05$) and a higher methylation at CpG 3 in HFD+Q compared to CD (50%; $p \leq 0.05$) and CD+Q ($p \leq 0.05$, Figure 4B). No significant differences at CpG1 and CpG3 were shown between CD and HFD.

5.3.2. Relative gene expression and CpG methylation of MLH1 in colon and liver cells

In colon cells no significant differences were shown between the diets related to MLH1. Only in the equol supplemented groups MLH1 tends to be higher in HFD+Q ($p = 0.153$) and CD+Q ($p = 0.274$, Figure 5A). In liver MLH1 relative gene expression is significantly reduced in CD+Q (64 %) and lower in HFD+Q (24 %; $p \leq 0.01$) compared to CD. Between the diets with equol intervention there was a higher expression in HFD+Q ($p \leq 0.01$) than in CD+Q and also between HFD and HFD+Q ($p \leq 0.01$; Figure 5B).

In case of relative methylation of MLH1 6 CpGs were investigated in the promoter region of colon and liver. MLH1 shows significant methylation patterns in CpG 1, 2 and 3. In colon there is a significant difference at CpG1 in CD compared to HFD ($p \leq 0.01$). CpG2 is lower methylated in HFD ($p \leq 0.01$) and 62 % lower in CD+Q ($p \leq 0.01$) compared to CD. HFD+Q is decreased 44 % at CpG2 ($p \leq 0.01$) and 50 % at CpG4 ($p \leq 0.01$) in contrast to CD. At CpG4 HFD is significantly higher methylated than CD ($p \leq 0.01$, Figure 6A).

In liver CpG1 of MLH1 is 53 % lower methylated in CD+Q ($p \leq 0.026$) and 68 % decreased in HFD+Q compared to CD ($p \leq 0.002$). CpG1 and CpG4 were lower methylated in HFD+Q compared to HFD ($p \leq 0.02$). At CpG2 MLH1 methylation was increased in CD+Q compared with HFD+Q ($p \leq 0.01$) whereas CpG3 was lower methylated in CD+Q than in HFD+Q ($p \leq 0.01$; (Figure 6B).

The methylation status of CpG5 and 6 were not analyzable thus they were excluded from statistical analysis.

5.3.3. Relative gene expression of IL-6 in colon and liver

There is a significant higher expression of IL-6 in HFD compared to CD ($p \leq 0.01$) and in CD compared with HFD+Q ($p \leq 0.01$) in colon (Figure 7). No differences were shown between the other groups. In liver analysis results were below the detection limit.

5.3.4. DNA damage with nuclei from colon and liver cells

Figure 8

6. Discussion

Gut microbial composition differs between CD and HFD: lower total bacterial abundance due to HFD, lower microbial diversity, higher *Firmicutes/Bacteroidetes* ratio, lower abundance of *F.*

prausnitzii, and *Akkermansia,* reduced incidence of *butyryl CoA: acetate CoA-transferase* gene and *butyrate kinase* gene*.* Additionally, we showed that HFD significantly induced inflammatory status in mice according to higher IL-6 expression status although only verifiable in colon. However, either the expression of DNA repair was higher due to HFD feeding also reflected by a lower methylation in the promoter region of MLH1. DNMT1 expression was decreased in HFD.

These research results were in line with previous published data, indicating a higher inflammatory status with at least partial responsibility on aberrant gut microbiota composition and reduced diversity (Remely et al., 2014; Tremaroli and Bäckhed, 2012). Thus, interventions with antioxidants, equol, are of interest. Due to the nonplanar structure of equol, which is important for its flexibility for conformational changes facilitating the penetration into the interior of the membrane, it prevents protein or lipid structures from oxidative damage. Equol is able to donate hydrogen/electron at the position C-4 for hydroxyl substitution (J.-P. Yuan et al., 2007) but affects also NO production or utilization through downregulation of O2-• formation and prevents LDL modification to an atherogenic particle (Hwang et al., 2003; Joy et al., 2006). Equol and daidzein also have the ability to invert the effects of NF-Kb signaling pathway and affect TNF-α on Jak/stat signaling cascade. In turn may lead to a down-regulation of gene expression of several inflammatory cytokines, adhesion molecules and enzymes like iNOS (Pinent et al., 2011).

However, only a limited number of humans are able to produce equol out of soy or rather daidzein. In comparison to animals like rodents, humans produce very low levels of equol one cause may be due to a shorter caecum and therefore less abundant microbiota. Although between humans the amount of conversion is also very diverging: In western countries only 25% to 30% of adults are able to produce equol in contrast to 50% to 60% of adults in Japan, China and Korea. One reason might be the different diets and dietary habits resulting in a altered composition of the intestinal microbiota (Yuan, Wang & Liu, 2007) (He & Chen, 2013). Three strains of bacteria are identified as equol-producer *Bacteroides ovatus* spp., the gram-positive *Strepotococcus* intermedius spp. and *Ruminococcus productus* spp.

6.1. Equol partially reversed HFD induced aberrancies in gut microbiota composition

Equol especially affected the *Firmicutes/Bacteroidetes* ratio which is almost higher due to obesity, metabolic syndrome etc. but decreased with equol supplementation, although it did not reach lean fed status. In detail *Lactobacilli* were increased in both supplemented groups. *Clostridial* cluster including *F. prausnitzii* and butyrate production were reduced abundant in HFD either detected in case of *Bacteroidetes* but improving with equol supplementation. *Akkermansia* were decreasing with equol supplementation.

The equol producer frequency is higher in vegetarians with 59% compared to non-vegetarians with 25% also represented in our study group (main part from fat contribution: lard). Suggesting that a high consumption of dietary fiber, plant proteins, less fat and higher carbohydrate intake is strongly associated with equol producers (J. P. Yuan et al., 2007). Gardana *et al*. (2009) stated the opposite: less dietary fibre and more lipids from animal origin for increasing equol production (Gardana et al., 2009). However, differences in gut microbiota induce either equol or O-

desmethylangolensin (ODMA) production from daidzein the later has lower estrogen effects as one of the phenolic rings is cleaved. Approximately 80–95% of humans harbour gut microbial communities producing ODMA whereas only 25–60% are capable in producing equol. An obese gut microbiota composition is 2.8-times more likely to result in an ODMA non-producer but no association was verifiable in case of equol production (Frankenfeld et al., 2014).

However, several metabolic compounds like fatty acids, organic acids and H_2O_2 produced by lactic acid bacteria have antimicrobial effects. *Lactobacillus gasseri* is suggested to suppress the production of equol and decreases the plasma equol concentration and the total amount of equol in the cecal content. Therefore, a high amount of lactobacilli might reduce intestinal equol production (Tamura et al, 2004) also represented in our mice: a higher *Lactobacilli* abundance due to equol supplementation might inhibit equol producing gut microbes.

6.2. Equol decreases DNMT1 expression reflected by a higher methylation status in the promoter region

HFD fed mice without equol showed the lowest expression of DNMT1 compared to CD and supplemented groups in colon. Whereas in the liver the expression of DNMT1 were in all groups lower compared to CD. The methylation status of DNMT1 in colon did not show any significance, but it tends to be higher in HFD and CD+Q compared to CD. In liver DNMT1 is lower methylated in HFD but tends to be higher in CD+Q and HFD+Q compared to CD.

The sequence [5'-TTTCCGCG-3'] within the genomic methylation analysis was identified as crucial site for the transcriptional regulation of *DNMT1* by the transcription factor E2F1 (Kimura et al., 2003; McCabe et al., 2005). DNMT1 forms a stable complex with retinoblastoma (Rb) tumor suppressor gene product, E2F1 and histone deacetylase 1 (HDAC1) preventing transcription from promoters containing E2F1-binding sites. Methylation targeting this region show implications for transcriptional control, DNA replication and tumorgenesis (Robertson et al., 2000). Our investigated site contains two CpGs, one was found to be significantly higher methylated in the HFD+Q preventing transcriptional activation of the gene also reflected by a reduced *DNMT1* expression in the liver. The methylation status is increased especially at CpG 1 and CpG 3 compared to CD and HFD. A suppression of DNMT1 activity in obese mice led to a stimulation of adiponectin expression and therefore inflammatory response and insulin sensitivity were increased (Kim et al., 2015). We also observed a higher IL-6 gene expression in the colon of HFD fed mice with no reduction due to equol supplementation. In turn obesity-induced, pro-inflammatory cytokines stimulate *DNMT1* expression and activity in adipocytes of mice (Kim et al., 2015). As we only investigated liver and colon cells we were not able to show an increase of DNMT1 gene expression in adipocytes. No effects were indicated in the expression of colon and liver in obese mice. Either induced oxidative stress was mentioned to transcriptionally up-regulate the expression of *DNMT1* in the lung of mice (Soberanes et al., 2012).

6.3. Equol decreases MLH1 promoter methylation resulting in tissue specific variances in gene expression

Equol decreased the methylation in the promoter of MLH1 either in HFD and CD in the liver but showed no significant differences in colon. Either the gene expression of MLH1 was lower in colon but higher in liver according to methylation status.

These results of a higher expression in colon maybe derive from a major need of repair systems in inflamed tissues caused by high fat intake and obesity which has been also indicated by an increased IL-6 expression in colon but not in liver. Equol could have a positive impact on the expression of MLH1 as a higher expression was shown.

Relating to the methylation status there is evidence that equol lowers the methylation compared to control groups. According to Harfe and Jinks-Roberts (2000) a hypermethylation of MLH1 implicates a complete loss of protein expression inducing colorectal carcinomas (Harfe and Jinks-Robertson, 2000). Either, Esteller et al. (2002) mentioned a MLH1 promoter hypermethylation with a promoter methylation-dependent down-regulation of the corresponding gene expression in some cancer tissues (Esteller, 2002). However, Switzeny et al. (2012) indicated a correlation between DNA strand breaks and methylation status with folate intervention in non-insulin dependent diabetes mellitus type 2 patients but no effect in gene-expression was shown. Thus, antioxidants may increase DNA repair or they may lower the activity of DNA demethylating enzymes by ROS scavenging (O J Switzeny et al., 2012). Our results suggest the hypothesis of induced DNA repair under equol interventions.

Even an inhibition of DNMTs, like equol as an inhibitor in our study, but not of histone deacetylases, results in a promoter demethylation of MLH1, to a gene reexpression and finally into a complete histone code reversal (Fahrner et al., 2002). Accordingly McGarvey (2006) indicated histone modifications, histone H3 lysine 9 (H3K9) and lysine 27 (H3K27) trimethylation and H3K9 dimethylation (H3K9me2), which tend to be associated with MLH1 promoter hypermethylation. Consequently histone modifications are absent in MLH1 hypomethylation status and fully expressed in a euchromatic state (McGarvey et al., 2006). Chromate exposure and therefore increased oxidative stress also induced H3K9me2 silencing in *MLH1* gene promoter and repressed its expression in A549 cells (Sun et al., 2009). In our study this would suggest a higher gene expression according to hypomethylation status of MLH1 promoter region as indicated in colon. However, histone modifications may not directly affect MLH1 expression but may serve as an additional epigenetic control of DNA methylation and gene expression.

7. Conclusion

Consolidated there is evidence that equol may have an influence on gene expression and methylation of DNA repair in obesity. Equol supplementation may be beneficial for persons not producing equol themselves. The reason for the different results in colon and liver may be due to different metabolisms, the enterohepatic pathway and also the colonization of gut bacteria. A more detailed analysis of equol metabolism, estrogenic effects, related to genome-wide and gene-specific changes will significantly add to our understanding of antioxidant properties.

8. References

Boqué, N., Campión, J., de la Iglesia, R., de la Garza, A.L., Milagro, F.I., San Román, B., Bañuelos, Ó., Martínez, J.A., 2013. Screening of polyphenolic plant extracts for anti-obesity properties in Wistar rats. J. Sci. Food Agric. 93, 1226–32. doi:10.1002/jsfa.5884
Esteller, M., 2002. CpG island hypermethylation and tumor suppressor genes: a booming present, a brighter future. Oncogene 21, 5427–40. doi:10.1038/sj.onc.1205600
Fahrner, J.A., Eguchi, S., Herman, J.G., Baylin, S.B., 2002. Dependence of Histone Modifications and Gene Expression on DNA Hypermethylation in Cancer. Cancer Res. 62.
Frankenfeld, C.L., Atkinson, C., Wähälä, K., Lampe, J.W., 2014. Obesity prevalence in relation to gut microbial environments capable of producing equol or O-desmethylangolensin from the isoflavone daidzein. Eur. J. Clin. Nutr. 68, 526–30. doi:10.1038/ejcn.2014.23
Furukawa, S., Fujita, T., Shimabukuro, M., Iwaki, M., Yamada, Y., Nakajima, Y., Nakayama, O., Makishima, M., Matsuda, M., Shimomura, I., 2004. Increased oxidative stress in obesity and its impact on metabolic syndrome. J. Clin. Invest. 114, 1752–1761. doi:10.1172/JCI200421625
Gardana, C., Canzi, E., Simonetti, P., 2009. The role of diet in the metabolism of daidzein by human faecal microbiota sampled from Italian volunteers. J. Nutr. Biochem. 20, 940–7. doi:10.1016/j.jnutbio.2008.08.006
Han, C.Y., Umemoto, T., Omer, M., Den Hartigh, L.J., Chiba, T., LeBoeuf, R., Buller, C.L., Sweet, I.R., Pennathur, S., Abel, E.D., Chait, A., 2012. NADPH oxidase-derived reactive oxygen species increases expression of monocyte chemotactic factor genes in cultured adipocytes. J. Biol. Chem. 287, 10379–93. doi:10.1074/jbc.M111.304998
Harfe, B.D., Jinks-Robertson, S., 2000. DNA mismatch repair and genetic instability. Annu. Rev. Genet. 34, 359–399. doi:10.1146/annurev.genet.34.1.359
Hodge, D.R., 2005. Interleukin 6 Supports the Maintenance of p53 Tumor Suppressor Gene Promoter Methylation. Cancer Res. 65, 4673–4682. doi:10.1158/0008-5472.CAN-04-3589
Hodge, D.R., Xiao, W., Clausen, P. a, Heidecker, G., Szyf, M., Farrar, W.L., 2001. Interleukin-6 regulation of the human DNA methyltransferase (HDNMT) gene in human erythroleukemia cells. J. Biol. Chem. 276, 39508–39511. doi:10.1074/jbc.C100343200
Hwang, J., Wang, J., Morazzoni, P., Hodis, H.N., Sevanian, A., 2003. The phytoestrogen equol increases nitric oxide availability by inhibiting superoxide production: an antioxidant mechanism for cell-mediated LDL modification. Free Radic. Biol. Med. 34, 1271–82.
Joy, S., Siow, R.C.M., Rowlands, D.J., Becker, M., Wyatt, A.W., Aaronson, P.I., Coen, C.W., Kallo, I., Jacob, R., Mann, G.E., 2006. The Isoflavone Equol Mediates Rapid Vascular Relaxation: Ca2+-INDEPENDENT ACTIVATION OF ENDOTHELIAL NITRIC-OXIDE SYNTHASE/Hsp90 INVOLVING ERK1/2 AND Akt PHOSPHORYLATION IN HUMAN ENDOTHELIAL CELL. J. Biol. Chem. 281, 27335–27345. doi:10.1074/jbc.M602803200
Kim, A.Y., Park, Y.J., Pan, X., Shin, K.C., Kwak, S.-H., Bassas, A.F., Sallam, R.M., Park, K.S., Alfadda, A. a., Xu, A., Kim, J.B., 2015. Obesity-induced DNA hypermethylation of the adiponectin gene mediates insulin resistance. Nat. Commun. 6, 7585. doi:10.1038/ncomms8585
Kimura, H., Nakamura, T., Ogawa, T., Tanaka, S., Shiota, K., 2003. Transcription of mouse DNA methyltransferase 1 (Dnmt1) is regulated by both E2F-Rb-HDAC-dependent and -independent pathways. Nucleic Acids Res. 31, 3101–3113. doi:10.1093/nar/gkg406
McCabe, M.T., Davis, J.N., Day, M.L., 2005. Regulation of DNA Methyltransferase 1 by the pRb/E2F1 Pathway. Cancer Res. 65, 3624–3632. doi:10.1158/0008-5472.CAN-04-2158
McGarvey, K.M., Fahrner, J.A., Greene, E., Martens, J., Jenuwein, T., Baylin, S.B., 2006. Silenced Tumor Suppressor Genes Reactivated by DNA Demethylation Do Not Return to a Fully Euchromatic Chromatin State. Cancer Res. 66.
Ness-Abramof, R., Apovian, C.M., n.d. Waist circumference measurement in clinical practice. Nutr. Clin. Pract. 23, 397–404. doi:10.1177/0884533608321700

Pinent, M., Espinel, A.E., Delgado, M.A., Baiges, I., Bladé, C., Arola, L., 2011. Isoflavones reduce inflammation in 3T3-L1 adipocytes. Food Chem. 125, 513–520. doi:10.1016/j.foodchem.2010.09.042
Remely, M., Aumueller, E., Jahn, D., Hippe, B., Brath, H., Haslberger, A., 2014. Microbiota and epigenetic regulation of inflammatory mediators in type 2 diabetes and obesity. Benef Microbes 5, 33–43. doi:QMQ61043P3L1J86L [pii] 10.3920/BM2013.006
Robertson, K.D., Ait-Si-Ali, S., Yokochi, T., Wade, P.A., Jones, P.L., Wolffe, A.P., 2000. DNMT1 forms a complex with Rb, E2F1 and HDAC1 and represses transcription from E2F-responsive promoters. Nat. Genet. 25, 338–42. doi:10.1038/77124
Schroder, A.L., Pelch, K.E., Nagel, S.C., 2009. Estrogen modulates expression of putative housekeeping genes in the mouse uterus. Endocrine 35, 211–9. doi:10.1007/s12020-009-9154-6
Setchell, K.D.R., Clerici, C., 2010. Equol: history, chemistry, and formation. J. Nutr. 140, 1355S–62S. doi:10.3945/jn.109.119776
Soberanes, S., Gonzalez, A., Urich, D., Chiarella, S.E., Radigan, K.A., Osornio-Vargas, A., Joseph, J., Kalyanaraman, B., Ridge, K.M., Chandel, N.S., Mutlu, G.M., De Vizcaya-Ruiz, A., Budinger, G.R.S., 2012. Particulate matter Air Pollution induces hypermethylation of the p16 promoter Via a mitochondrial ROS-JNK-DNMT1 pathway. Sci. Rep. 2, 275. doi:10.1038/srep00275
Sun, H., Zhou, X., Chen, H., Li, Q., Costa, M., 2009. Modulation of histone methylation and MLH1 gene silencing by hexavalent chromium. Toxicol. Appl. Pharmacol. 237, 258–66. doi:10.1016/j.taap.2009.04.008
Switzeny, O.J., Mullner, E., Wagner, K.H., Brath, H., Aumuller, E., Haslberger, A.G., 2012. Vitamin and antioxidant rich diet increases MLH1 promoter DNA methylation in DMT2 subjects. Clin Epigenetics 4, 19. doi:1868-7083-4-19 [pii]10.1186/1868-7083-4-19
Switzeny, O.J., Müllner, E., Wagner, K.-H., Brath, H., Aumüller, E., Haslberger, A.G., 2012. Vitamin and antioxidant rich diet increases MLH1 promoter DNA methylation in DMT2 subjects. Clin. Epigenetics 4, 19. doi:10.1186/1868-7083-4-19
Tremaroli, V., Bäckhed, F., 2012. Functional interactions between the gut microbiota and host metabolism. Nature 489, 242–9. doi:10.1038/nature11552
Wellen, K.E., Hotamisligil, G.S., 2005. Inflammation, stress, and diabetes. J. Clin. Invest. 115, 1111–9. doi:10.1172/JCI25102
WHO Consultation on Obesity., 2000. Obesity: preventing and managing the global epidemic. Report of a WHO consultation. World Health Organ. Tech. Rep. Ser.
Yuan, J.P., Wang, J.H., Liu, X., 2007. Metabolism of dietary soy isoflavones to equol by human intestinal microflora--implications for health. Mol Nutr Food Res 51, 765–781. doi:10.1002/mnfr.200600262
Yuan, J.-P., Wang, J.-H., Liu, X., 2007. Metabolism of dietary soy isoflavones to equol by human intestinal microflora – implications for health. Mol. Nutr. Food Res. 51, 765–781. doi:10.1002/mnfr.200600262

9. Tables

Table 1: Body weight, food and water intake of C57BL/6J male mice over a period of 4 months

		Water intake [ml]				Chow intake [g]				Weight [mg]			
Month		1	2	3	4	1	2	3	4	1	2	3	4
Inter-vention	**CD**	5.60 ± 0.99	5.36 ± 0.99	5.40 ± 0.91	5.05 ± 1.27	2.64 ± 0.17	2.11 ± 0.62	2.08 ± 0.61	1.99 ± 0.64	23.99 ± 1.50	25.92 ± 1.09	26.94 ± 1.42	27.88 ± 1.49

	CD+Q	5.38 ± 0.48	5.30 ± 0.47	5.29 ± 0.85	5.30 ± 1.22	2.65 ± 0.21	2.64 ± 0.22	2.65 ± 0.27	2.66 ± 0.34	23.83 ± 2.49	25.36 ± 2.45	26.4 ± 2.
	HFD	5.30 ± 0.43	5.13 ± 0.47	4.97 ± 0.54	5.07 ± 0.39	2.56 ± 0.10	2.59 ± 0.15	2.60 ± 0.13	2.56 ± 0.13	30.54 ± 3.43	37.62 ± 4.11	42.8 ± 4.
	HFD+Q	5.42 ± 0.59	4.94 ± 0.06	4.98 ± 0.08	4.58 ± 0.44	3.53 ± 4.43	2.61 ± 0.36	2.52 ± 0.18	2.20 ± 0.50	30.49 ± 2.99	37.47 ± 3.16	42.5 ± 3.

Table 2: Sequence to analyze and primers for CpG Methylation analysis

Gene	**Primer**	**Sequence (5′->3′)**	**Size (bp)**	**GC%**
DNMT1	FW	Biotin - GTA GGT TGT AGA AGA TAG AAT AGT TTT GA	29	31
	RW	CCC ACT CTC TTA CCC TAT ATA ATA CAT	27	37
	Seq	CCC CTC CCA ATT AAT TTC	18	44.4
	Sequence ID: gb|AH009208.2| ***DNMT1:*** at reverse strand of chromosome 9: 20907205–20959888 (52684 bp).			
Sequence to analyze	**7104 – CGCGCGCGCG**AAAAAGC**CG**GGGTCT**CG**T - **7131**		27	7 CpGs
MLH1	FW	AGG GTA TTT TAG TTT TTA TTG GTT GGA GA	29	31
	RW	TTA CAC CTC AAT TCC TAA AAT CTC TAT CCC – Biotin	30	37
	Seq	TTT AGT TTT TAG AAA TGA GTT AAT A	25	16
	Sequence ID: ref|XR_379849.3 **MLH1:** at reverse strand of Chromosome 9: 111228228–111271786 (43559 bp)			
Sequence to analyze	19 - GAAGAG**CG**GAC**CG**TGAACTTTGA**CGCG**CAAG**CGCG** TTGCCTTCTA-GCCTGGTGT**CG**GGC**CG**CTG - 82		64	8 CpGs

10. Figures

Figure 1: Body weight gain of C57BL/6J male mice over 4 month. (CD= control diet, HFD= high fat diet, CD+Q= control diet with equol; HFD+Q= high fat diet with equol)

Figure 2: 16S rDNA qPCR quantification of total bacterial abundance (A), *Firmicutes/ Bacteroidetes ratio* (B), and *F. prausnitzii* (C). The error bar represents a 95% confidence interval. (CD= control diet; HFD= high fat diet; CD+EGCG= control diet plus EGCG; HFD+EGCG= high fat diet plus EGCG Stars indicates significance: *p-value ≤ 0.05, **p-value ≤ 0.01, *p-value ≤ 0.01)

Figure 3: Relative gene expression of DNMT1 in colon and liver. Mean gene expression data is shown for DNMT1 in colon (A) and liver (B) for six mice per group. All gene expression data is relative to control diet and normalized to the house keeping gene GAPDH. The error bar represents a 95% confidence interval. (CD= control diet, HFD= high fat diet, CD+Q= control diet plus

Equol; HFD+Q= high fat diet plus Equol; Stars indicates significance: *p-value ≤ 0.05, **p-value ≤ 0.01, *p-value ≤ 0.001)

Figure 4: Relative methylation status in promoter region of DNMT1 in colon and liver. Mean methylation data is shown for DNMT1 in colon (A) and liver (B) for six mice in each group. All methylation data are relative to control diet. The error bar represents a 95% confidence interval. (CD= control diet, HFD= high fat diet, CD+Q= control diet plus Equol; HFD+Q= high fat diet plus Equol; Stars indicates significance: *p-value ≤ 0.05, **p-value ≤ 0.01, *p-value ≤ 0.001)

Figure 5: Relative gene expression of MLH1 in colon and liver. Mean gene expression data is shown for MLH1 in colon (A) and liver (B) for six mice in each group. All gene expression data is relative to control diet and normalized to the house keeping gene GAPDH. The error bar represents a 95% confidence interval. (CD= control diet, HFD= high fat diet, CD+Q= control diet plus Equol; HFD+Q= high fat diet plus Equol; Stars indicates significance: *p-value ≤ 0.05, **p-value ≤ 0.01, *p-value ≤ 0.001)

Figure 6: Relative methylation status in promoter region of MLH1 in colon (A) and liver (B). Mean methylation data is shown for MLH1 in colon (A) and liver (B) for six mice in each group. Mean methylation data are shown for MLH1 in each intervention group. All methylation data are relative to CD. Error bar represent a 95% confidence interval. In figure 4A significance is shown for CpG 4, 5 and 6. 4B shows significant differences in methylation status in CpG1. (CD= control diet; HFD= high fat diet; CD+EGCG= control diet plus EGCG; HFD+EGCG= high fat diet plus EGCG; Stars indicates significance: *p-value ≤ 0.05, **p-value ≤ 0.01, *p-value ≤ 0.001)

Figure 7: Relative gene expression of IL-6. Mean gene expression data is shown for IL-6 in colon for six mice in each group. All gene expression data is relative to control diet and normalized to the house keeping gene GAPDH. The error bar represents a 95% confidence interval. (CD= control diet, HFD= high fat diet, CD+Q= control diet plus Equol; HFD+Q= high fat diet plus Equol; Stars indicates significance: *p-value ≤ 0.05, **p-value ≤ 0.01, *p-value ≤ 0.001)

14.2 EGCG prevents high-fat diet-induced changes in gut microbiota, decreases of DNA strand breaks, and changes in expression and DNA methylation of *Dnmt1* and *MLH1* in C57BL/6J male mice

Submitted at Oxidative Medicine and Cellular Longevity

Remely Marlene[1a], Ferk Franziska[2b], Sterneder Sonja[1c], Setayesh Tahereh[2d], Roth Sylvia[1f], Tatjana Kepcija[1e], Rahil Noorizadeh [2g], Rebhan Irene[1h], Greunz Martina[1i], Beckmann Johanna[1j], Wagner Karl-Heinz[1k], Knasmüller Siegfried[2l], Haslberger Alexander[1*]

[1] Department of Nutritional Sciences, University Vienna, Vienna, Austria

[2] Institute of Cancer Research, Department of Medicine I, Medical University of Vienna, Vienna, Austria

1. Abstract

Obesity as a multifactorial disorder involves low-grade inflammation, increased ROS incidence, gut microbiota aberrations, and epigenetic consequences. Thus, prevention and therapies with epigenetic active antioxidants, EGCG, are of increasing interest, to determine their role in obesity.

We investigated C57BL/6J male mice fed a high-fat (HFD) or a control diet (CD) with and without EGCG supplementation (25 mg/kg b. w.). DNA damage was analyzed by SCGE assay in liver and colon. DNA promoter of *Dnmt1* and *MLH1* methylation was measured using pyrosequencing. Gene expression of inflammatory mediators (*IL-6*), *Dnmt1* and DNA repair gene (*MLH1*) were assayed in liver and colon. Gut microbiota was analyzed on the basis of 16s rDNA with quantitative real time polymerase chain reaction.

EGCG supplementation showed a decreased DNA damage in liver in the HFD group, although the effect was not shown in colon. In the CD+EGCG even an increased DNA damage was shown in colon but not in the liver.

EGCG supplementation induced a significant lower gene expression of Dnmt1 in both intervention groups in the liver whereas in colon a reduction was only shown in HFD compared to CD. Additionally the mean methylation status of *Dnmt1* promoter region was higher in supplemented groups compared to both reference groups (CD, HFD). In colon a significantly lower *IL-6* gene expression was induced by EGCG, but did not affect significantly *MLH1* gene expression. In liver EGCG supplemented groups showed a decreased *MLH1* gene expression. The methylation status was higher in CD+EGCG compared to CD whereas in HFD+EGCG a decrease was shown in comparison to HFD.

HFD feeding caused a significant lower bacterial abundance in both HFD groups (HFD, HFD+EGCG) resulting in a lower microbial diversity compared to CD. The *Firmicutes/Bacteroidetes* ratio is significantly lower in HFD+EGCG but higher in CD+EGCG compared to each control group.

The results demonstrate the impact of EGCG on the one hand on gut microbiota composition and gut microbial metabolite profile which together with dietary components affect host health. On the other hand effects may derive from antioxidative activities as well as epigenetic modifications observed on CpG methylation but also likely to include other epigenetic elements.

2. Abbreviations

bw.	body weight
CD	control diet
CD+EGCG	control diet plus EGCG
cDNA	complementary DNA
DNMT1	DNA methyltransferase 1
DGGE	denaturing gradient gel electrophoresis
EGC	epigallocatechin
EGCG	(-)-Epigallocatechin-3-gallate
FFAs	free fatty acids
GA	gallic acid
GAPDH	glycerinaldehyd-3-phosphat-dehydrogenase
HAT	histone acetyl transferase
HFD	high fat diet
HFD+EGCG	high fat diet plus EGCG
IC	inhibitory concentration
IL-6	interleukin-6
MGMT	O6-methylguanine-deoxyribonucleic acidmethyltransferase
MLH1	MutL homologue 1
MMR	DNA mismatch repair
Nrf2	Nuclear factor-erythroid 2-related factor 2
ROS	reactive oxygen species
SAH	S-adenosylhomocysteine
SAM	S-Adenosylmethionin
SCFA	short-chain fatty acids
SCGE	single cell gel electrophoresis
SD	standard deviation
TNFα	tumor necrosis factor α
T	time point

3. Introduction

Metabolic syndrome, a multifactorial disorder, results from a long-term imbalance of diet and physical activity, genetic predisposition, and an imbalanced gut microbiota influencing several metabolic pathways including epigenetic regulation. In 2015 the prevalence of metabolic syndrome was determined at 1.9 billion adults being overweight (BMI ≥ 25 kg/m² (body mass index)) and more than 600 billion obese (BMI ≥ 30 kg/m²) [1]. Thus, this high incidence of obesity and associated diseases like type 2 diabetes (hyperglycemia on basis of an insulin resistance) are a challenge and financial burden for the national health care system.

The increased adipose tissue is an important energy storage organ but also a key endocrine organ with active metabolism relevant in energy homeostasis, lipid and glucose metabolism, fibrinolysis, coagulation, blood pressure, and inflammation (like interleukin-6 (IL-6), tumor necrosis factor α (TNFα)) [2,3], but also in increased reactive oxygen species (ROS) and free fatty acids (FFAs) production, and increased oxidative stress [4,5]. Oxidative stress in turn is associated with both genome-wide hypomethylation and

promoter hypermethylation of the DNA [6], resulting in transcriptional silencing of key antioxidant enzymes as well as tumor suppressor genes [7,8]. Diets rich in bioactive anti-inflammatory compounds, such as polyphenols, have been recommended to reduce oxidative stress and to decrease inflammation [9].

EGCG (-)-Epigallocatechin-3-gallate), the main catechin form green-tea (50-75 %), has been shown to support many potential health effects, including antioxidant, anticarcinogenic, hypocholesterolemic, and cardioprotective epigenetic activities [10]. It is named to increase energy expenditure, weight loss, reduce fat mass, and facilitates weight maintenance after weight loss [11]. Antiobesity effects might be mediated through antioxidative and singlet oxygen quencher properties. Inhibition of destructive effects of ROS might act through selective inhibition of specific enzyme activities such as DNMTs, repair of DNA aberrations [12], and suppressing inflammation in the development of obesity [9]. EGCG supplementation (0.1 %) in obese and diabetic C57BL/KsJ-db/db mice decreased levels of insulin, IGF-1, IGF-2, free fatty acid, and TNF-α as well as the expression of *TNF-α*, interleukin (*IL)-6*, *IL-1β*, and *IL-18* mRNAs in the livers [13]. EGCG inhibits DNMT activity resulting in a decreased 5-methlcytosine concentration, 20 µmol/L of EGCG already inhibit DNMT activity in oesophageal (KYSE-150), colon (HT-29), prostate (PC-3), and breast (MCF7 and MDA-MB-231) cancer cells. Although no effects of EGCG on DNMT activity (2–50 µmol/L) are also shown in cancer cells. Another DNMT inhibitory pathway of flavan-3-ols results from an increase of S-adenosyl-l-homocysteine (SAH) [14].

A reduced DNMT activity reactivates methylation-silenced genes in a dose- (5-50 µmM of EGCG) and time-dependent (12-144 h) manner [15]. According to Fang et al. (2003) *MLH1* and *O6-methylguanine-deoxyribonucleicacidmethyltransferase (MGMT)*, both part of the DNA mismatch repair (MMR) system, are hypomethylated in the CpG reach promoter regions [15] accompanied by a higher expression of mRNA [15]. In contrast ROS-induced oxidative stress contributes to hypermethylation of normally unmethylated promoter regions, resulting in transcriptional silencing of key antioxidant enzymes as well as tumor suppressor genes [7,8]. EGCG also alters histone acetyl transferase (HAT) activity, histone acetylation resulting in aberrant chromatin structures, but also miRNA expression in hepatocellular carcinoma cells is named to be effected [14].

However, above small-intestinal absorption, tea catechins could reach the large intestine, and be processed by the gut microbiota into gallic acid (GA) and epigallocatechin (EGC) [16,17]. Alterations in gut microbiota composition, differences in gut microbial metabolite profile, due to different dietary feeding offer insights that may be relevant for

several chronic conditions, including obesity. The obesity related gut microbiota is composed by a less bacterial diversity and altered abundance, gene-representation, and metabolic pathways [18]. These differences include a higher abundance of *Firmicutes*, whereas *Bacteroidetes* are reduced resulting in a higher *Firmicutes/Bacteroidetes* ratio in obese individuals. An increased abundance of *Lactobacilli* is mentioned as growth promoter and is associated with weight gain and inflammatory processes during obesity [19]. Genes encoding for carbohydrate metabolism enzymes are increased in the gut microbiome of obese mice provoking a greater capacity to extract energy from the diet and to generate short-chain fatty acids (SCFAs) [20,21]. SCFAs are essential for the microbial community and play a role in regulation of energy balance, inflammatory processes, health, and obesity [22].

Whereas intervention with EGCG resulted in a reduction of *Clostridium spp.* abundance, increased *Bacteroides*, but also influenced *Bifidobacterium* and *Prevotella* to a lesser extent resulting in lower levels of acetic and butyric acids and little influence on propionic acid levels in caecum. Thus, effects on weight reduction, weight maintenance due to dietary intervention with EGCG could be responsible for regulating energy metabolism in the body [23].

In the present study, we investigate the effects of physiologically applicable dose of EGCG on gut microbiota, DNA damage, DNA methylation, and gene expression of inflammatory mediators: *IL-6; DNMT1*, and DNA repair: *MLH1* in liver and colon due to metabolic syndrome induced by a high-fat diet (HFD) and due to control diet (CD). We investigated the colon as direct nutrient contact is given, whereas in liver, the main organ in glucose and insulin metabolism, only metabolites are further catabolized and influenced by the enterohepatic pathway. In addition, gut microbiota composition and diversity was analyzed on the basis of stool samples. Effects of dietary EGCG in alleviating conditions associated with obesity and metabolic syndromes are reported.

4. Materials and Methods

The Ethical Committee of the Medical University of Vienna approved this animal experiment (BMWFW-66.009/0329-WF/V/3b/2014) implemented with 6 weeks old C57BL/6J male mice (n=60) (Janvier Labs, France). The mice were kept by three animals per cage (Macrolon type III, Techniplast GmbH, Germany) under standard conditions (24 ± 1 ºC, humidity 50 ± 5 %, 12 hrs light/dark cycle). The animals were divided into four groups after an acclimatization time of two weeks with control diet (EF R/M Control, 12 % fat ssniff Spezialdiäten GmbH, Soest, Germany): 1) CD group (EF R/M Control, 11 kJ % fat,

ssniff Spezialdiäten GmbH, Soest, Germany), 2) CD plus EGCG group (CD+EGCG) (EGCG: 25 mg/kg body weight per day), 3) HFD group (54 % kJ fat ssniff EF acc.D12492 (I) mod., ssniff Spezialdiäten GmbH, Soest, Germany) and 4) HFD plus EGCG group (HFD+EGCG). Food and water were provided ad libitum, supplemented with EGCG in the intervention groups (25 mg/kg b. w.). EGCG was provided as pure EGCG (System Biologie, Wollerau). Water/ EGCG uptake was measured daily. Once per week the mice were weight and food intake was determined (Table 1). Animals were killed by cervical dislocation after 4 months.

4.1. SCGE (single cell gel electrophoresis) assay

DNA migration in an electric field was analyzed in hepatocytes and colonocytes from mice in SCGEassays according to the protocol of Tice et al. (2000) [24]. Nuclei from livers and cells from colons were collected according to the method developed by Sasaki et al., (2002) [25]. 1.0 g liver tissue was homogenized by use of a Potter Elvehjem-type (B. Braun, Melsungen, Germany) at 400 rpm in 4.0 mL chilled homogenization buffer (pH 7.5). Subsequently, the homogenates were centrifuged (800*g*, 10 min, 4 ºC). Colon cells were isolated by scratching from the colon mucosa and kept on ice in 2.0 mL homogenisation buffer. The nuclei were suspended in LMPA (0.5 %, Gibco, Paisley, UK) and transferred to slides which were pre-coated with NMPA (1.0 %, Gibco, Paisley, UK).

The experiments were carried out according to Burlinson et al. (2007) [26]. After lysis (pH 10.0) and electrophoresis (20 min, 300 mA, 25 V, at 4 ˚C, pH > 13), the gels were stained with ethidium bromide (20 µg/mL, Sigma-Aldrich, Germany).

With nuclei from each organ, three slides were prepared per experimental point and 50 cells were evaluated from each slide. Slides were examined under a fluorescence microscope (Nikon EFD-3, Japan) using 25-fold magnification. DNA migration was determined with a computer aided comet assay image analysis system (Comet Assay IV, Perceptive Instruments, UK).

4.2. Gene expression analysis

Liver and colon samples were stored at -80 °C until RNA and DNA isolation using the AllPrep DNA/RNA/miRNA Universal Kit (Qiagen, Germany) according to the manufacturer's protocol. Concentration respectively purity were controlled with a Picodrop100 (Picodrop, UK). Complementary DNA (cDNA) was synthesized by reverse transcription using RT2 First Strand Kit (Qiagen, Germany). cDNA was analyzed in real-time PCR using qPCR Primer Assays (Qiagen, Germany) and RT2 SYBR Green Mastermix (Qiagen, Germany) according to manufacturer’s protocol. PCR conditions were as follows:

initial step of 95°C for 10 min, followed by 40 cycles of 95°C for 15 s and 60°C for 1 min, ending with melting curve analysis (gradient melting of the products was performed at 0.5°C/10 s from 65°C to 95°C). Each sample was analyzed in duplicate, with normalization to the housekeeping gene GAPDH (glycerinaldehyd-3-phosphat-dehydrogenase).

4.3. Methylation analysis

Genomic DNA was bisulfite converted with EpiTect® Fast Bisulfite Conversion kit (Qiagen, Germany) and amplified by PCR using the PyroMark PCR Kit (Qiagen, Germany) according to manufacturer's instructions with primers for *DNMT1* and *MLH1* designed by PyroMark Assay Design SW 2.0 Software (Table 2).

The PCR was carried out in a total reaction volume of 25.0 µL, containing 12.5 µL Pyromark 2X PCR master mix, 10 pmol (*DNMT1*) or 7 pmol (*MLH1*) of each primer, 2.5 µL Coralload Concentrate 10X (Qiagen, Germany), and 10.0 ng (*DNMT1*) or 15.0 ng (*MLH1*) bisulfite converted DNA. Thermocycling condition started with initial denaturation at 95 C for 15 min, followed by 45 cycles at 94°C for 30 s, 55.5°C for 45 s, 72°C for 45 s and a final extension at 72°C for 10 min. PCR product quality was investigated with agarose gel-electrophoresis. CpG methylation analysis was performed in a Pyromark Q24 MDx (Qiagen, Germany).

4.4. Gut microbiota analysis

Stool was collected before intervention and continuously after 1 month until the end of the study period and stored at -20 °C until microbial DNA extraction by using the QIAamp® Fast DNA Mini Kit (Qiagen, Germany) following the manufacturer‘s protocol including two steps of 45 sec beadbeating at 4000 rpm with a 60 sec break in-between to increase the DNA yield. DNA concentration and purification was measured using the Pico100 (Picodrop Ltd., Cambridge UK).

The abundance of gut microbial subgroups were determined by 16s rDNA using quantitative real-time PCR with SYBR green or TaqMan-Probe mastermix with specific primer pairs (Table 3-4) in a Rotor Gene 3000 (Corbett Life Science, Australia). The PCR reaction mixtures and serial DNA dilution of typical strains were prepared according to Remely et al. (2013) [27].

The diversity of gut microbiota was analyzed using denaturing gradient gel electrophoresis (DGGE) [27].

4.5. Statistical analysis

For SCGE assays statistical analyses GraphPad Prism 5.02 (GraphPad Software, USA) was used. The means and standard deviation (SD) of % DNA in the comet tails of the nuclei from the different treatment groups were calculated. Comparisons of groups were done by student´s t-test based on the means of three slides/animal.

All statistical analyses of gene expression and methylation analysis were performed using IBM SPSS Advanced Statistics 20.0 (SPSS, USA). All data are shown mean±SD. ΔCT values were calculated by normalization to GAPDH (ΔCT = CT-Target – CT-GAPDH). The ΔΔCT value shows the difference between the two groups. (ΔΔCT = ΔCT+EGCG - ΔCT-Control). Relative changes in gene expression between the intervention and control group are determined by the 2-ΔΔCT equation (fold change = 2-ΔΔCT). Kolmogorov-Smirnov-Test was used to test the normalization of the data. The Mann-Whitney-U Test was used to examine significant relationships. For all comparisons p-values ≤ 0.05 were considered as statistical significant.

5. Results

5.1. Body weight, food intake and EGCG uptake

Body weight and food intake were measured weekly, water/EGCG uptake daily. According to Table 1 food intake and total water consumption did not differ between the groups (Table 1). Mean EGCG uptake was about 0.64 ± 0.07 mg in the CD group and about 0.97 ± 0.09 mg in the HFD group of each mouse per day. Mice fed a HFD (T1: 30.54 ± 3.43 g; T4: 45.99 ± 4.46 g) and HFD+EGCG (T1: 30.74 ± 3.43 g; T4: 47.69 ± 3.45 g) increased significantly more weight in comparison to CD fed mice (T1: 23.99 ± 1.50 g; T4: 27.88 ± 1.49 g) and CD+EGCG (T1: 24.16 ± 1.52 g; T4: 28.43 ± 1.76 g) ($p \leq 0.01$, Figure 1). The body weight increase over study period was significant in all groups ($p \leq 0.01$).

5.2. SCGE experiments with nuclei from colon and liver cells

HFD induced significant DNA damage in liver and colon compared with CD. In liver of animals fed with HFD and supplemented with EGCG in drinking water the extent of DNA migration was significantly decreased by 31.5% ($p \leq 0.05$) after supplementation (Figure 2). No effect was detected in colon of HFD group after EGCG supplementation (Figure 2).

Supplementation with EGCG in CD group in colon of animals caused slight DNA damage, while no effect was detected between CD and CD + EGCG in liver of the animals.

5.3. Relative gene expression and CpG methylation of the promoter region of MLH1 in liver and colon cells

In liver cells the relative gene expression of *MLH1* decreased significantly in HFD fed mice compared to the CD (49%, $p \leq 0.001$). EGCG supplementation showed significant reduction in CD+EGCG compared to CD (56%; $p \leq 0.001$), as well in HFD+EGCG compared to HFD (44%; $p \leq 0.01$). Moreover the reduction of EGCG was significantly higher in HFD+EGCG than in CD+EGCG (38%; $p \leq 0.05$) (Figure 3A).

The relative gene expression of *MLH1* in colon did not result in any significant difference between the interventions (Figure 3B).

In *MLH1* promoter region the relative methylation of six CpGs was investigated in liver and in colon (Figure 4-5). In liver cells of CD+EGCG the mean methylation was higher compared to CD (CD: 2.83%; CD+EGCG: 3.23%), but in HFD+EGCG decreased mean methylation status compared to HFD was shown (HFD: 3.36%; HFD+EGCG: 3.18%). Particular, at CpG1 HFD (57%) either CD+EGCG (44%) showed a significant decrease in methylation status compared to CD ($p \leq 0.01$). Furthermore a significant hypomethylation in the HFD+EGCG group was seen compared to CD+EGCG (24%; $p \leq 0.01$; Figure 4B). At CpG4 (73%; $p \leq 0.01$) and at CpG6 (60%; $p \leq 0.05$) the methylation status significantly increased with HFD compared to CD. A hypermethylation was seen in both supplementation groups at CpG4 CD+EGCG (172 %) and HFD+EGCG at CpG 2 with an increase of 80 % normalized to respectively CD or HFD ($p \leq 0.01$). By comparing CD+EGCG with HFD+EGCG the CD group showed a significant hypomethylation at CpG 3 (22%; $p \leq 0.01$) and CpG5 (20%; $p \leq 0.01$) (Figure 4A).

The mean methylation of *MLH1* in colon cells increased with EGCG in the CD group (CD: 2.79%; CD+EGCG: 2.97%), but decreased in the HFD group with EGCG (HFD: 3.41%; HFD+EGCG: 3.01%, Figure 5). In colon cells the methylation status of *MLH1* showed a significant reduction at CpG2 in HFD compared to CD (60%; $p \leq 0.01$). Furthermore, EGCG supplementation significantly reduced the methylation status of CpG2 in HFD+EGCG group compared to HFD (35%; $p \leq 0.01$). A significant decrease at CpG1 was seen in CD with EGCG supplementation compared to CD (62%, $p \leq 0.01$) whereas HFD+EGCG were significantly higher methylated compared to CD+EGCG (82% $p \leq 0.05$). At CpG 4 HFD resulted in a hypermethylation of 113% compared to CD. Furthermore supplementation with EGCG in the CD decreased the methylation status significantly 38% when normalized to CD ($p \leq 0.01$). CpG5 of *MLH1* was significantly higher methylated in HFD (24%; $p \leq 0.01$) and in CD+EGCG (75%; $p \leq 0.01$) compared to CD whereas in the HFD+EGCG a significant hypomethylation was shown when normalized

to CD (45%; $p \leq 0.01$). A significant reduction was shown between CD+EGCG and HFD+EGCG (61%; $p \leq 0.01$). CD+EGCG resulted in a significant hypomethylation at CpG6 of *MLH1* in colon cells compared to CD (63%; $p \leq 0.05$) and respectively in HFD with (34%; $p \leq 0.01$).

5.4. Relative gene expression of IL-6 in colon

A significant lower expression of IL-6 has been measured between CD and HFD ($p \leq 0.01$) and CD and HFD+EGCG ($p \leq 0.01$) in colon (Figure 8). In liver the gene expression of IL-6 was under detection limit in the study group.

5.5. Relative gene expression and CpG methylation of the promoter region of Dnmt1 in liver and colon cells

Relative gene expression of *Dnmt1* in liver cells was lower in HFD compared to CD (61%; $p \leq 0.01$). Supplementation with EGCG resulted in a significantly reduced gene expression compared to respectively CD (75%; $p \leq 0.01$) and HFD (51%; $p \leq 0.01$) (Figure 6A). In colon the relative gene expression of *Dnmt1* decreased significantly in HFD compared to CD (69%, $p \leq 0.01$). Although the decrease of HFD compared to CD is compensated by EGCG in HFD with a more than three times higher gene expression of *Dnmt1* compared to HFD ($p \leq 0.01$, Figure 6B).

In the promoter region of *Dnmt1* in liver and colon four CpGs were analyzed. Mean methylation of *Dnmt1* in liver cells was higher in CD+EGCG (3.21%) and HFD+EGCG (3.09%) compared to each diet CD (2.28%) and HFD (2.37%). Significant differences in methylation status of *Dnmt1* were determined in CpG 1 and CpG 3. In both diets EGCG significantly increased the methylation status of CpG 1 (CD+EGCG: CD 71%; $p \leq 0.05$; HFD+EGCG: HFD 62%; $p \leq 0.05$). The same effect of EGCG was seen in at CpG 3 in the CD group with a significant increase (37%; $p \leq 0.01$). Furthermore the supplementation with EGCG resulted in a significantly higher methylation of CpG 3 in HFD+EGCG than in CD+EGCG (28%, $p \leq 0.05$). CpG 2 and CpG 4 did not show any significant changes in methylation status (Figure 7A).

In colon cells CpG 2 and CpG 4 showed significant changes in the methylation status of *Dnmt1*. A significant higher methylation status in CpG 2 was observed due to EGCG in the HFD group (19%; $p \leq 0.05$). In CD+EGCG supplementation resulted in a significant hypermethylation at CpG4 (28%; $p \leq 0.05$). No significant changes were observed at methylation status of *Dnmt1* at CpG 1 and CpG 3 (Figure 7B).

5.6. Gut microbiota composition and diversity

Differences in total bacterial abundance were shown between CD and HFD ($p < 0.0001$) as well as between CD+EGCG and HFD+EGCG but also between HFD and HFD+EGCG ($p = 0.039$). HFD feeding caused a lower bacterial abundance in both HFD groups resulting in a lower microbial diversity compared to CD (HFD bands = 21.4 ± 5.08, HFD+EGCG bands = 19.6 ± 3.84, CD bands = 20.4 ± 4.62, CD+EGCG bands = 17.02 ± 5.07).

The *Firmicutes/Bacteroidetes* ratio is significantly higher in both HFD groups compared to CD groups ($p < 0.0001$). EGCG treatment induced a significantly lower ratio in HFD+EGCG compared to HFD ($p < 0.0001$) but a significantly higher ratio in CD+EGCG compared to CD ($p < 0.0001$). Lactobacilli decrease with EGCG intervention. Both clostridial clusters (Clostridium cluster IV, Clostridium cluster XIVa) were significantly lower in HFD groups compare to CD groups ($p < 0.0001$). *Clostridium cluster IV* significantly increased in HFD+EGCG compared to HFD ($p = 0.005$). *Clostidium cluster XIVa* increased in CD+EGCG compared to CD ($p = 0.189$) and were significantly higher abundant in comparison to HFD+EGCG ($p < 0.0001$). In turn, *F. prausnitzii* is less abundant in HFD groups compared to CD groups ($p < 0.0001$) and were most abundant in CD compared to all other groups (CD+EGCG: HFD+EGCG: $p < 0.0001$; CD: CD+EGCG: $p = 0.001$).

In HFD mice *butyryl CoA: acetate CoA-transferase* gene was significantly lower in comparison to CD mice ($p < 0.0001$). Intervention with EGCG in CD group resulted in a significant decrease ($p < 0.0001$) whereas in HFD no significant effect was shown. Results of the *butyrate kinase* gene showed similar results whereas HFD+EGCG group showed a significant increase (CD: HFD $p < 0.0001$; CD: CD+EGCG $p = 0{,}001$; HFD: HFD+EGCG $p = 0.005$).

Bacteroidetes were significantly lower abundant in HFD compared to CD ($p < 0.0001$) and significantly increase with EGCG intervention in HFD mice ($p = 0{,}001$). An increase was shown in CD mice due to EGCG treatment.

Akkermansia showed a lower abundance in HFD fed mice compared to CD ($p = 0.092$). EGCG treatment resulted in a lower abundance in CD+EGCG ($p = 0{,}001$) but no significant change in abundance of HFD+EGCG was observable ($p=0.574$).

6. Discussion

We showed that HFD induced significantly DNA damage in liver and colon compared with CD. These results were also reflected by a lower gene expression of *Dnmt1* in liver and colon of HFD fed mice. In turn DNA methylation status was higher in this group. As well as *MLH1* methylation status was higher compared to CD, but gene expression lower

due to HFD feeding in both organs. Especially CpG 1 showed a decreased methylation status in contrast to CpG 4 with an increased methylation in liver. In colon CpG2, CpG4, CpG5, and CpG6 of *MLH1* promoter region were affected due to different feeding. *IL-6* gene expression was significantly higher in HFD compared to CD. Either gut microbial composition differs between CD and HFD: lower total bacterial abundance due to HFD, lower microbial diversity, higher *Firmicutes/Bacteroidetes* ratio, lower abundance of *F. prausnitzii,* and *Akkermansia,* reduced incidence of *butyryl CoA: acetate CoA-transferase* gene and *butyrate kinase* gene.

On the basis of microbial analysis we are able to support the results of our previous publications on human fecal analysis [27]. Mice fed a HFD differ in microbial subpopulations especially the *Firmicutes/Bacteroidetes* ratio which is already handled as a marker in obesity epidemic. Although other researches also show converse or not diverging results [28–32]. However, additionally we can support results of gut microbial metabolites/ cell wall components influencing the host via epigenetic mechanisms too. The *Firmicutes/Bacteroidetes* ratio causes or occurs due to low-grade inflammation which was shown due to increased *IL-6* gene expression but also by increased DNA damage and by increased *MLH1* methylation status and reduced expression of the gene.

Interventions with EGCG as an epigenetic active antioxidant may provide valuable impact in the therapy of metabolic syndrome. Bose et al. (2008) showed an effect of EGCG on HFD fed mice: the percentage of body fat and the visceral fat weight were reduced significantly ($p \leq 0.05$) due to the supplementation of EGCG (3.2 g/kg diet) for 16 weeks when compared to control mice [11]. EGCG on the one hand influences gut microbiota composition in dependence on polymersiation degree: higher polymerization results in a higher bioavailability in the gut as the absorption in the small intestine is negligible in contrast to low degree of polymerization [33]. Methylated catechins, ring fission products (like valerolactone), and phenolic products are indicative of gut microbial transformations. On the other hand EGCG has valuable direct impact as antioxidant. However, EGCG acts also as epigenetic active substance influencing histone modification and/or DNA methylation patterns [17].

6.1. EGCG protects DNA damage caused by HFD in the liver

EGCG supplementation showed a decreased DNA migration in liver but no effects were shown in colon in the HFD group. In the CD+EGCG even an increased DNA damage in colon was shown but not in liver. Our findings are in agreement with result published by Kager et al. (2010) who gave EGCG orally to normal weight mice as in present experiment they found no evidence for a protective effect in standard SCGE experiment in

colon and liver. However, a clear protective effect was seen in hepatocytes but not in colonocytes in this experiment in regard to formation of oxidized DNA bases [34].
Oršolić et al. (2013) published results which were obtained with diabetic mice, they found even an increase of DNA migration in the liver after injection of EGCG for 7 days [35]. Notably, the authors use relatively high dose of catechin in this experiment (i.e. 50 mg/kg b.w.) and it is known from *in vitro* study that high concentration of EGCG and other tea catechins causes DNA damage as a consequence of radical formation [36,37] .
The pattern of gene expression of *DNMT1* and *MLH1* which were observed in the liver is in partial agreement with results from SCGE experiments i.e. a decrease was observed in hepatocytes in obese animals ocompared to controls. However, EGCG did not compensate this effect but cause further decline of the expression of both genes.
On the contrary a clear increase of *DNMT1* was seen with the catechin in the colon of HFD animals while obesity itself had no impact on the transcriptional activity of both genes in colonocytes. It is well documented that the *MLH1* and *DNMT1* play a key role in DNA repair processes; in particular mismatch repair [38,39]. However, distinct differences which we found between the induction of DNA migration in SCGE experiment and decreased gene expression levels distract from the assumption of direct relation between comet formation and repair processes which are controlled by *MLH1* and *DNMT1*.

6.2. EGCG decreases inflammatory IL-6 and MLH1 gene expression reflected by a higher MLH1 promoter methylation

In colon a significantly lower *IL-6* gene expression was induced by EGCG, but did not affect significantly *MLH1* gene expression. In liver EGCG reduced *MLH1* gene expression in both diet groups. The mean methylation was higher in CD+EGCG compared to CD whereas in HFD+EGCG a decrease was shown in comparison to HFD. However, methylation status varies CpG specific and additionally diet specific.
EGCG reduced the expression levels of TNF-α, IL-6, IL-18, and IL-1β mRNAs, the serum levels of TNF-α, and the activation of Stat3 and JNK proteins in diethylnitrosamine (DEN)-induced liver tumor genesis treated C57BL/KsJ-*db/db* (*db/db*) obese mice [13], but also IL-6 synthesis in a rat adjuvant-induced arthritis by administration of 100 mg/kg EGCG, intraperitoneally daily [40]. Ahmed et al. (2008) showed an increase in the synthesis of soluble gp130 protein, an endogenous inhibitor of IL-6 signaling and trans-signaling [40]. Additionally EGCG induced a concentration and time-dependent reversal hypermethylation of tumor suppressor genes such as *p16, RAR, MGMT*, and *MLH1* genes in human esophageal cancer cells [12].

6.3. EGCG increases Dnmt1 DNA methylation resulting in tissue specific variances in gene expression

EGCG supplementation resulted in a significantly reduced gene expression compared to respectively CD and HFD in the liver. In the colon EGCG compensates the decrease in gene expression due to HFD and results equalized to CD and with a three times higher gene expression of *Dnmt1* compared to HFD. The methylation status in the promoter region of *Dnmt1* was higher in supplemented groups compared to both control groups (CD, HFD). A significant increase was shown in CpG1 and CpG3 in the liver. In colon CpG 2 and CpG4 were affected respectively in HFD+EGCG or in CD+EGCG.

EGCG was already shown to be the most efficacious inhibitor of enzymatic DNA methylation *in vitro* in comparison to other tea polyphenols (catechin, epicatechin) and bioflavonoids (quercetin, fisetin, and myricetin). Inhibitory effects for SssI nmt- and *Dnmt1*-mediated DNA methylation were shown at a half maximal inhibitory concentration (IC50) of 0.21 and 0.47 μM, respectively. Inhibitory mechanisms are mentioned at the one hand via direct pathways and on the other hand indirect via DNMT-mediated DNA methylation through increased formation of SAH, a potent inhibitor of S-adenosylmethionine (SAM)-mediated reactions [41] and via altering the availability of methyl groups which are used to methylate catechol groups on polyphenols by catechol-O-methyltransferase [17]. Although Lee et al. (2005) mentioned rather an important influence of the presence of a physiologically relevant concentration of Mg2+ (such as 2 mM) on inhibitory potency of EGCG than a dependence on its own methylation [41]. EGCG is also suggested to induce Foxp3 promoter demethylation inducing differentiation and expansion of Treg via DNMT inhibitory activity and to reduce T cell proliferation and cytokine production [42]. An inhibition of DNMTs together with an inhibition of histone deacetylase is suggested to prevent the hypermethylation and the silencing of key genes [41]. Either gut microbial derived metabolites of EGCG, gallic acid (GA) and epigallocatechin (EGC) influence epigenetic gene expression via HAT inhibitors to a lesser extent [17].

6.4. EGCG changes obese gut microbial profile to lean phenotype

HFD feeding caused a significant lower bacterial abundance in both HFD groups (HFD, HFD+EGCG) resulting in a lower microbial diversity compared to CD. The *Firmicutes/Bacteroidetes* ratio is significantly lower in HFD+EGCG but higher in CD+EGCG compared to each control group. Main changes due to EGCG intervention are derived in *Lactobacilli* (decrease), but also in *Clostridia* cluster resulting in a lower abundance of *F. prausnitzii* in HFD groups with highest abundance in CD. *Butyryl CoA: acetate CoA-*

transferase gene significantly increased in CD+EGCG whereas in HFD+EGCG the *butyrate kinase* significantly increased. *Akkermansia* are reduced abundant with EGCG supplementation.

It is already known that HFD, Western lifestyle, impacts gut microbiota composition. Diet quality and quantity are important influencing factors on bacterial community composition and metabolic/immunological activity of the host gut microbiota. Phytochemicals are generally poorly absorbed in the small intestine, thus they are in close contact with the gut microbiota in turn affecting health benefits attributed to natural compounds. Results from green tea polyphenols, EGCG, give evidence to have a positive influence on gut microbiota composition. Unno et al. (2014) not only shows changes in body and stool composition due to EGCG treatment but also changes in gut microbiota composition. However, these changes were dependent on dosage: 0.3 % EGCG supplementation induced *Bifidobacterium*, *Lactobacillales*, *Bacteroides*, but reduced the abundance of *Clostridium* clusters. A concentration of 0.6 % EGCG supplementation increased the abundance of *Lactobacillales, Bacteroides*, but nearly depleted the abundance of *Clostridium* clusters and *Bifidobacterium* [16]. However, Unno et al. (2014) used Wistar rats and fed a commercial chow, thus comparison of both projects in gut microbiota composition, especially *Lactobacilli,* may be impaired on induced metabolic syndrome due to HFD feeding. However, we showed also an increase in *Bacteroidetes* and a decrease in *Clostridium* clusters impairing butyrate metabolism. Unno et al. (2014) showed lower levels of acetic and butyric acid but little influence on propionic acid due to 0.6 % EGCG supplementation [16]. We even showed differences in butyrate formation pathways. The butyrate kinase pathway is more related to a Western diet, reflected in HFD fed mice (main fat resource: lard). Whereas the b*utyryl CoA: acetate CoA-transferase* gene is associated with vegetarian feeding and to a lesser content available in omniovores [43].

7. Conclusions

According to our results, EGCG might be suggested for the potential use for the prevention or in the therapy of obesity-related and oxidative stress-induced health risks. One effect may derive from changes in GI microbiota and their anti-inflammatory effects by metabolites. Another effect may derive from antioxidative activities as well as epigenetic modifications observed on CpG methylation but also likely to include other elements of the epigenetic machinery. Interactions between antioxidative and epigenetic effects, e.g. via ROS mediated breaks of DNMT pathways need to be explored.

8. Acknowledgement

The work was funded by the Austrian Science Fund (FWF; AP2658721).

9. Ethics Approval

The animal experiment was approved by the Ethical Committee of the Medical University of Vienna (BMWFW-66.009/0329-WF/V/3b/2014).

10. Competing Interests

The authors declare to have no actual or potential competing interests that might be perceived as influencing the results or interpretation of a reported study.

11. References

1. World Health Statistics 2015. 2015.
2. Fernández-Sánchez A, Madrigal-Santillán E, Bautista M, Esquivel-Soto J, Morales-González Á, Esquivel-Chirino C, et al. Inflammation, oxidative stress, and obesity. Int. J. Mol. Sci. 2011;12:3117–32.
3. Kershaw EE, Flier JS. Adipose Tissue as an Endocrine Organ. J. Clin. Endocrinol. Metab. 2004;89:2548–56.
4. Savini I, Catani MV, Evangelista D, Gasperi V, Avigliano L. Obesity-associated oxidative stress: Strategies finalized to improve redox state. Int. J. Mol. Sci. 2013;14:10497–538.
5. Le Lay S, Simard G, Martinez MC, Andriantsitohaina R. Oxidative Stress and Metabolic Pathologies: From an Adipocentric Point of View. Oxid. Med. Cell. Longev. 2014;2014:908539.
6. Thanan R, Oikawa S, Hiraku Y, Ohnishi S, Ma N, Pinlaor S, et al. Oxidative Stress and Its Significant Roles in Neurodegenerative Diseases and Cancer. Int. J. Mol. Sci. 2014;16:193–217.
7. Ziech D, Franco R, Pappa A, Panayiotidis MI. Reactive oxygen species (ROS)--induced genetic and epigenetic alterations in human carcinogenesis. Mutat. Res. Elsevier B.V.; 2011;711:167–73.
8. Franco R, Schoneveld O, Georgakilas AG, Panayiotidis MI. Oxidative stress, DNA methylation and carcinogenesis. Cancer Lett. 2008;266:6–11.
9. Wang S, Moustaid-Moussa N, Chen L, Mo H, Shastri A, Su R, et al. Novel insights of dietary polyphenols and obesity. J. Nutr. Biochem. [Internet]. 2014 [cited 2016 Jan 11];25:1–18. Available from: http://www.pubmedcentral.nih.gov/articlerender.fcgi?artid=3926750&tool=pmcentrez&rendertype=abstract
10. Chen Y-K, Cheung C, Reuhl KR, Liu AB, Lee M-J, Lu Y-P, et al. Effects of green tea polyphenol (-)-epigallocatechin-3-gallate on newly developed high-fat/Western-style diet-induced obesity and metabolic syndrome in mice. J. Agric. Food Chem. [Internet]. NIH Public Access; 2011 [cited 2016 Jul 11];59:11862–71. Available from: http://www.ncbi.nlm.nih.gov/pubmed/21932846
11. Bose M, Lambert JD, Ju J, Reuhl KR, Shapses SA, Yang CS. The major green tea polyphenol, (-)-epigallocatechin-3-gallate, inhibits obesity, metabolic syndrome, and fatty liver disease in high-fat-fed mice. J. Nutr. [Internet]. NIH Public Access; 2008 [cited 2016 Jul 11];138:1677–83. Available from: http://www.ncbi.nlm.nih.gov/pubmed/18716169
12. Singh BN, Shankar S, Srivastava RK. Green tea catechin, epigallocatechin-3-gallate (EGCG): mechanisms, perspectives and clinical applications. Biochem. Pharmacol. [Internet]. 2011 [cited

2016 Feb 12];82:1807–21. Available from: http://www.pubmedcentral.nih.gov/articlerender.fcgi?artid=4082721&tool=pmcentrez&rendertype=abstract
13. Shimizu M, Sakai H, Shirakami Y, Yasuda Y, Kubota M, Terakura D, et al. Preventive effects of (-)-epigallocatechin gallate on diethylnitrosamine-induced liver tumorigenesis in obese and diabetic C57BL/KsJ-db/db Mice. Cancer Prev. Res. (Phila). [Internet]. 2011 [cited 2016 Mar 1];4:396–403. Available from: http://www.ncbi.nlm.nih.gov/pubmed/21372039
14. Busch C, Burkard M, Leischner C, Lauer UM, Frank J, Venturelli S. Epigenetic activities of flavonoids in the prevention and treatment of cancer. Clin. Epigenetics [Internet]. 2015 [cited 2016 Feb 1];7:64. Available from: http://www.pubmedcentral.nih.gov/articlerender.fcgi?artid=4497414&tool=pmcentrez&rendertype=abstract
15. Fang MZ, Wang Y, Ai N, Hou Z, Sun Y, Lu H, et al. Tea polyphenol (-)-epigallocatechin-3-gallate inhibits DNA methyltransferase and reactivates methylation-silenced genes in cancer cell lines. Cancer Res. [Internet]. 2003 [cited 2016 Mar 1];63:7563–70. Available from: http://www.ncbi.nlm.nih.gov/pubmed/14633667
16. Unno T, Sakuma M, Mitsuhashi S. Effect of dietary supplementation of (-)-epigallocatechin gallate on gut microbiota and biomarkers of colonic fermentation in rats. J. Nutr. Sci. Vitaminol. (Tokyo). [Internet]. 2014 [cited 2016 May 3];60:213–9. Available from: http://www.ncbi.nlm.nih.gov/pubmed/25078378
17. Hullar MAJ, Fu BC. Diet, the gut microbiome, and epigenetics. Cancer J. [Internet]. 2014 [cited 2016 Jun 14];20:170–5. Available from: http://www.ncbi.nlm.nih.gov/pubmed/24855003
18. Tremaroli V, Bäckhed F. Functional interactions between the gut microbiota and host metabolism. Nature [Internet]. 2012 [cited 2016 Jul 11];489:242–9. Available from: http://www.ncbi.nlm.nih.gov/pubmed/22972297
19. Armougom F, Henry M, Vialettes B, Raccah D, Raoult D. Monitoring Bacterial Community of Human Gut Microbiota Reveals an Increase in Lactobacillus in Obese Patients and Methanogens in Anorexic Patients. Ratner AJ, editor. PLoS One [Internet]. Public Library of Science; 2009 [cited 2016 Jul 11];4:e7125. Available from: http://dx.plos.org/10.1371/journal.pone.0007125
20. Turnbaugh PJ, Ley RE, Mahowald MA, Magrini V, Mardis ER, Gordon JI. An obesity-associated gut microbiome with increased capacity for energy harvest. Nature [Internet]. 2006 [cited 2014 Jul 10];444:1027–31. Available from: http://www.ncbi.nlm.nih.gov/pubmed/17183312
21. Turnbaugh PJ, Hamady M, Yatsunenko T, Cantarel BL, Duncan A, Ley RE, et al. A core gut microbiome in obese and lean twins. Nature [Internet]. 2009 [cited 2016 Jul 11];457:480–4. Available from: http://www.ncbi.nlm.nih.gov/pubmed/19043404
22. Delzenne NM, Cani PD. Interaction between obesity and the gut microbiota: relevance in nutrition. Annu. Rev. Nutr. [Internet]. 2011 [cited 2016 Jul 11];31:15–31. Available from: http://www.ncbi.nlm.nih.gov/pubmed/21568707
23. UNNO T, SAKUMA M, MITSUHASHI S. Effect of Dietary Supplementation of (^|^minus;)-Epigallocatechin Gallate on Gut Microbiota and Biomarkers of Colonic Fermentation in Rats. J. Nutr. Sci. Vitaminol. (Tokyo). [Internet]. 2014 [cited 2016 Mar 2];60:213–9. Available from: https://www.jstage.jst.go.jp/article/jnsv/60/3/60_213/_article
24. Tice RR, Agurell E, Anderson D, Burlinson B, Hartmann A, Kobayashi H, et al. Single cell gel/comet assay: guidelines for in vitro and in vivo genetic toxicology testing. Env. Mol Mutagen [Internet]. 2000/03/29 ed. 2000;35:206–21. Available from: http://www.ncbi.nlm.nih.gov/entrez/query.fcgi?cmd=Retrieve&db=PubMed&dopt=Citation&list_uids=10737956
25. Sasaki YF, Kawaguchi S, Kamaya A, Ohshita M, Kabasawa K, Iwama K, et al. The comet assay with 8 mouse organs: results with 39 currently used food additives. Mutat. Res. [Internet].

2002 [cited 2016 Feb 16];519:103–19. Available from: http://www.ncbi.nlm.nih.gov/pubmed/12160896
26. Burlinson B, Tice RR, Speit G, Agurell E, Brendler-Schwaab SY, Collins AR, et al. Fourth International Workgroup on Genotoxicity testing: results of the in vivo Comet assay workgroup. Mutat Res [Internet]. 2006/11/23 ed. 2007;627:31–5. Available from: http://www.ncbi.nlm.nih.gov/entrez/query.fcgi?cmd=Retrieve&db=PubMed&dopt=Citation&list_uids=17118697
27. <p>Remely Marlene DSHBZJAEBH and HA. Abundance and Diversity of Microbiota in Type 2 Diabetes and Obesity. J. Diabetes Metab. [Internet]. [cited 2015 Nov 25]; Available from: http://www.omicsonline.org/abundance-and-diversity-of-microbiota-in-type-2-diabetes-and-obesity-2155-6156.1000253.php&&aid=11463
28. Duncan SH, Lobley GE, Holtrop G, Ince J, Johnstone AM, Louis P, et al. Human colonic microbiota associated with diet, obesity and weight loss. Int. J. Obes. (Lond). [Internet]. Macmillan Publishers Limited; 2008 [cited 2015 Nov 26];32:1720–4. Available from: http://dx.doi.org/10.1038/ijo.2008.155
29. Schwiertz A, Taras D, Schäfer K, Beijer S, Bos NA, Donus C, et al. Microbiota and SCFA in lean and overweight healthy subjects. Obesity (Silver Spring). [Internet]. 2010 [cited 2016 Jun 13];18:190–5. Available from: http://www.ncbi.nlm.nih.gov/pubmed/19498350
30. Cani PD, Delzenne NM. Interplay between obesity and associated metabolic disorders: new insights into the gut microbiota. Curr. Opin. Pharmacol. [Internet]. 2009 [cited 2016 Jun 13];9:737–43. Available from: http://www.ncbi.nlm.nih.gov/pubmed/19628432
31. Arumugam M, Raes J, Pelletier E, Le Paslier D, Yamada T, Mende DR, et al. Enterotypes of the human gut microbiome. Nature [Internet]. 2011 [cited 2016 Jun 13];473:174–80. Available from: http://www.ncbi.nlm.nih.gov/pubmed/21508958
32. Abdolrasulnia M, Menachemi N, Shewchuk RM, Ginter PM, Duncan WJ, Brooks RG. Market effects on electronic health record adoption by physicians. Health Care Manage. Rev. [Internet]. [cited 2016 Jun 13];33:243–52. Available from: http://www.ncbi.nlm.nih.gov/pubmed/18580304
33. Marín L, Miguélez EM, Villar CJ, Lombó F. Bioavailability of dietary polyphenols and gut microbiota metabolism: antimicrobial properties. Biomed Res. Int. [Internet]. 2015 [cited 2016 Jun 13];2015:905215. Available from: http://www.ncbi.nlm.nih.gov/pubmed/25802870
34. Kager N, Ferk F, Kundi M, Wagner K-H, Misík M, Knasmüller S. Prevention of oxidative DNA damage in inner organs and lymphocytes of rats by green tea extract. Eur. J. Nutr. [Internet]. 2010 [cited 2016 Jul 11];49:227–34. Available from: http://www.ncbi.nlm.nih.gov/pubmed/19851801
35. Oršolić N, Sirovina D, Gajski G, Garaj-Vrhovac V, Jazvinšćak Jembrek M, Kosalec I. Assessment of DNA damage and lipid peroxidation in diabetic mice: effects of propolis and epigallocatechin gallate (EGCG). Mutat Res. [Internet]. 2013;18:36–44. Available from: http://www.ncbi.nlm.nih.gov/pubmed/23859956
36. Tobi SE, Gilbert M, Paul N, McMillan TJ. The green tea polyphenol, epigallocatechin-3-gallate, protects against the oxidative cellular and genotoxic damage of UVA radiation. Int. J. cancer [Internet]. 2002 [cited 2016 Jul 11];102:439–44. Available from: http://www.ncbi.nlm.nih.gov/pubmed/12432544
37. Lu LY, Ou N, Lu Q-B. Antioxidant induces DNA damage, cell death and mutagenicity in human lung and skin normal cells. Sci. Rep. [Internet]. 2013 [cited 2016 Jul 11];3:3169. Available from: http://www.ncbi.nlm.nih.gov/pubmed/24201298
38. Loughery JEP, Dunne PD, O'Neill KM, Meehan RR, McDaid JR, Walsh CP. DNMT1 deficiency triggers mismatch repair defects in human cells through depletion of repair protein levels in a process involving the DNA damage response. Hum. Mol. Genet. [Internet]. 2011 [cited 2016 Jul 11];20:3241–55. Available from: http://www.ncbi.nlm.nih.gov/pubmed/21636528

39. Jin B, Robertson KD. DNA methyltransferases, DNA damage repair, and cancer. Adv. Exp. Med. Biol. [Internet]. 2013 [cited 2016 Jul 11];754:3–29. Available from: http://www.ncbi.nlm.nih.gov/pubmed/22956494
40. Ahmed S, Marotte H, Kwan K, Ruth JH, Campbell PL, Rabquer BJ, et al. Epigallocatechin-3-gallate inhibits IL-6 synthesis and suppresses transsignaling by enhancing soluble gp130 production. Proc. Natl. Acad. Sci. U. S. A. [Internet]. 2008 [cited 2016 Jun 14];105:14692–7. Available from: http://www.ncbi.nlm.nih.gov/pubmed/18796608
41. Lee WJ, Shim J-Y, Zhu BT. Mechanisms for the inhibition of DNA methyltransferases by tea catechins and bioflavonoids. Mol. Pharmacol. 2005;68:1018–30.
42. Wong CP, Nguyen LP, Noh SK, Bray TM, Bruno RS, Ho E. Induction of regulatory T cells by green tea polyphenol EGCG. Immunol. Lett. [Internet]. 2011 [cited 2016 May 4];139:7–13. Available from: http://www.pubmedcentral.nih.gov/articlerender.fcgi?artid=4125122&tool=pmcentrez&rendertype=abstract
43. Hippe B, Zwielehner J, Liszt K, Lassl C, Unger F, Haslberger AG. Quantification of butyryl CoA:acetate CoA-transferase genes reveals different butyrate production capacity in individuals according to diet and age. FEMS Microbiol. Lett. [Internet]. 2011 [cited 2016 May 3];316:130–5. Available from: http://www.ncbi.nlm.nih.gov/pubmed/21204931

12. Table

Table 1: Body weight, food and water intake of C57BL/6J male mice over a period of 4 months.

Mean ± SD		**Chow intake [g per day]**				**Water intake [ml per day]**				**Weight [g]**			
Month		1	2	3	4	1	2	3	4	1	2	3	4
Intervention	**CD**	2.64 ± 0.17	2.11 ± 0.62	2.08 ± 0.61	1.99 ± 0.64	5.60 ± 0.99	5.36 ± 0.99	5.40 ± 0.91	5.05 ± 1.27	23.99 ± 1.50	25.92 ± 1.09	26.94 ± 1.42	27.88 ± 1.49
	CD+ EGCG	2.67 ± 0.12	2.61 ± 0.13	2.63 ± 0.12	2.62 ± 0.28	5.19 ± 0.61	5.13 ± 0.54	4.83 ± 0.65	4.60 ± 0.39	24.16 ± 1.52	25.81 ± 1.32	26.98 ± 1.53	28.43 ± 1.76
	HFD	2.56 ± 0.10	2.59 ± 0.15	2.60 ± 0.13	2.56 ± 0.13	5.30 ± 0.43	5.13 ± 0.47	4.97 ± 0.54	5.07 ± 0.39	30.54 ± 3.43	37.62 ± 4.11	42.88 ± 4.58	45.99 ± 4.46
	HFD+ EGCG	2.57 ± 0.10	2.50 ± 0.10	2.58 ± 0.13	2.55 ± 0.16	5.07 ± 0.61	4.56 ± 0.40	4.43 ± 0.41	4.55 ± 0.31	30.74 ± 3.43	38.79 ± 3.07	44.72 ± 3.68	47.69 ± 3.45

Table 2: Sequence to analyze and primers for CpG Methylation analysis

Gene	**Primer**	**Sequence (5′->3′)**	**Size (bp)**	**GC%**
DNMT1	FW	Biotin - GTA GGT TGT AGA AGA TAG AAT AGT TTT GA	29	31
	RW	CCC ACT CTC TTA CCC TAT ATA ATA CAT	27	37
	Seq	CCC CTC CCA ATT AAT TTC	18	44.4
	Sequence ID: gb|AH009208.2|			

	DNMT1: at reverse strand of chromosome 9: 20907205–20959888 (52684 bp).			
Sequence to analyse	7104 – CGCGCGCGCGAAAAAGCCGGGGTCTCGT - 7131		27	7 CpGs
MLH1	FW	AGG GTA TTT TAG TTT TTA TTG GTT GGA GA	29	31
	RW	TTA CAC CTC AAT TCC TAA AAT CTC TAT CCC – Biotin	30	37
	Seq	TTT AGT TTT TAG AAA TGA GTT AAT A	25	16
	Sequence ID: ref|XR_379849.3 MLH1: at reverse strand of Chromosome 9: 111228228–111271786 (43559 bp)			
Sequence to analyse	19 - GAAGAGCGGACCGTGAACTTTGACGCGCAAGCGCG TTGCCTTCTA-GCCTGGTGTCGGGCCGCTG - 82		64	8 CpGs

Table 3: Primers and TaqMan®-probes targeting 16rRNA coding regions of bacteria

Target organism	**Primer/ Probe**	**Sequence (5' - 3')**	**Size (bp)**	**Conc. [pmol/µL]**	**Reference**
All Bacteria	Fwd primer	ACT CCT ACG GGA GGC AG	468	10	[44]
	Rev primer	GAC TAC CAG GGT ATC TAA TCC		10	
	Probe	(6-FAM)-TGC CAG CAG CCG CGG TAA TAC-(BHQ-1)		2	
Clostridium cluster IV (Ruminococcaceae)	Fwd primer	GCA CAA GCA GTG GAG T	239	4	[45]
	Rev primer	CTT CCT CCG TTT TGT CAA		4	
	Probe	(6-FAM)-AGG GTT GCG CTC GTT-(BHQ-1)		2	
Cluster XIVa (Lachnospiraceae)	Fwd primer	GCA GTG GGG AAT ATT GCA	477	5	[45]
	Rev primer	CTT TGA GTT TCA TTC TTG CGA A		5	
	Probe	(6-FAM)-aaa tga cgg tac ctg act aa-(BHQ-1)		1,5	
Bacteroi-detes	Fwd primer	GAG AGG AAG GTC CCC CAC	106	3	[46]
	Rev primer	CGC TAC TTG GCT GGT TCA G		3	

	Probe	(6-FAM)-CCA TTG ACC AAT ATT CCT CAC TGC TGC CT-(BHQ-1)		1	
Bifidobacterium spp.	Fwd primer	GCG TGC TTA ACA CAT GCA AGT C	125	3	[47]
	Rev primer	CAC CCG TTT CCA GGA GCT ATT		3	
	Probe	(6-FAM)-TCA CGC ATT ACT CAC CCG TTC GCC-(BHQ-1)		1.5	

Table 4: Primers (SYBR® Green) targeting 16rRNA coding regions of bacteria, *butyryl-coenzyme A (CoA) CoA transferase* genes, and *butyrate kinase* gene

Target organism	**Primer**	**Sequence (5' - 3')**	**Size (bp)**	**Conc. [pmol/µL]**	**Reference**
Lactobacilli	Fwd primer	AGC AGT SGG GAA TCT TCC A	352-700	4	[48]
	Rev primer	ATT YCA CCG CTA CAC ATG		4	
Enterobacteria	Fwd primer	AGC ACC GGC TAA CTC CGT	492-509	3	[49]
	Rev primer	GAA GCC ACG CCT CAA GGG CAC AA	834 - 856	3	
Prevotella	Fwd primer	CACCAAGGCGAC-GATCA	1458	2,5	[50]
	Rev primer	GGATAACGCCYG-GACCT		2,5	
Akkermansia	Fwd primer	CAGCAC-GTGAAGGTGGGGAC	1505	2,5	[51]
	Rev primer	CCTTGCGGTT-GGCTTCAGAT		2,5	
BCoAT gene	Fwd primer	GCIGAICATTTCACITG-GAAYWSITGGCAYATG	~540	27	[52]
	Rev primer	CCTGCCTTTGCA ATRTCIACRAANGC		27	
Butyrate kinase	Fwd primer	TGCTGTWGTTGG-WAGAGGYGGA	273	18	[53]
	Rev Primer	GCAACIGCYTTTTGAT-TTAATGCATGG		18	

Table 5: DNA methylation results, presented as relative methylation (mean ± SD) compared to CD or HFD respectively for every CpG. (Stars indicates significance: *p-value ≤ 0.05, **p-value ≤ 0.01)

Mean ± SD in %	**CD+EGCG compared to CD**	**HFD compared to CD**	**HFD+EGCG compared to HFD**
***Dnmt1* liver**			
CpG1	1.71 ± 0.32*	0.93 ± 0.25	1.62 ± 0.33*
CpG2	1.14 ± 0.21	0.81 ± 0.12	1.10 ± 0.39
CpG3	1.37 ±0.14**	1.48 ± 0.73	1.18 ± 0.19
CpG4	1.19 ± 0.40	0.88 ± 0.48	1.39 ± 0.21
***Dnmt1* colon**			
CpG1	1.07 ± 0.16	1.17 ± 0.24	0.89 ± 0.06
CpG2	1.15 ± 0.30	1.12 ± 0.14	1.19 ± 0.14*
CpG3	0.98 ± 0.27	1.01 ± 0.19	1.23 ± 0.42
CpG4	1.28 ± 0.09*	1.17 ± 0.12	0.98 ± 0.13
***MLH1* colon**			
CpG1	0.38 ± 0.20*	1.08 ± 0.46	0.98 ± 0.48
CpG2	0.66 ± 0.39	0.40 ± 0.03*	0.65 ± 0.13*
CpG3	1.04 ± 0.27	1.36 ± 0.44	0.87 ± 0.31
CpG4	0.62 ± 0.11*	2.13 ± 0.12*	0.76 ± 0.42
CpG5	1.75 ± 0.10*	1.24 ± 0.09*	0.55 ± 0.11*
CpG6	0.37 ± 0.14*	1.53 ± 0.37	0.68 ± 0.70*
***MLH1* liver**			
CpG1	0.56 ± 0.02**	0.43 ± 0.03	0.98 ± 0.21
CpG2	1.65 ± 0.61	1.27 ± 0.37**	1.80 ± 0.42**
CpG3	1.11 ± 0.09	0.75 ± 0.13	1.16 ± 0.10
CpG4	2.73 ± 1.06**	1.73 ± 0.08**	1.13 ± 0.15
CpG5	1.20 ± 0.08**	1.12 ± 0.26**	0.86 ± 0.05**
CpG6	1.20 ± 0.10*	1.60 ± 0.47	0.68 ± 0.16**

13. Figures

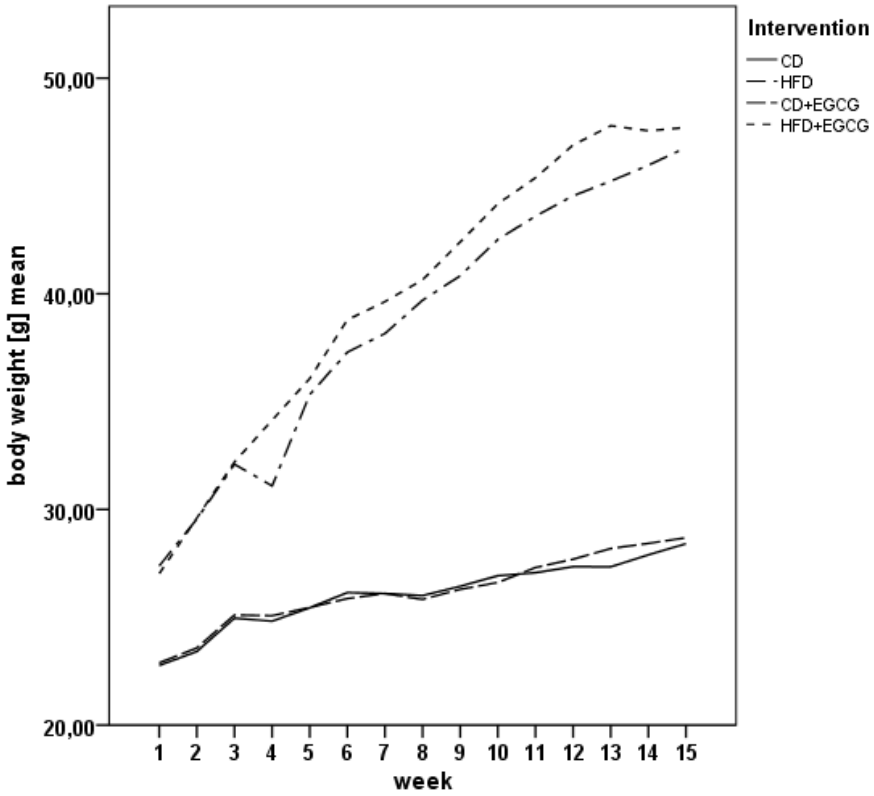

Figure 1: Body weight gain of C57BL/6J male mice over 4 month. (CD= control diet, HFD= high fat diet, CD+EGCG= control diet plus EGCG, HFD+EGCG= high fat diet plus EGCG)

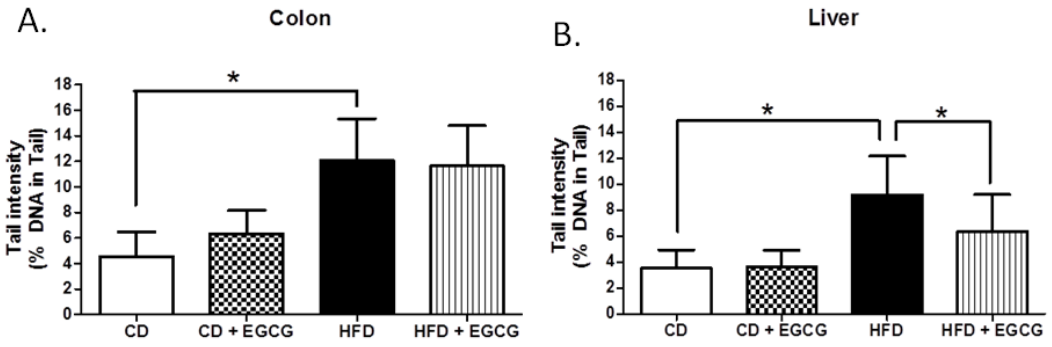

Fig. 2: Impact of EGCG supplementation on DNA damage in colon (A) and liver (B) of C57BL/6J male mice Bars indicate means ± SD of results obtained with 15 animals per group. From each sample, three slides were made and 50 cells were evaluated per slide. (CD= control diet, HFD= high fat diet, CD+EGCG= control diet plus EGCG; HFD+EGCG= high fat diet plus EGCG; Stars indicates significance: *p-value ≤ 0.05)

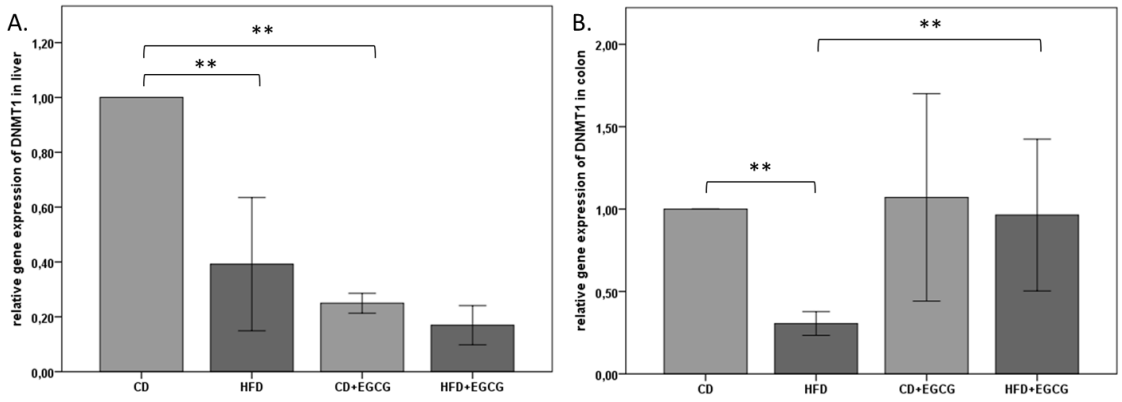

Figure 3: Relative gene expression of *MLH1* in colon (A) and liver (B) of C57BL/6J male mice. All gene expression data are relative to CD and normalized to the house keeping gene *GAPDH*. The error bar represents a 95% confidence interval. (CD= control diet, HFD= high fat diet, CD+EGCG= control diet plus EGCG; HFD+EGCG= high fat diet plus EGCG; Stars indicates significance: *p-value ≤ 0.05, **p-value ≤ 0.01, *p-value ≤ 0.001)

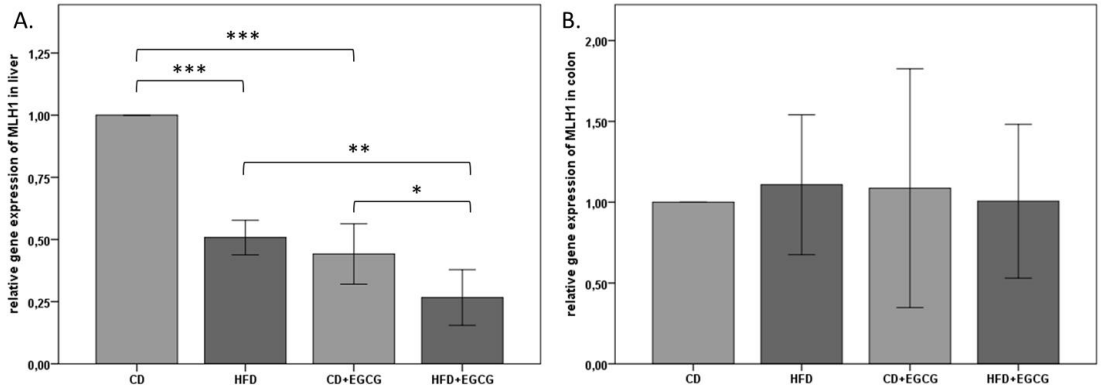

Figure 4: Relative CpG methylation status in promotor region of *MLH1* in liver of C57BL/6J male mice. Mean methylation data are shown for *MLH1* in each intervention group. All methylation data are relative to CD. Error bar represent a 95% confidence interval. In figure 4A significance is shown for CpG 4, 5 and 6. 4B shows significant differences in methylation status in CpG1. (CD= control diet; HFD= high fat diet; CD+EGCG= control diet plus EGCG; HFD+EGCG= high fat diet plus EGCG; Stars indicates significance: *p-value ≤ 0.05, **p-value ≤ 0.01, *p-value ≤ 0.001)

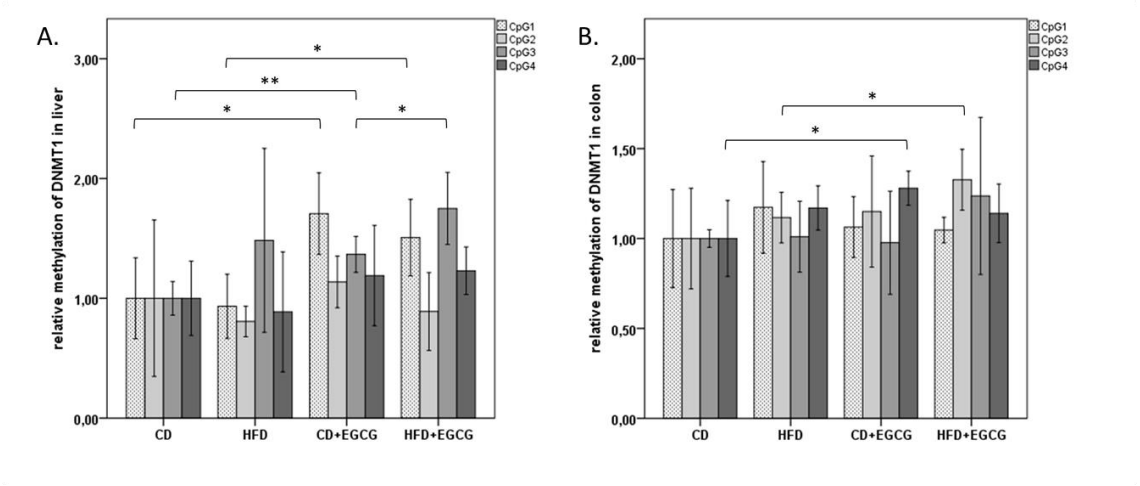

Figure 5: Relative CpG methylation status in promotor region of *MLH1* in colon. Mean methylation data are shown for *MLH1* as an overview 5A (significant for CpG 1, 2, 4) and CpG1 5B. All methylation data are relative to control diet. Error bar represent a 95% confidence interval. (CD= control diet; HFD= high fat diet; CD+EGCG= control diet plus EGCG; HFD+EGCG= high fat diet plus EGCG; Stars indicates significance: *p-value ≤ 0.05, **p-value ≤ 0.01, *p-value ≤ 0.001)

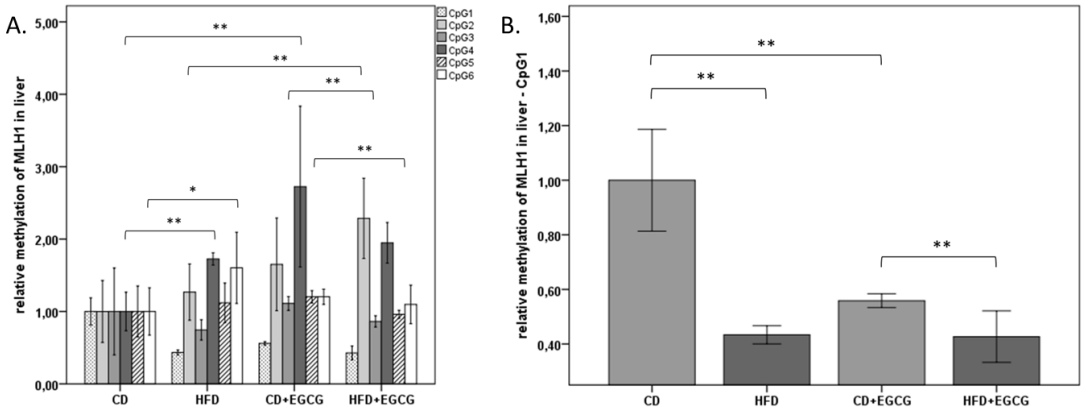

Figure 6: Relative gene expression of *Dnmt1* in colon (A) and liver (B) of C57BL/6J male mice. All gene expression data are relative to CD and normalized to the house keeping gene *GAPDH*. Error bar represents a 95% confidence interval. (CD= control diet; HFD= high fat diet; CD+EGCG= control diet plus EGCG; HFD+EGCG= high fat diet plus EGCG; Stars indicate significances: *p-value ≤ 0.05, **p-value ≤ 0.01, *p-value ≤ 0.001)

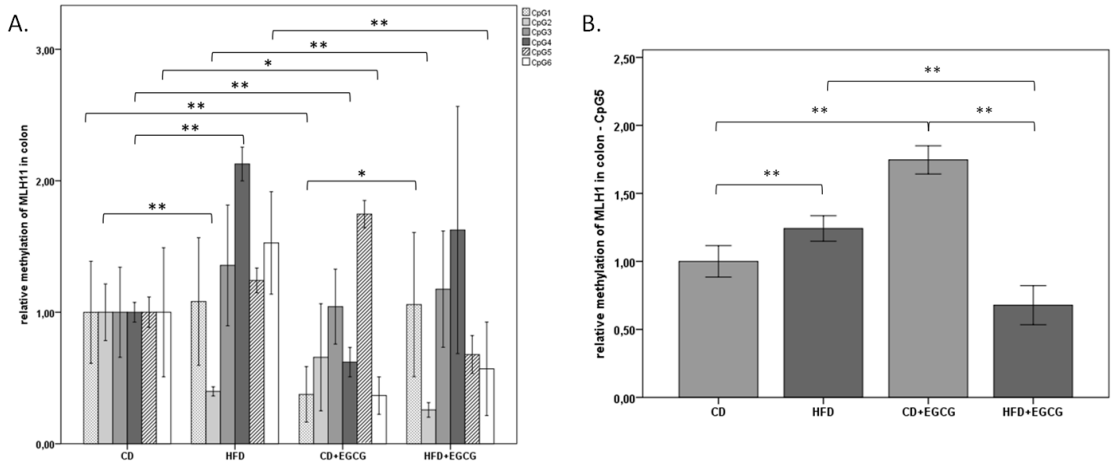

Figure 7: Relative CpG methylation status in promoter region of *Dnmt1* in colon (A) and liver (B) of C57BL/6J male mice. Mean methylation data are shown relative to control diet. Error bar represents a 95% confidence interval. (CD= control diet; HFD= high fat diet; CD+EGCG= control diet plus EGCG; HFD+EGCG= high fat diet plus EGCG Stars indicates significance: *p-value ≤ 0.05, **p-value ≤ 0.01, *p-value ≤ 0.001)

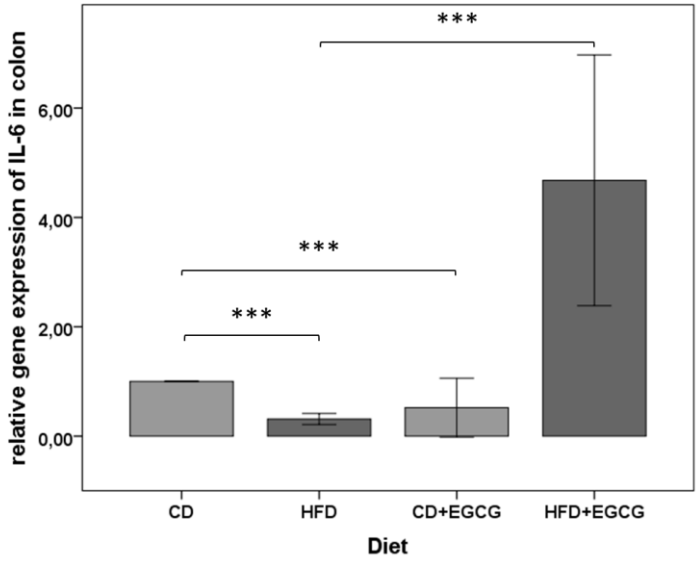

Figure 8: Relative gene expression of IL-6 in colon. All gene expression data are relative to CD and normalized to the house keeping gene *GAPDH*. Error bar represents a 95% confidence interval. (CD= control diet; HFD= high fat diet; CD+EGCG= control diet plus EGCG; HFD+EGCG= high fat diet plus EGCG; Stars indicate significances: *p-value ≤ 0.05, **p-value ≤ 0.01, *p-value ≤ 0.001)

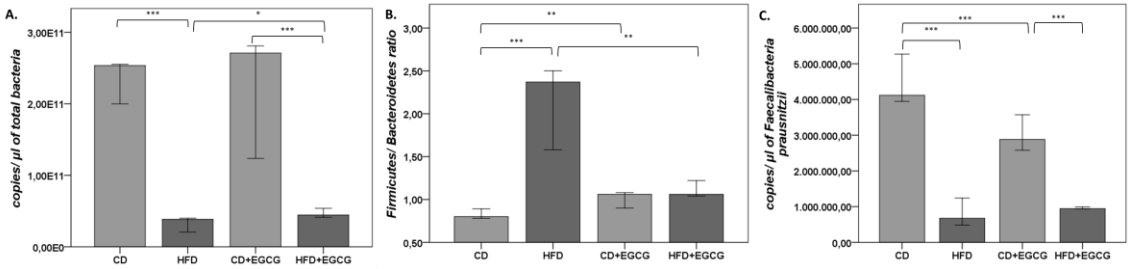

Figure 9: 16S rDNA qPCR quantification of total bacterial abundance (A), *Firmicutes/ Bacteroidetes ratio* (B), and *F. prausnitzii* (D). The error bar represents a 95% confidence interval. (CD= control diet; HFD= high fat diet; CD+EGCG= control diet plus EGCG; HFD+EGCG= high fat diet plus EGCG Stars indicates significance: *p-value ≤ 0.05, **p-value ≤ 0.01, *p-value ≤ 0.01)

14.3 Vitamin E modifies high-fat diet-induced increase of DNA strand breaks, and changes in expression and DNA methylation of *Dnmt1* and *MLH1* in C57BL/6J male mice

Submitted at Genes & Nutrition

Remely Marlene[1a], Ferk Franziska[2b], Sterneder Sonja[1c], Setayesh Tahereh[2d], Tatjana Kepcija[1e], Roth Sylvia[1f], Noorizadeh Rahil [2g], Greunz Martina[1h], Rebhan Irene[1i], Wagner Karl-Heinz[1j], Knasmüller Siegfried[2k], Haslberger Alexander[1*]

1 Department of Nutritional Sciences, University Vienna, Vienna, Austria

1. Abstract

Background:

Obesity is associated with a low-grade inflammation, increased ROS production and DNA damage. Supplementation with antioxidants might ameliorate DNA damage and support epigenetic regulation of DNA repair.

Results:

C57BL/6J male mice were fed a high-fat (HFD) or a control diet (CD) with and without vitamin E supplementation (4.5 mg/kg b.w.). DNA damage was analyzed by SCGE assay, DNA promoter methylation using pyrosequencing. Gene expression of Dnmt1 and a DNA repair gene (MLH1) were assayed in liver and colon to determine the role of HFD and vitamin E in inflammatory processes and DNA damage due to obesity.

Mice increased significantly weight during the study period (4 months). In the HFD group a significant increase in DNA damage in both liver and colon was observed, with a significant decrease in DNA migration due to vitamin E supplementation. The relative expression of the Dnmt1 gene in the colon decreased significantly in the HFD group, whereas vitamin E supplementation caused a significant increase of Dnmt1 gene expression in CD but a significant decrease in HFD. In liver a significant reduction of Dnmt1 gene expression was observed with the HFD and HFD+E compared too respectively CD and CD+E. Of the four analysed CpGs in the promoter region of Dnmt1, CpG 1 showed significant differences in methylation status in the liver and in the colon.

MLH1 relative gene expression in the colon showed a significant increase in CD+E whereas in HFD animals a significant decrease was detected. In colon the gene expression decreased with HFD and with vitamin E supplementation in both groups. In the MLH1 promoter region the relative methylation was analyzed in 6 CpGs, with significant differences appearing in CpG 1 and 2.

Conclusion:

The HFD resulted in organ specific changes in DNA damage, the epigenetically important *Dnmt1* gene, and the DNA repair gene *MLH1*. Vitamin E reduced DNA damage and showed organ-specific effects on *MLH1* and *Dnmt1* gene expression and methylation. These results suggest that intervention with antioxidants and epigenetic active food ingredients should be developed as an effective prevention in obesity- and oxidative stress-induced health risks.

2. Keywords

MLH1 – Dnmt1– DNA damage – gene expression – DNA methylation – SCGE assay

3. Background

Obesity is associated with a positive energy balance, an abnormal increase of adipose tissue and weight gain that impairs health [1]. Genetic factors like single nucleotide polymorphisms, the environment, social status, dietary behavior, metabolism, microbiota, and physical activity are proposed to influence its development [2]. However, the adipose tissue is not merely an energy depot: it is also a highly active metabolic and endocrine organ. Various bioactive peptides, called adipokines, are involved in energy homeostasis, lipid and glucose metabolism, inflammation, fibrinolysis, coagulation, and blood pressure. Among others, they include cytokines such as interleukin-6 (IL-6) and tumor necrosis factor α (TNFα), leptin, monocyte chemoattractant protein-1 (MCP-1), plasminogen activator inhibitor-1 (PAI-1), adiponectin, and resistin, both of which affect insulin [3,4].
In addition to these, an increased reactive oxygen species (ROS) production due to adipocytokines and free fatty acids (FFAs) and increased oxidative stress are reported [5,6]. In obese mice, the ROS production increases in adipose tissue along with an elevated expression of nicotinamide adenine dinucleotide phosphate (NADPH) oxidase and decreased expression of antioxidative enzymes such as superoxide dismutase (SOD), glutathione peroxidase (GPX), and catalase (CAT) as well as altered production of adipocytokines in accumulated fat. Together with a positive correlation of biomarkers for systemic oxidative stress, it is likely that adipose tissue is the main source of elevated

plasma ROS [7]. Oxidative stress is involved in both genome-wide hypomethylation and promoter hypermethylation of DNA [8].

Increased levels of oxygen radicals are involved in DNA damage including base modifications, deletions, strand breaks, and chromosomal rearrangements, which interfere with DNA methylation [9,10]. Guanine within CpG dinucleotides is the favored base for oxidative damage, resulting in the production of 8-oxoguanine (8-oxoG). Substitution of guanine to 8-oxoG reduces the binding capacity of transcription repressor proteins causing persistent transcription of affected genes. However, the methyl group of 5-methylcytosine is similarly accessible to oxidation, forming 5-hydroxy-methylcytosine [10]. Another product of oxidative damage is 8-hydroxy-2-deoxyguanosine within CpG dinucleotides, leading to strong inhibition of cytosine methylation [9]. On the other hand ROS-induced oxidative stress contributes to hypermethylation of normally unmethylated promoter regions, resulting in transcriptional silencing of key antioxidant enzymes as well as tumor suppressor genes [11].

O^6-methylguanine-deoxyribonucleic acidmethyltransferase (MGMT) is a DNA repair enzyme, which is able to repair O^6-methylguanine by eliminating mutagenic and cytotoxic alkyl groups [12,13]. Either the repair protein MutL homologue 1 (MLH1) is part of the DNA mismatch repair (MMR) system [14,15]. This correction of replication errors involves recognition of mismatches and selective removal of the affected DNA region. If the repair of DNA lesions is not accurate, an increase of DNA mutations is the consequence and can cause cellular dysfunctions and diseases including sporadic and hereditary human cancers. In patients with hereditary non-polyposis colorectal cancer, but also a wide variety of other cancers, increased mutations in microsatellite sequences, known as microsatellite instability (MSI), are associated with defects in MMR system [16]. MSI is often associated with promoter hypermethylation, resulting in inactivation of MLH1 [15,16].

The methyl donor *S*-Adenosylmethionin (SAM) is also impaired due to oxidative stress, as methionine is transformed to cysteine, part of the endogenous glutathione to scavenge ROS in cells [17]; an altered expression of DNA methyltransferase 1 (*Dnmt1*) is also reported. In turn the expression changes and may promote health disorders: e.g. in cancer an increased expression has been mentioned [18]. In a mouse model of asthma disease Dnmt1 was down-regulated [19]. Hodge et al. (2001, 2005, 2007) extensively studied the connection between Dnmt1 and the inflammatory cytokine: IL-6. Treatment of cells with IL-6 increased Dnmt1 expression and activity due to transcriptional activation in the promoter [20–22]. Furthermore, the elevated expression of *Dnmt1* coordinated by

IL-6 is negatively correlated with the expression level of tumor suppressor gene p53. It is suggested that IL-6 has the ability to induce p53 promoter methylation through up-regulation of *Dnmt1* [21]. Thus, chronic exposure to low-grade inflammation, especially IL-6, might induce dysregulation of *Dnmt1* gene.

Nutritional interventions, e.g. with antioxidants, may improve DNA methylation and nucleotide biosynthesis reactions and as a consequence DNA repair. We reported previously that a diet rich in antioxidants and vitamins (in particular folate) alters DNA methylation and ameliorates ROS induced epigenetic lesions [23]. It was shown that vitamin E plays a key role in antagonizing oxidative stress associated with lipid metabolism [24] as a direct scavenger of toxic free radicals and induction of antioxidant enzymes, enhancing inflammatory/immune response, modulation of DNA repair systems, and of signal transduction pathways [25]. Tocopherols are known to induce Nuclear factor-erythroid 2-related factor 2 (Nrf2) which plays a central role in transcriptional regulation of antioxidant and detoxification genes and consequently antioxidant and anti-inflammatory processes [26].

Hydroxyl radicals also initiate lipid peroxidation reactions with lipid peroxyl radicals: in the colon tocopherols react with lipid soluble peroxyl radicals and quench the further propagation of free radicals [27]. In the liver oxidative stress is involved in the pathogenesis of various diseases such as non-alcoholic fatty liver disease (NAFLD). NAFLD is the hepatic manifestation of metabolic syndrome and frequently associated with diabetes, hyperlipidemia, and obesity. Antioxidant treatment of NAFLD with vitamin E is a well-established pharmacological approach [28].

Several earlier findings with rodent and humans indicate that obesity induces low-grade inflammatory processes in the following genomic instability [29–31]. One of the strategies to prevent adverse effects of obesity and co-morbidities may be nutritional interventions. In the present study we investigated the impact of vitamin E intake on genomic instability, DNA methylation, and gene expression of *Dnmt1*, and of the DNA repair molecule *MLH1*, assayed in liver and colon of C57BL/6J mice. The colon plays an important role in nutrient absorption, while the liver has important impact on glucose and insulin metabolism as the main organ for insulin clearance from blood. DNA damage was measured in single cell gel electrophoresis (SCGE) experiments which are based on the determination of DNA migration in an electric field: the extent of the size of “comets” reflects formation of single and double strand breaks and apurinic site [32]. DNA methylation was analyzed

with bisulfite converted DNA in a Pyromark, and the expression of candidate genes was assayed from reverse-transcribed complementary DNA (cDNA).

4. Materials and Methods

The animal experiment was approved by the Ethical Committee of the Medical University of Vienna (BMWFW-66.009/0329-WF/V/3b/2014). 6-week-old C57BL/6J male mice (n=60, 15 mice/group, Janvier Labs, France) were used for the animal experiment. 3 animals were kept per cage (Macrolon type III, Techniplast GmbH, Germany) under standard conditions (24 ± 1ºC, humidity 50 ± 5%, 12 hrs light/dark cycle); food and water were provided ad libitum. After 14 days of acclimatization with CD (control diet, EF R/M Control, 11 kJ % fat, ssniff Spezialdiäten GmbH, Soest, Germany) mice were divided into four groups (time point T1: start of intervention): i) a CD group; ii) a CD plus vitamin E group (CD+E; 4.5 mg/kg body weight per day); iii) a HFD group (high fat diet: 54 kJ % fat ssniff EF acc.D12492 (I) mod., ssniff Spezialdiäten GmbH, Soest, Germany); and iv) a HFD plus vitamin E group (HFD+E).

The drinking water of animals was supplemented with vitamin E. The “Aqua E” (Aqua E, http://www.acgrace.com/aqua-e/) containing 20 IU d-alpha-tocopherol, 15 mg other tocopherols, and 2 mg tocotrienols per mL. Aqua E has been used to guarantee an equivalent Vitamin E absorption: according to Papas et al. (2007), Aqua E showed a better bioavailability in malabsorbing patients compared to conventional based supplements [33]. Body weight and food intake were measured weekly, water/vitamin E uptake daily. Animals were sacrificed by cervical dislocation after 4 months (T4: end of intervention).

4.1. SCGE (single cell gel electrophoresis) assay

DNA migration was studied in hepatocytes and colonocytes of mice in SCGE assay. These experiments are based on the measurement of DNA migration in an electric field [34]. Cells from livers and colons were collected according to the method developed by Sasaki et al., (2000) [35]. Briefly, 1.0 g liver tissue was homogenized by use of a Potter Elvehjem-type (B. Braun, Melsungen, Germany) at 400 rpm in 4.0 mL chilled homogenization buffer (pH 7.5). Subsequently, the homogenates were centrifuged (800*g*, 10 min, 4 ºC). Colon cells were isolated by scratching from the colon mucosa and kept on ice in 2.0 mL homogenisation buffer. The nuclei were re-suspended in LMPA (low melting point agarose, 0.5 %, Gibco, Paisley, UK) and transferred to slides which were pre-coated with NMPA (normal melting point agarose, 1.0 %, Gibco, Paisley, UK).

The experiments were carried out according to international guidelines for SCGE experiments [36]. After lysis (pH 10.0) and electrophoresis (30 min, 300 mA, 25 V, at 4 ˚C, pH > 13), the gels were stained with ethidium bromide (20 µg/mL, Sigma-Aldrich, Germany). Three slides were prepared per experimental time point and 50 cells were evaluated from each slide. Slides were examined under a fluorescence microscope (Nikon EFD-3, Japan) using 25-fold magnification. DNA migration was determined with a computer-aided comet assay image analysis system (Comet Assay IV, Perceptive Instruments, UK).

4.2. Gene expression analysis

Colon and liver samples were stored at -80°C. RNA and DNA were isolated from liver and colon using the AllPrep DNA/RNA/miRNA Universal Kit (Qiagen, Germany) according to the manufacturer's protocol and concentration measured respectively purity controlled with a Picodrop100 (Picodrop, UK). Complementary DNA (cDNA) was synthesized from 1 µg of total RNA by reverse transcription using RT2 First Strand Kit (Qiagen, Germany). cDNA was analyzed in real-time PCR using qPCR Primer Assays (Qiagen, Germany) and RT^2 SYBR Green Mastermix (Qiagen, Germany) according to protocol. PCR conditions were as follows: initial step of 95°C for 10 min, followed by 40 cycles of 95°C for 15 s and 60°C for 1 min, ending with melting curve analysis (gradient melting of the products was performed at 0.5°C/10 s from 65°C to 95°C). Each sample was analyzed in duplicate, with normalization to the housekeeping gene glycerinaldehyde-3-phosphate-dehydrogenase (GAPDH) as an internal control.

4.3. Methylation analysis

2.0 µg of genomic DNA was bisulfite converted with EpiTect® Fast Bisulfite Conversion kit (Qiagen, Germany) and amplified by PCR using the PyroMark PCR Kit (Qiagen, Germany) according to manufacturer’s instructions with primers for Dnmt1 and MLH1 designed by PyroMark Assay Design SW 2.0 Software (Table 2).

The PCR was carried out in a total reaction volume of 25.0 µL, containing 12.5 µL Pyromark 2X PCR master mix, 10 pmol (Dnmt1) or 7 pmol (MLH1) of each primer, 2.5 µL Coralload Concentrate 10X (Qiagen, Germany), and 10.0 ng (Dnmt1) or 15.0 ng (MLH1) bisulfite converted DNA. Thermocycling started with initial denaturation at 95 C for 15 min, followed by 45 cycles at 94°C for 30 s, 55.5°C for 45 s, 72°C for 45 s and a final

extension at 72°C for 10 min. PCR product quality was examined with agarose gel-electrophoresis. Analysis of CpG methylation was performed with a Pyromark Q24 MDx (Qiagen, Germany).

4.4. Statistical analyses

In SCGE assays, statistical analyses were performed using GraphPad Prism 5.02 (GraphPad Software, USA). The means and SD of % DNA in the comet tails of the nuclei from the different treatment groups were calculated. Group means were compared using Student´s *t*-test based on the means of three slides.

All statistical analyses of gene expression and methylation analyses were performed using IBM SPSS Advanced Statistics 20.0 (SPSS, USA). All data are shown mean ± SD.

ΔCT values of each gene were calculated by normalization to the housekeeping gene GAPDH (ΔCT = CT-Target – CT-GAPDH). The ΔΔCT value shows the difference between the two groups. The ΔCT value of the control group was deducted from the ΔCT value of the vitamin E group (ΔΔCT = ΔCT-Vitamin E – ΔCT-Control). Relative changes in gene expression between the intervention and control group are determined by the 2-ΔΔCT equation (fold change = 2-ΔΔCT). The Kolmogorov-Smirnov-Test was used to test the normality of the data distribution. To examine significant relationships, Mann-Whitney-U Test was used. The interaction between DNA damage and mean methylation was tested by Spearman correlation test. For all difference-of-mean and correlation tests p-values ≤ 0.05 were considered as significant.

5. Results

5.1. Body weight, food intake and vitamin E uptake

Body weight and food intake were measured weekly and water/vitamin E uptake daily. As shown in Table 1 food intake and total water consumption did not differ between the groups. The body weight of mice fed a HFD (T1: 32.57 ± 2.09 g; T4: 47.09 ± 0.83 g) and of HFD+E (T1: 32.77 ± 2.3 g; T4: 47.67 ± 0.49 g) increased significantly in comparison to CD-fed mice (T1: 24.66 ± 0.75 g; T4: 28.31 ± 0.24 g) and CD+E (T1: 24.94 ± 0.77 g; T4: 28.63 ± 0.14 g) over study period ($p < 0.01$, Figure 1). The body weight increase over study period was significant in all groups ($p < 0.01$, Figure 1).

Mean Vitamin E uptake was 3.90 ± 0.14 µl of Aqua E in the CD group and 5.89 ± 0.11 µl of Aqua E in the HFD group of each mouse per day. The alpha-tocopherol intake was 0.08 IE (CD) and 0.12 IE (HFD) per day and mouse.

5.2. SCGE experiments from colon and liver cells

HFD caused significant induction of DNA damage in both organs compared to CD (Figure 2). The extent of DNA migration was more pronounced in the colon (2.6-fold) than in the liver (2.3-fold). In HFD+E the extent of DNA migration was significantly decreased by 17 % ($p \leq 0.05$) in the colon while no effect was seen in the liver compared to HFD fed mice (Figure 2).
Supplementation with vitamin E in CD group caused significant DNA migration in both organs (1.7-fold in colon and 1.3-fold in liver).

5.3. Relative gene expression (Figure 3) and CpG methylation (Figure 4) of Dnmt1 in colon and liver cells

In colon cells the relative expression of Dnmt1 decreased 61% in HFD compared to CD ($p \leq 0.01$). With vitamin E supplementation Dnmt1 relative gene expression was significantly lower (86%) in HFD+E in comparison to CD+E ($p \leq 0.01$). The relative gene expression of Dnmt1 in colon cells of HFD showed no significant differences in comparison to HFD+E ($p = 0.394$). Relative to CD mice, the vitamin E supplementation (CD+E) resulted in 87 % higher expression of Dnmt1 ($p \leq 0.01$; Figure 3). In the liver a significantly lower expression of Dnmt1 in HFD compared to CD was shown with a reduction of 61 % ($p \leq 0.01$). CD compared to CD+E (79%) and HFD compared to HFD+E (68%) showed both a lower gene expression of Dnmt1 in the liver ($p \leq 0.01$). The relative gene expression of Dnmt1 in liver cells was 25% lower in HFD+E compared to CD+E ($p \leq 0.01$, Figure 3).

Four CpGs were analyzed in the promoter region of Dnmt1 in liver and in colon (Figure 4). In colon cells, significant differences in methylation status were measured in CpG numbers 3 and 4. In CD+E, CpG 3 showed 33.67% lower methylation ($p \leq 0.01$) when compared to CD, and 25.67% lower when compared to HFD+E. Moreover, a significant decrease in methylation of both CpG 3 (17.13%, $p \leq 0.01$) and CpG 4 (21.57%, $p \leq 0.05$) was indicated in HFD+E in comparison to HFD. By comparing HFD with CD, a slight increase in methylation levels was observed in HFD, however, no significant difference

was detected between those two groups (p = 0.394, Figure 4A). In CD a negative correlation between DNA damage and the mean methylation of Dnmt1 in colon was seen (r2 = - 0.837, p≤0.05).

In liver cells, CpG 3 showed the highest relative methylation among all intervention groups. When compared to CD animals, increased methylation levels of CpG 3 were found in HFD, CD+E as well as in HFD+E. Particularly in CD+E, vitamin E supplementation caused a significant hypermethylation of CpG 3 (59.67 %, p ≤ 0.01). No significant difference in Dnmt1 methylation in liver was observed between the HFD and HFD+E group (Figure 4B). Furthermore, in HFD DNA damage correlated positively with the mean methylation of Dnmt1 in the liver (r2 = 0.956, p≤ 0.01).

5.4. Relative gene expression (Figure 5) and CpG methylation (Figure 6-7) of MLH1 in colon and liver cells

The relative gene expression of *MLH1* in colon did not result in significant difference between CD and HFD animals (p = 0.659). However, vitamin E supplementation induced a higher gene expression of *MLH1* in CD+E in comparison to CD (36%, p ≤ 0.01). In contrast HFD vitamin E supplementation caused a significant reduction of 72 % compared to HFD (p ≤ 0.01, Figure 5).

The relative gene expression of *MLH1* in liver was significantly lower in the HFD animals (49 %) compared to CD and HFD+E (53 %) compared to HFD. Vitamin E supplementation induced a significant (58 %) lower expression of *MLH1* in liver compared to CD (p ≤ 0.01; Figure 5).

In the *MLH1* promoter region the relative methylation was analyzed of 6 CpGs in colon (Figure 6) and liver (Figure 7). In colon cells, vitamin E supplementation significantly reduced methylation of CpG number 1 (CD+E: 40.17 %, p ≤ 0.05; HFD+E: 59.30 %, p ≤ 0.01) and 2 (CD+E: 55.00 %, p ≤ 0.01; HFD+E: 76.53 %, p ≤ 0.01) in comparison to CD (Figures 6A and 6B). The same effect has been observed over all six CpGs in HFD+E compared to HFD (all p ≤ 0.01). Significantly different methylation levels between CD and HFD were found in CpG numbers 2, 4 and 5 (all p ≤ 0.01). In general, HFD showed a higher relative methylation over all CpGs with exception of CpG 2, where *MLH1* methylation decreased by 60.17 % in comparison to CD (p ≤ 0.01) (Figures 6A and 6C). In liver cells, similar to the colon, hypomethylation of CpG 1 was found in both supplementation groups (CD+E: 59.63 %; HFD+E: 60.63 %; all p ≤ 0.01) in comparison to CD, and the methylation of CpG 1 was reduced by 56.63 % in HFD (p ≤ 0.01) (Figure 7B). On the contrary, the HFD showed significant hypermethylation of CpG 4 (72.11 %, p ≤ 0.01) and

CpG 6 (11.93 %, $p \leq 0.05$) when compared to CD. In comparison to HFD, vitamin E treatment (HFD+E) significantly decreased the methylation levels of CpG 1 (9.23 %, $p \leq 0.05$) and 6 (35.37 %, $p \leq 0.01$), whereas methylation of CpG 3 significantly increased by 27.57 % ($p \leq 0.05$) (Figure 7A).

6. Discussion

HFD induced a significant increase of DNA damage in liver and colon compared with CD in mice. *Dnmt1* relative gene expression decreased significantly in both organs, whereas methylation status showed a slight increase in HFD compared to CD. The relative gene expression of *MLH1* in colon did not show significant differences between the two different diets, although in liver significantly lower *MLH1* expression was shown in HFD compared to CD. The methylation status of all CpGs was generally higher in HFD in comparison to CD.

Although *IL-6* expression was below the detection limit in our experiment, low-grade inflammation is known as a major cause of obesity caused by the release of FFAs from adipocytes, related to the increased amount of adipose tissue. FFAs are usually stored as triglycerides or provide energy through β-oxidation by cell´s mitochondria. Minor products, ROS, are potentially harmful for cellular functions. A complex antioxidant system provides some protection, although an imbalance due to obesity results in oxidative stress, potentiating comorbidities. Antioxidant therapies have been shown to reduce the oxidative stress, to reduce susceptibility of low-density lipoprotein (LDL) to oxidation, and also to inhibit secretion of pro-inflammatory cytokines[37], to improve insulin signaling *in vitro* [38], and to improve glycemic control in individuals with type 2 diabetes [39–41]. Vitamin E interrupts lipid peroxidation due to the presence of the phenolic hydroxyl group on the chroman ring of the molecule resulting in tocopheroxyl radicals, which are regenerated by means of hydrogen donors. However, due to incomplete reduction, tocopheroxyl radicals can also induce oxidative stress by reaction with polyunsaturated fatty acids in the LDL particles. Thus, Aqua E has been used in concentrations in accordance to recommended daily allowance, although further studies testing different concentrations would be of interest.

Natural vitamin E comprises four tocopherols and four tocotrienols. Therefore, we used a mixture of tocopherols and tocotrienols, which reflects the human diet more accurately than pure alpha- tocopherol, which was used in previous animal and human studies. All forms of the vitamin E family are absorbed and delivered to the liver. Only α-tocopherol

accumulates in this organ, whereas the other isoforms are rapidly metabolized and excreted. The accumulation of mainly α-tocopherol in hepatic tissue is the consequence of the expression of a cytosolic protein (α-tocopherol transfer protein, α-TTP) with high selectivity for α-tocopherol and low or very low affinity for the other tocopherols [42]. α-TTP and other bound vitamin E forms are prevented from being catabolized in the liver. Among the isoforms γ-tocopherol is slightly less efficient than α-tocopherol as a scavenger of oxygen radicals, but it is an efficient scavenger of reactive nitrogen species [43]. In addition tocotrienols have more pronounced cancer protective effects than tocopherol [44], and tocotrienols are notably also more effective in NF-κB inhibition than tocopherols [45].

6.1. Vitamin E protects DNA damage caused by HFD

We found a significant increase of DNA damage with HFD in both organs. Vitamin E supplementation decreased DNA damage. Bardowell et al (2012) estimated that unmetabolized tocopherols and tocotrienols are discarded via biliary excretion in feces [46]. This observation may provide an explanation for more pronounced protective effects in the colon. Ju and coworkers [47] evaluated 32 animal studies published since 1980 with regard to cancer-preventive activities of tocopherols and tocotrienols. Only 12 studies focused on colon tumorigenesis and aberrant crypt foci formation, and only two out of twelve studies showed a protective effect of vitamin E family compounds in colon. Vitamin E has also been shown to protect against liver damage induced by oxidative stress in animal experiments [48,49].

Taken together, this study showed that supplementation of Aqua E with HFD for 4 months significantly improves DNA damage in colon and liver of mice. This identifies vitamin E as an important nutritional factor for preventing of DNA damage caused by oxidative stress due to obesity although the dosage has to be taken into account.

6.2. Vitamin E supplementation affects specific CpG sites of Dnmt1, resulting in altered relative gene expression of *Dnmt1*

As mentioned above oxidative stress due to obesity is involved in both genome-wide hypomethylation and promoter hypermethylation of the DNA [8] as oxygen radicals impair DNA lesions. These lesions interfere with methylation activity since damaged DNA cannot serve as acceptor for methyl groups, causing global hypomethylation [9,10].

The methyl donor SAM and the expression of *Dnmt1* are also impaired by oxidative stress [17,18]. Both are important in the maintenance of epigenetic modifications by adding methyl groups to the C5 position of cytosine in CpG dinucleotides at the replication

fork and are responsible to copy DNA methylation patterns to newly synthesized daughter strands [18]. Thus, altered expression of Dnmt1 can lead to hypo- or hypermethylation of other genes, resulting in expression changes of mRNAs or proteins. Altered levels of Dnmt1 can disrupt cellular mechanisms and may lead to pathological changes of different gene functions [18].

We showed a lower expression of *Dnmt1* in colon of HFD with no changes due to vitamin E supplementation, although in CD animals an increase with supplementation was noted (Figure 3). Methylation status of CpG 3 and 4 in the promoter region of *Dnmt1* in colon is significantly lower in CD+E compared to CD and HFD+E. The same CpGs showed a significantly lower methylation in HFD+E compared with HFD control group. HFD showed a slightly higher promoter methylation status compared to CD (Figure 5). In all intervention groups a decreased gene expression was noted in liver (Figure 3) although the methylation status of CpG 3 was increased in HFD, CD+E as well as in HFD+E. However, no significant differences were observed between the two HFD groups, while in the CD+E group vitamin E supplementation caused a significant hypermethylation of CpG3 (Figure 5). Furthermore, in the liver a positive correlation of *Dnmt1* mean methylation and DNA damage has been observed in liver whereas in CD a correlation has been found in the colon.

In adipose tissue Dnmt1 expression/activity is stimulated by pro-inflammatory signals such as TNFα, IL-1β [50], and IL-6 [20]. IL-6 produced by macrophages, monocytes, lymphocytes, fibroblasts and many other cell types [51,52] plays a crucial role in the defense against stress (infections and injury) [52], in the regulation of the immune system, inflammation, acute immune response, energy expenditure, lipid metabolism, and carcinogenesis [53,54]. We did not detect a higher gene expression of *IL-6* between the groups in colon and liver. However, others showed a significant decrease of the inflammatory status in type 2 diabetics due to vitamin E supplementation (800 IU/day), indicated by decreased plasma levels of C reactive protein (CRP) [55]. Inhibition of IL-1β release decreases the expression of IL-6 and further of CRP [37]. However, an antioxidant-independent effect via a decrease of 5-lipoxygenase activity is suggested [56], although no changes of inflammatory markers and of plasma CRP levels were observed due to vitamin E supplementation (800 IU/day and 1200 IU/day) in overweight individuals [41]. Adverse effects were also shown, such as increased risk for heart failure [57] or increased risk of hemorrhagic stroke [58]. Furthermore, tumor suppressor genes or cell

cycle regulation may be affected leading to aberrant cell growth [20]. Thus, a routine vitamin E supplementation due to obesity is not recommended at the present.

Recent research indicated the requirement of an ubiquitin interacting motif (UIM) in the N-terminal regulatory domain of *Dnmt1*, which binds to ubiquitinated H3 tails and is essential for DNA methylation *in vivo*. H3 ubiquitination and subsequent DNA methylation were shown to require UHRF1 (Ubiquitin-like, Containing PHD and RING Finger Domains, 1) PHD (plant
homeodomain) binding to H3R2 [59]. In addition, we should consider that the methylation status and gene expression are only snapshots, and cell cycle information is missing. However, Fuks et al. (2000) disclosed the interaction of *Dnmt1* with histone deacetylase activity and repression of gene transcription *in vivo* [60]. In diet induced obesity (DIO) mice the binding of HDACs is increased at the leptin promoter whereas histones H3 and H4 are hypoacetylated, lysine 4 of histone H3 (H3K4) is hypomethylated. The methylation and the binding of DNMTs and methyl-CpG-binding domain protein 2 (MBD2) are increased and RNA Pol II is decreased, resulting in a negative correlation of leptin promoter methylation and leptin gene transcription. These modifications may indicate a feedback loop for the maintenance of leptin concentrations due to obesity [61]. In another DIO mouse model, *Dnmt1* expression and enzymatic activity were elevated in adipocytes, leading to promoter hypermethylation and following decreased adiponectin expression [50]. Vitamin E supplementation might improve insulin sensitivity and the associated features of insulin resistance in overweight individuals.

Potential compensatory effects in response to a lack or oversupply of methyl groups for DNA methylation may also affect *Dnmt1* expression [62]. The sequence [5'-TTTCCGCG-3'] within the genomic methylation analysis (CpG 1, 2 in our study), was identified as crucial site for the transcriptional regulation of Dnmt1 by the transcription factor E2F1 [63,64]. However, we were not able to show significant changes on these specific CpG sites. These results disclose the various mechanisms controlling Dnmt1 activity and the multifaceted interplay between DNA and histone modifications, or even the diverse effects on other CpG methylation of target gene promoters. Thus, we were not able to elucidate how and if Dnmt1 regulates the MMR system in the current study, although a coherence is shown with *MLH1*.

6.3. Vitamin E supplementation affects specific CpG sites of MLH1, inducing a lower gene expression of MLH1 with high-fat diet

MLH1 is part of the MMR system that is responsible for ensuring overall DNA integrity [14]. Enhanced oxidative stress, as a consequence of overweight and obesity, can cause elevated DNA damage [65] which in turn requires optimal function of the MMR system, including MLH1.

We showed a higher gene expression of *MLH1* in CD+E in comparison to CD and HFD in colon, whereas in HFD+E *MLH1* gene expression decreased (Figure 4). The methylation status of 6 CpGs in the promoter region of *MLH1* in colon showed a higher methylation over all CpGs in comparison to CD (Figure 6). In addition, vitamin E supplementation induced a lower methylation of specific CpG sites in both supplemented groups, also shown in liver cells. Vitamin E supplementation induced a lower expression of *MLH1* in liver (Figure 4). Both HFD groups also had lower expression compared to CD. CpG 4 and 6 were significantly hypermethylated in HFD compared to CD. Comparisons between HFD and HFD+E showed significant differences in methylation levels of 3 CpG sites (Figure 7).

Switzeny et al. (2012) showed a significant higher CpG methylation in two particular *MLH1* promoter regions. The methylation status and DNA strand breaks correlated significantly [23], although no changes in gene expression of *MLH1* due to dietary intervention with folate in non-insulin dependent diabetes mellitus type 2 was shown. Thus, our results are in accordance with previously published data using antioxidants. Sinicrope et al. (2015) indicated a “less likely” deficient MMR in colon cancers from obese patients, suggesting that obesity-associated colon cancers are predominantly caused by sufficient MMR, a molecular subtype showing chromosomal instability with significantly worse survival rates. Although only the deficient MMR colon cancers are associated with a higher DNA methylation near gene promoter regions of MLH1. Higher estradiol levels in both sexes due to obesity might be the cause of the lower frequency of deficient MMR system [66].

In summary, differences in gene expression might indicate tissue specificity, different metabolic pathways, especially as a higher nutrient bioavailability is indicated in colon, main transit organ, but not in the metabolizing organ (liver), with substance dependence in the enterohepatic pathway or the transport system (blood). Differences in methylation status might already indicate an adaption to dietary intervention, although the duration is not sufficient for ROS-dependent defects in gene expression. Differences of methylation

status of different CpG-sites in promoter regions are rarely known, although some CpG sites show more profound results between our groups. The involvement of other epigenetic modifications has to be taken also into account: DNA methylation at gene promoters regulates gene expression through a complicated mechanism involving multiple modifications, including histone modifications and miRNAs. Similar results seen in *in vitro* experiments with Caco2 cells will be submitted for publication soon.

7. Conclusions

Our study with C57BL/6J male mice fed a HFD or CD with or without supplemental vitamin E shows significant effects of HFD on DNA damage, analyzed in SCGE assays. HFD also resulted in significant organ-specific changes in the epigenetically important *Dnmt1* gene and the DNA repair gene *MLH1*. Vitamin E reduced DNA damage and affected *Dnmt1* and *MLH1* gene expression and methylation, also organ specific. These results suggest that intervention with vitamin E, as an epigenetic active food ingredient, can be developed as an effective prevention of obesity-related and oxidative stress-induced health risks.

8. Acknowledgement

The work was funded by the Austrian Science Fund (FWF; AP2658721). The authors thank Dr. Brian Metscher for the English corrections.

9. List of abbreviations

α -TTP	α -tocopherol transfer protein
CAT	catalase
CD	control diet
CD+E	control diet plus vitamin E
cDNA	complementary DNA
CRP	C reactive protein
CYPs	cytochrome P450s
DIO	diet induced obesity
Dnmt1	DNA methyltransferase 1
FFAs	free fatty acids
GAPDH	glycerinaldehyd-3-phosphat-Dehydrogenase
GPX	glutathione peroxidase
H	histone
HFD	high fat diet
HFD+E	high fat diet plus vitamin E
IL-6	interleukin-6
LDL	low-density lipoprotein
LMPA	low melting point agarose
MBD2	methyl-CpG-binding domain protein 2
MCP-1	monocyte chemoattractant protein-1
MGMT	O6-methylguanine-deoxyribonucleic acidmethyltransferase
MLH1	MutL homologue 1

MMR	DNA mismatch repair
MSI	microsatellite instability
NADPH	nicotinamide adenine dinucleotide phosphate
NAFLD	non-alcoholic fatty liver diseases
NMPA	normal melting point agarose
Nrf2	Nuclear factor-erythroid 2-related factor 2
PAI-1	plasminogen activator inhibitor-1
PHD	plant homeodomain
ROS	reactive oxygen species
SAM	S-Adenosylmethionin
SCGE	single cell gel electrophoresis
SOD	superoxide dismutase
TNFα	tumor necrosis factor α
T	time point
UHRF1	Ubiquitin-like, Containing PHD and RING Finger Domains 1
UIM	ubiquitin interacting motif

10. Ethics Approval

The animal experiment was approved by the Ethical Committee of the Medical University of Vienna (BMWFW-66.009/0329-WF/V/3b/2014).

11. Availability of data and supporting materials section

Please find enclosed.

12. Competing Interests

The authors declare to have no actual or potential competing interests that might be perceived as influencing the results or interpretation of a reported study.

13. Funding

The work has been funded by FWF (AP2658721).

14. Authors' contribution

MR together with AH, Univ. Prof. KHW, and SK were the main coordinators for the project: project design, realization, availability of resources etc. MR in addition was responsible to establish analysis methods with the master students IR and MG. Together with SS, SR and TK she did the animal care and analysis of epigenetic markers and gene expression. SS additionally contributed to statistical analysis. FF, ST and NR performed the SCGE experiments. MS was the main contributor to the manuscript, FF contributed the according parts of SCGE experiments and helped improving the manuscript as well as AH, KHW, and SK.

15. References

1. WHO Consultation on Obesity. Obesity: preventing and managing the global epidemic. Report of a WHO consultation. World Health Organ. Tech. Rep. Ser. 2000. p. i – xii, 1–253.

2. Fazel S, Luigi G, Daglia M, Mohammad S. Role of quercetin as an alternative for obesity treatment : You are what you eat ! 2015;179:305–10.

3. Fernández-Sánchez A, Madrigal-Santillán E, Bautista M, Esquivel-Soto J, Morales-González Á, Esquivel-Chirino C, et al. Inflammation, oxidative stress, and obesity. Int. J. Mol. Sci. 2011;12:3117–32.

4. Kershaw EE, Flier JS. Adipose Tissue as an Endocrine Organ. J. Clin. Endocrinol. Metab. 2004;89:2548–56.

5. Savini I, Catani MV, Evangelista D, Gasperi V, Avigliano L. Obesity-associated oxidative stress: Strategies finalized to improve redox state. Int. J. Mol. Sci. 2013;14:10497–538.

6. Le Lay S, Simard G, Martinez MC, Andriantsitohaina R. Oxidative Stress and Metabolic Pathologies: From an Adipocentric Point of View. Oxid. Med. Cell. Longev. 2014;2014:908539.

7. Furukawa S, Fujita T, Shimabukuro M, Iwaki M, Yamada Y, Nakajima Y, et al. Increased oxidative stress in obesity and its impact on metabolic syndrome. J. Clin. Invest. 2004;114:1752–61.

8. Thanan R, Oikawa S, Hiraku Y, Ohnishi S, Ma N, Pinlaor S, et al. Oxidative Stress and Its Significant Roles in Neurodegenerative Diseases and Cancer. Int. J. Mol. Sci. 2014;16:193–217.

9. Franco R, Schoneveld O, Georgakilas AG, Panayiotidis MI. Oxidative stress, DNA methylation and carcinogenesis. Cancer Lett. 2008;266:6–11.

10. Donkena KV, Young CYF, Tindall DJ. Oxidative stress and DNA methylation in prostate cancer. Obstet. Gynecol. Int. 2010;2010:302051.

11. Ziech D, Franco R, Pappa A, Panayiotidis MI. Reactive oxygen species (ROS)--induced genetic and epigenetic alterations in human carcinogenesis. Mutat. Res. Elsevier B.V.; 2011;711:167–73.

12. Chahal M, Xu Y, Lesniak D, Graham K, Famulski K, Christensen JG, et al. MGMT modulates glioblastoma angiogenesis and response to the tyrosine kinase inhibitor sunitinib. Neuro. Oncol. 2010;12:822–33.

13. Kovalchuk O, Burke P, Besplug J, Slovack M, Filkowski J, Pogribny I. Methylation changes in muscle and liver tissues of male and female mice exposed to acute and chronic low-dose X-ray-irradiation. Mutat. Res. 2004;548:75–84.

14. Harfe BD, Jinks-Robertson S. DNA mismatch repair and genetic instability. Annu. Rev. Genet. 2000;34:359–99.

15. Peltomäki P. Role of DNA mismatch repair defects in the pathogenesis of human cancer. J. Clin. Oncol. 2003;21:1174–9.

16. Li G-M. Mechanisms and functions of DNA mismatch repair. Cell Res. 2008;18:85–98.

17. Hitchler MJ, Domann FE. An epigenetic perspective on the free radical theory of development. Free Radic. Biol. Med. 2007;43:1023–36.

18. Subramaniam D, Thombre R, Dhar A, Anant S. DNA methyltransferases: a novel target for prevention and therapy. Front. Oncol. 2014;4:80.

19. Verma M, Chattopadhyay BD, Paul BN. Epigenetic regulation of DNMT1 gene in mouse model of asthma disease. Mol. Biol. Rep. 2013;40:2357–68.

20. Hodge DR, Xiao W, Clausen P a, Heidecker G, Szyf M, Farrar WL. Interleukin-6 regulation of the human DNA methyltransferase (HDNMT) gene in human erythroleukemia cells. J. Biol. Chem. 2001;276:39508–11.

21. Hodge DR. Interleukin 6 Supports the Maintenance of p53 Tumor Suppressor Gene Promoter Methylation. Cancer Res. 2005;65:4673–82.

22. Hodge DR, Cho E, Copeland TD, Guszczynski T, Yang E, Seth AK, et al. IL-6 enhances the nuclear translocation of DNA cytosine-5-methyltransferase 1 (DNMT1) via phosphorylation of the nuclear localization sequence by the AKT kinase. Cancer Genomics Proteomics [Internet]. 2007 [cited 2016 Feb 23];4:387–98. Available from: http://www.ncbi.nlm.nih.gov/pubmed/18204201

23. Switzeny OJ, Mullner E, Wagner KH, Brath H, Aumuller E, Haslberger AG. Vitamin and antioxidant rich diet increases MLH1 promoter DNA methylation in DMT2 subjects. Clin Epigenetics [Internet]. 2012/10/03 ed. 2012;4:19. Available from: http://www.ncbi.nlm.nih.gov/entrez/query.fcgi?cmd=Retrieve&db=PubMed&dopt=Citation&list_uids=23025454

24. Colombo ML. An update on vitamin E, tocopherol and tocotrienol-perspectives. Molecules [Internet]. Molecular Diversity Preservation International; 2010 [cited 2015 Aug 31];15:2103–13. Available from: http://www.mdpi.com/1420-3049/15/4/2103

25. Mocchegiani E, Costarelli L, Giacconi R, Malavolta M, Basso A, Piacenza F, et al. Vitamin E-gene interactions in aging and inflammatory age-related diseases: implications for treatment. A systematic review. Ageing Res. Rev. [Internet]. 2014 [cited 2015 Aug 31];14:81–101. Available from: http://www.sciencedirect.com/science/article/pii/S1568163714000026

26. Li G, Lee M-J, Liu AB, Yang Z, Lin Y, Shih WJ, et al. The antioxidant and anti-inflammatory activities of tocopherols are independent of Nrf2 in mice. Free Radic. Biol. Med. [Internet]. 2012 [cited 2015 Sep 15];52:1151–8. Available from: http://www.sciencedirect.com/science/article/pii/S0891584911012305

27. Stone WL, Papas AM. Tocopherols and the etiology of colon cancer. J. Natl. Cancer Inst. [Internet]. 1997 [cited 2015 Sep 23];89:1006–14. Available from: http://www.ncbi.nlm.nih.gov/pubmed/9230882

28. Traussnigg S, Kienbacher C, Halilbasic E, Rechling C, Kazemi-Shirazi L, Hofer H, et al. Challenges and Management of Liver Cirrhosis: Practical Issues in the Therapy of Patients with Cirrhosis due to NAFLD and NASH. Dig. Dis. [Internet]. 2015 [cited 2015 Sep 23];33:598–607. Available from: http://www.ncbi.nlm.nih.gov/pubmed/26159280

29. Dias FM, Leffa DD, Daumann F, Marques S de O, Luciano TF, Possato JC, et al. Acerola (Malpighia emarginata DC.) juice intake protects against alterations to proteins involved in inflammatory and lipolysis pathways in the adipose tissue of obese mice fed a cafeteria diet. Lipids Health Dis. [Internet]. BioMed Central; 2014 [cited 2016 Apr 19];13:24. Available from: http://lipidworld.biomedcentral.com/articles/10.1186/1476-511X-13-24

30. Hakkak R, Korourian S, Pavliv O, Evans T, Melnyk S. Effects of obesity on development of oxidative stress and DNA damages in liver of the obese Zucker rat (643.1). FASEB J [Internet]. 2014 [cited 2016 Apr 19];28:643.1 – . Available from: http://www.fasebj.org/content/28/1_Supplement/643.1

31. Al-Aubaidy HA, Jelinek HF. Oxidative DNA damage and obesity in type 2 diabetes mellitus. Eur. J. Endocrinol. [Internet]. 2011 [cited 2016 Apr 19];164:899–904. Available from: http://www.ncbi.nlm.nih.gov/pubmed/21436346

32. Collins AR, Oscoz AA, Brunborg G, Gaivão I, Giovannelli L, Kruszewski M, et al. The comet assay: topical issues. Mutagenesis [Internet]. 2008 [cited 2016 Apr 18];23:143–51. Available from: http://mutage.oxfordjournals.org/content/23/3/143.full

33. Papas K, Kalbfleisch J, Mohon R. Bioavailability of a novel, water-soluble vitamin E formulation in malabsorbing patients. Dig. Dis. Sci. [Internet]. 2007 [cited 2016 Jan 27];52:347–52. Available from: http://www.ncbi.nlm.nih.gov/pubmed/17216337

34. Tice RR, Agurell E, Anderson D, Burlinson B, Hartmann A, Kobayashi H, et al. Single cell gel/comet assay: guidelines for in vitro and in vivo genetic toxicology testing. Env. Mol Mutagen [Internet]. 2000/03/29 ed. 2000;35:206–21. Available from: http://www.ncbi.nlm.nih.gov/entrez/query.fcgi?cmd=Retrieve&db=PubMed&dopt=Citation&list_uids=10737956

35. Sasaki YF, Kawaguchi S, Kamaya A, Ohshita M, Kabasawa K, Iwama K, et al. The comet assay with 8 mouse organs: results with 39 currently used food additives. Mutat. Res. [Internet]. 2002 [cited 2016 Feb 16];519:103–19. Available from: http://www.ncbi.nlm.nih.gov/pubmed/12160896

36. Burlinson B, Tice RR, Speit G, Agurell E, Brendler-Schwaab SY, Collins AR, et al. Fourth International Workgroup on Genotoxicity testing: results of the in vivo Comet assay workgroup. Mutat Res [Internet]. 2006/11/23 ed. 2007;627:31–5. Available from: http://www.ncbi.nlm.nih.gov/entrez/query.fcgi?cmd=Retrieve&db=PubMed&dopt=Citation&list_uids=17118697

37. Devaraj S, Jialal I. The effects of alpha-tocopherol on critical cells in atherogenesis. Curr. Opin. Lipidol. [Internet]. 1998 [cited 2016 Jan 12];9:11–5. Available from: http://www.ncbi.nlm.nih.gov/pubmed/9502329

38. Maddux BA, See W, Lawrence JC, Goldfine AL, Goldfine ID, Evans JL. Protection Against Oxidative Stress--Induced Insulin Resistance in Rat L6 Muscle Cells by Micromolar Concentrations of -Lipoic Acid. Diabetes [Internet]. American Diabetes Association; 2001 [cited 2016 Jan 13];50:404–10. Available from: http://paperity.org/p/45165484/protection-against-oxidative-stress-induced-insulin-resistance-in-rat-l6-muscle-cells-by

39. Paolisso G, D'Amore A, Galzerano D, Balbi V, Giugliano D, Varricchio M, et al. Daily vitamin E supplements improve metabolic control but not insulin secretion in elderly type II diabetic patients. Diabetes Care [Internet]. 1993 [cited 2016 Jan 13];16:1433–7. Available from: http://www.ncbi.nlm.nih.gov/pubmed/8299431

40. Jacob S, Ruus P, Hermann R, Tritschler H., Maerker E, Renn W, et al. Oral administration of rac-α-lipoic acid modulates insulin sensitivity in patients with type-2 diabetes mellitus: a placebo-controlled pilot trial. Free Radic. Biol. Med. [Internet]. 1999 [cited 2016 Jan 13];27:309–14. Available from: http://www.sciencedirect.com/science/article/pii/S0891584999000891

41. Manning PJ, Sutherland WHF, Walker RJ, Williams SM, De Jong SA, Ryalls AR, et al. Effect of high-dose vitamin E on insulin resistance and associated parameters in overweight subjects. Diabetes Care [Internet]. 2004 [cited 2016 Jan 13];27:2166–71. Available from: http://www.ncbi.nlm.nih.gov/pubmed/15333479

42. Sato Y, Hagiwara K, Arai H, Inoue K. Purification and characterization of the alpha-tocopherol transfer protein from rat liver. FEBS Lett. [Internet]. 1991 [cited 2016 Feb 16];288:41–5. Available from: http://www.ncbi.nlm.nih.gov/pubmed/1879562

43. Raederstorff D, Wyss A, Calder PC, Weber P, Eggersdorfer M. Vitamin E function and requirements in relation to PUFA. Br. J. Nutr. [Internet]. 2015 [cited 2016 Feb 16];114:1113–22. Available from: http://www.pubmedcentral.nih.gov/articlerender.fcgi?artid=4594047&tool=pmcentrez&rendertype=abstract

44. Krebs und Ernährung - Thieme.de - Thieme Webshop - Siegfried Knasmüller [Internet]. [cited

2016 Apr 18]. Available from: https://www.thieme.de/shop/Endokrinologie--Diabetologie/Knasmueller-Krebs-und-Ernaehrung-9783131542113/p/000000000269440101

45. Aggarwal BB, Sundaram C, Prasad S, Kannappan R. Tocotrienols, the vitamin E of the 21st century: its potential against cancer and other chronic diseases. Biochem. Pharmacol. [Internet]. 2010 [cited 2016 Apr 18];80:1613–31. Available from: http://www.pubmedcentral.nih.gov/articlerender.fcgi?artid=2956867&tool=pmcentrez&rendertype=abstract

46. Bardowell SA, Duan F, Manor D, Swanson JE, Parker RS. Disruption of mouse cytochrome p450 4f14 (Cyp4f14 gene) causes severe perturbations in vitamin E metabolism. J. Biol. Chem. [Internet]. 2012 [cited 2016 Feb 16];287:26077–86. Available from: http://www.pubmedcentral.nih.gov/articlerender.fcgi?artid=3406691&tool=pmcentrez&rendertype=abstract

47. Ju J, Picinich SC, Yang Z, Zhao Y, Suh N, Kong A-N, et al. Cancer-preventive activities of tocopherols and tocotrienols. Carcinogenesis [Internet]. 2010 [cited 2016 Feb 16];31:533–42. Available from: http://www.pubmedcentral.nih.gov/articlerender.fcgi?artid=2860705&tool=pmcentrez&rendertype=abstract

48. Factor VM, Laskowska D, Jensen MR, Woitach JT, Popescu NC, Thorgeirsson SS. Vitamin E reduces chromosomal damage and inhibits hepatic tumor formation in a transgenic mouse model. Proc. Natl. Acad. Sci. U. S. A. [Internet]. 2000 [cited 2016 Feb 16];97:2196–201. Available from: http://www.pnas.org/content/97/5/2196.abstract

49. Kakizaki S, Takagi H, Fukusato T, Toyoda M, Horiguchi N, Sato K, et al. Effect of alpha-tocopherol on hepatocarcinogenesis in transforming growth factor-alpha (TGF-alpha) transgenic mice treated with diethylnitrosamine. Int. J. Vitam. Nutr. Res. Int. Zeitschrift für Vitamin- und Ernährungsforschung. J. Int. Vitaminol. Nutr. [Internet]. 2001 [cited 2016 Feb 16];71:261–7. Available from: http://www.ncbi.nlm.nih.gov/pubmed/11725690

50. Kim AY, Park YJ, Pan X, Shin KC, Kwak S-H, Bassas AF, et al. Obesity-induced DNA hypermethylation of the adiponectin gene mediates insulin resistance. Nat. Commun. Nature Publishing Group; 2015;6:7585.

51. Ireland SJ, Monson NL, Davis LS. Seeking balance: Potentiation and inhibition of multiple sclerosis autoimmune responses by IL-6 and IL-10. Cytokine. Elsevier Ltd; 2015;73:236–44.

52. Mesquida M, Leszczynska A, Llorenç V, Adán A. Interleukin-6 blockade in ocular inflammatory diseases. Clin. Exp. Immunol. 2014;176:301–9.

53. Yoshida Y, Tanaka T. Interleukin 6 and rheumatoid arthritis. Biomed Res. Int. 2014;2014.

54. Ma Y, Gao M, Sun H, Liu D. Interleukin-6 gene transfer reverses body weight gain and fatty liver in obese mice. Biochim. Biophys. Acta - Mol. Basis Dis. Elsevier B.V.; 2015;1852:1001–11.

55. Upritchard JE, Sutherland WH, Mann JI. Effect of supplementation with tomato juice, vitamin E, and vitamin C on LDL oxidation and products of inflammatory activity in type 2 diabetes. Diabetes Care [Internet]. 2000 [cited 2016 Jan 13];23:733–8. Available from: http://www.ncbi.nlm.nih.gov/pubmed/10840987

56. Devaraj S, Jialal I. Alpha-tocopherol decreases interleukin-1 beta release from activated human monocytes by inhibition of 5-lipoxygenase. Arterioscler. Thromb. Vasc. Biol. [Internet]. 1999 [cited 2016 Jan 13];19:1125–33. Available from: http://www.ncbi.nlm.nih.gov/pubmed/10195945

57. Lonn E, Bosch J, Yusuf S, Sheridan P, Pogue J, Arnold JMO, et al. Effects of long-term vitamin E

supplementation on cardiovascular events and cancer: a randomized controlled trial. JAMA [Internet]. American Medical Association; 2005 [cited 2016 Jan 3];293:1338–47. Available from: http://jama.jamanetwork.com/article.aspx?articleid=200541

58. Sesso HD, Buring JE, Christen WG, Kurth T, Belanger C, MacFadyen J, et al. Vitamins E and C in the prevention of cardiovascular disease in men: the Physicians' Health Study II randomized controlled trial. JAMA [Internet]. 2008 [cited 2015 Sep 3];300:2123–33. Available from: http://www.pubmedcentral.nih.gov/articlerender.fcgi?artid=2586922&tool=pmcentrez&rendertype=abstract

59. Qin W, Wolf P, Liu N, Link S, Smets M, La Mastra F, et al. DNA methylation requires a DNMT1 ubiquitin interacting motif (UIM) and histone ubiquitination. Cell Res. [Internet]. Shanghai Institutes for Biological Sciences, Chinese Academy of Sciences; 2015 [cited 2016 Jan 22];25:911–29. Available from: http://dx.doi.org/10.1038/cr.2015.72

60. Fuks F, Burgers WA, Brehm A, Hughes-Davies L, Kouzarides T. DNA methyltransferase Dnmt1 associates with histone deacetylase activity. Nat. Genet. [Internet]. 2000 [cited 2016 Jan 7];24:88–91. Available from: http://www.ncbi.nlm.nih.gov/pubmed/10615135

61. Shen W, Wang C, Xia L, Fan C, Dong H, Deckelbaum RJ, et al. Epigenetic modification of the leptin promoter in diet-induced obese mice and the effects of N-3 polyunsaturated fatty acids. Sci. Rep. [Internet]. Nature Publishing Group; 2014 [cited 2016 Feb 11];4:5282. Available from: http://www.nature.com/srep/2014/140613/srep05282/full/srep05282.html

62. Martínez JA, Milagro FI, Claycombe KJ, Schalinske KL. Epigenetics in adipose tissue, obesity, weight loss, and diabetes. Adv. Nutr. [Internet]. 2014 [cited 2016 Jan 17];5:71–81. Available from: http://advances.nutrition.org/content/5/1/71.full

63. Kimura H, Nakamura T, Ogawa T, Tanaka S, Shiota K. Transcription of mouse DNA methyltransferase 1 (Dnmt1) is regulated by both E2F-Rb-HDAC-dependent and -independent pathways. Nucleic Acids Res. 2003;31:3101–13.

64. McCabe MT, Davis JN, Day ML. Regulation of DNA Methyltransferase 1 by the pRb/E2F1 Pathway. Cancer Res. 2005;65:3624–32.

65. Roberts CK, Sindhu KK. Oxidative stress and metabolic syndrome. Life Sci. Elsevier Inc.; 2009;84:705–12.

66. Sinicrope FA, Foster NR, Yoon HH, Smyrk TC, Kim GP, Allegra CJ, et al. Association of obesity with DNA mismatch repair status and clinical outcome in patients with stage II or III colon carcinoma participating in NCCTG and NSABP adjuvant chemotherapy trials. J. Clin. Oncol. [Internet]. 2012 [cited 2016 Jan 27];30:406–12. Available from: http://www.pubmedcentral.nih.gov/articlerender.fcgi?artid=3269966&tool=pmcentrez&rendertype=abstract

Tables

Table 1: Body weight, food and water intake of C57BL/6J male mice over a period of 4 months.

		Chow intake [g]				Water intake [ml]				Weight [g]			
Month		1	2	3	4	1	2	3	4	1	2	3	4
Intervention	**CD**	2.64 ±0.07	2.11 ±0.01	2.08 ±0.04	2.06 ±0.03	5.58 ±0.21	5.29 ±0.22	5.39 ±0.28	4.95 ±0.56	24.66 ±0.75	26.17 ±0.16	27.17 ±0.18	28.31 ±0.24
	CD + E	2.70 ±0.08	2.70 ±0.05	2.76 ±0.06	2.76 ±0.51	5.80 ±0.21	5.76 ±0.15	5.97 ±0.17	5.55 ±0.27	24.94 ±0.77	26.58 0.15	27.75 ±0.19	28.63 ±0.14
	HFD	2.56 ±0.04	2.59 ±0.02	2.60 ±0.02	2.56 ±0.06	5.34 ±0.20	4.93 ±0.24	5.10 ±0.14	5.01 ±0.18	32.57 ±2.09	39.00 ±1.37	43.97 ±1.02	47.09 ±0.83
	HFD + E	2.51 ±0.02	2.45 ±0.06	2.50 ±0.05	2.54 ±0.01	5.21 ±0.20	4.69 ±0.06	5.05 ±0.04	5.09 ±0.11	32.77 ±2.3	39.49 ±1.64	44.67 ±1.23	47.67 ±0.49

Table 2: Sequence to analyze and primers for CpG methylation analysis

Gene	**Primer**	**Sequence (5′->3′)**	**Size (bp)**	**GC%**
DNMT1	FW	Biotin - GTA GGT TGT AGA AGA TAG AAT AGT TTT GA	29	31
	RW	CCC ACT CTC TTA CCC TAT ATA ATA CAT	27	37
	Seq	CCC CTC CCA ATT AAT TTC	18	44.4
	Sequence ID: gb|AH009208.2| ***DNMT1:*** at reverse strand of chromosome 9: 20907205–20959888 (52684 bp).			
Sequence to analyze	**7104 – CGCGCGCGCG**AAAAAGC**CG**GGGTCT**CG**T - **7131**		27	7 CpGs
MLH1	FW	AGG GTA TTT TAG TTT TTA TTG GTT GGA GA	29	31
	RW	TTA CAC CTC AAT TCC TAA AAT CTC TAT CCC – Biotin	30	37
	Seq	TTT AGT TTT TAG AAA TGA GTT AAT A	25	16
	Sequence ID: ref|XR_379849.3 **MLH1:** at reverse strand of Chromosome 9: 111228228–111271786 (43559 bp)			
Sequence to analyze	19 – GAAGAG**CG**GAC**CG**TGAACTTTGA**CGCG**C AA-G**CGCG**TTGCCTTCTAGCCTGGTGT**CG**GGC**CG** CTG - 82		64	8 CpGs

Table 3: DNA methylation results presented as relative methylation (mean ± SD) compared to CD or HFD respectively for every CpG. (Stars indicates significance: *p-value ≤ 0.05, **p-value ≤ 0.01)

Mean ±SD in %	CD+E compared to CD	HFD compared to CD	HFD+E compared to HFD
DNMT1 colon			
CpG1	0.92 ± 0.17	1.17 ± 0.24	0.79 ± 0.17
CpG2	0.86 ± 0.28	1.12 ± 0.14	0.94 ± 0.05
CpG3	0.67 ± 0.18 *	1.01 ± 0.19	0.83 ± 0.02 *
CpG4	0.90 ± 0.16	1.17 ± 0.12	0.78 ± 0.12 *
DNMT1 liver			
CpG1	1.00 ± 0.37	0.93 ± 0.25	1.06 ± 0.18
CpG2	0.67 ± 0.15	0.81 ± 0.12	0.91 ± 0.34
CpG3	1.60 ± 0.15 *	1.48 ± 0.73	1.00 ± 0.02
CpG4	0.88 ± 0.08	0.88 ± 0.48	1.29 ± 0.54
MLH1 colon			
CpG1	0.60 ± 0.19 *	1.08 ± 0.46	0.38 ± 0.08 **
CpG2	0.45 ± 0.17 **	0.40 ± 0.03 **	0.59 ± 0.15 **
CpG3	1.31 ± 0.56	1.36 ± 0.44	0.57 ± 0.06 **
CpG4	1.52 ± 0.54	2.13 ± 0.12 **	0.46 ± 0.14 **
CpG5	0.91 ± 0.09	1.24 ± 0.09 **	0.67 ± 0.10 **
CpG6	0.73 ± 0.16	1.53 ± 0.37	0.57 ± 0.07 **
MLH1 liver			
CpG1	0.40 ± 0.05 **	0.43 ± 0.03 **	0.91 ± 0.09 *
CpG2	1.47 ± 0.60	1.27 ± 0.37	0.74 ± 0.11
CpG3	0.84 ± 0.17	0.75 ± 0.13	1.28 ± 0.26 *
CpG4	1.62 ± 0.73	1.73 ± 0.08 **	0.86 ± 0.23
CpG5	1.21 ± 0.24	1.12 ± 0.26	1.06 ± 0.27
CpG6	1.31 ± 0.50	1.60 ± 0.47 *	0.65± 0.03 **

Figures

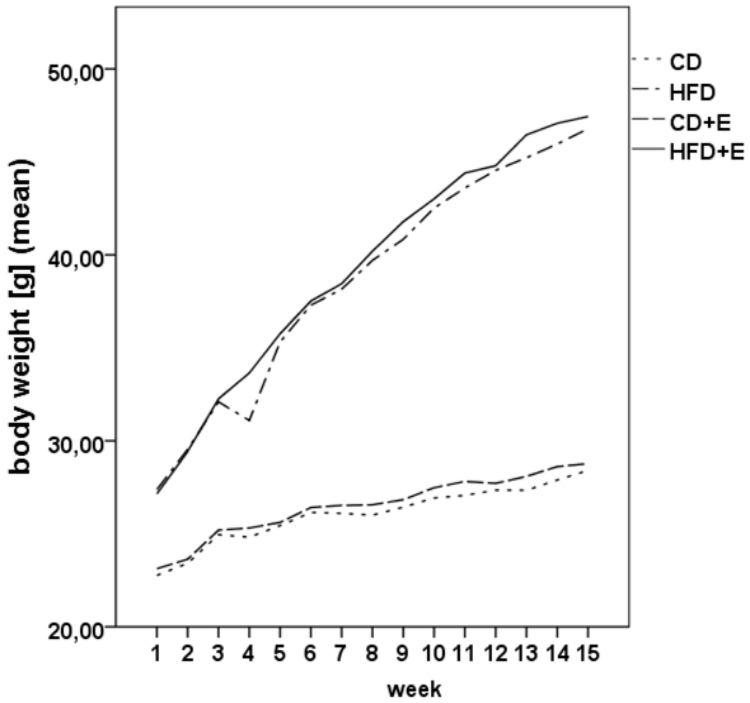

Figure 1: Body weight gain of C57BL/6J male mice over 4 months shown as mean ± confidence interval of 95%. (CD= control diet, HFD= high fat diet, CD+E= control diet plus vitamin E, HFD+E= high fat diet plus vitamin E)

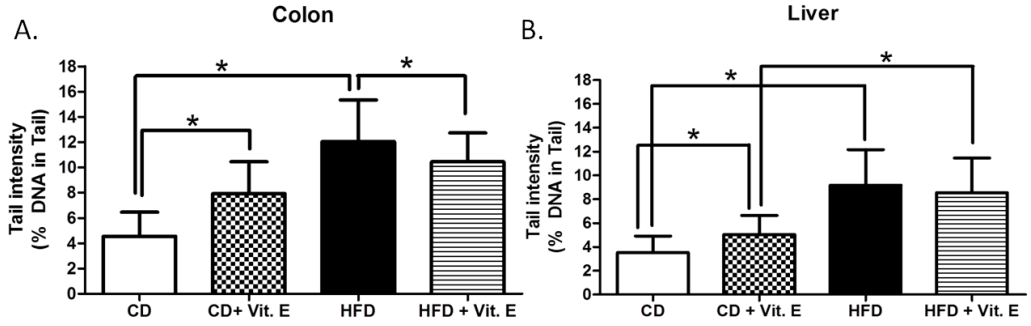

Figure 2: Impact of vitamin E supplementation on DNA damage in colon (A) and liver (B) of C57BL/6J male mice. Bars indicate means ± SD of results obtained with 15 animals per group. From each sample, three slides were made and 50 cells were evaluated per slide. (CD= control diet, HFD= high fat diet, CD+E= control diet plus vitamin E, HFD+E= high fat diet plus vitamin E; *p-value ≤ 0.05, **p-value ≤ 0.01, ***p-value ≤ 0.001).

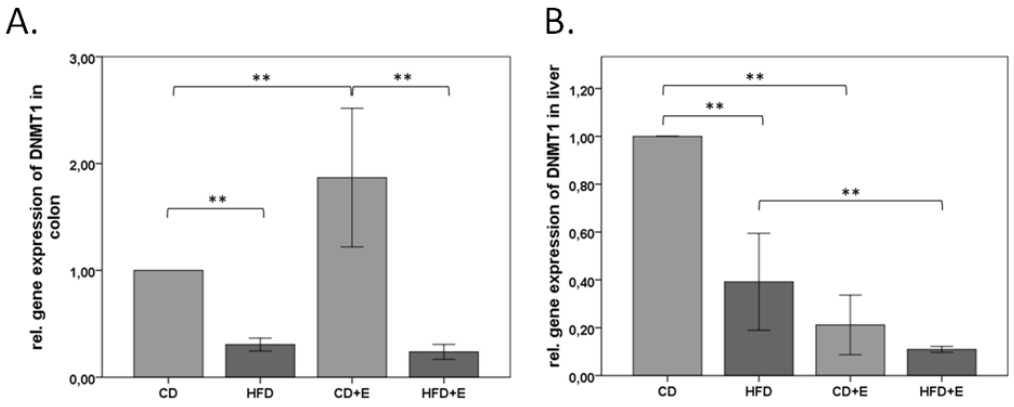

Figure 3: Relative gene expression of Dnmt1 in colon (A) and liver (B) of C57BL/6J male mice. Gene expression data were calculated relative to CD-data and normalized to the house keeping gene GAPDH. The error bar represents a 95 % confidence interval. (CD= control diet, HFD= high fat diet, CD+E= control diet plus vitamin E, HFD+E= high fat diet plus vitamin E, *p-value ≤ 0.05, **p-value ≤ 0.01, ***p-value ≤ 0.001)

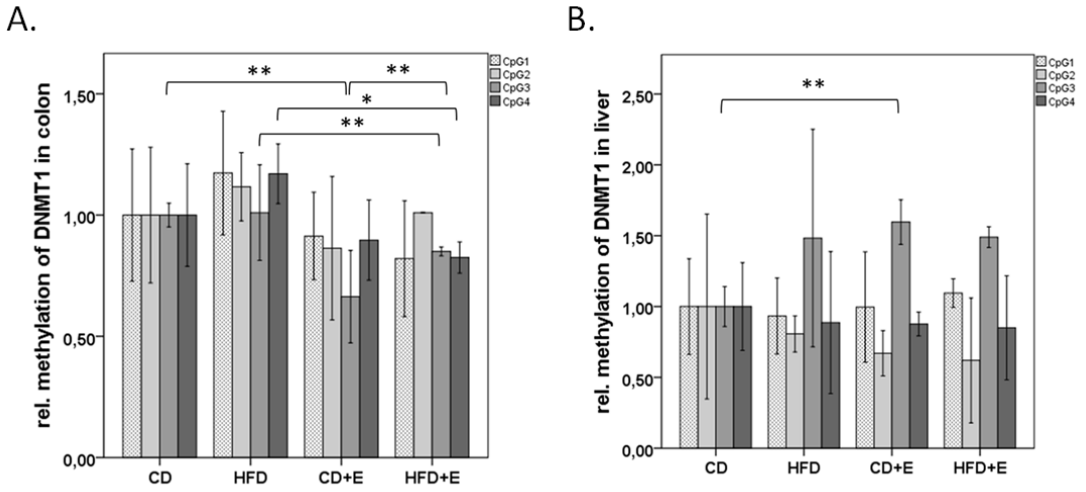

Figure 4: Relative CpG methylation status in promoter region of Dnmt1 in colon (A) and liver (B) of C57BL/6J male mice. All methylation data are relative to CD. The eror bar represents a 95% confidence interval. (CD= control diet, HFD= high fat diet, CD+E= control diet plus vitamin E, HFD+E= high fat diet plus vitamin E, *p-value ≤ 0.05, **p-value ≤ 0.01, ***p-value ≤ 0.001)

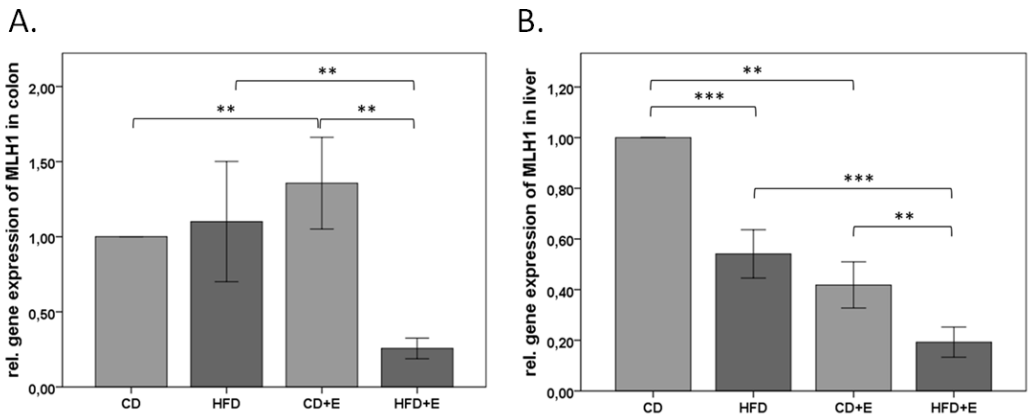

Figure 5: Relative gene expression of MLH1 in colon (A) and liver (B) of C57BL/6J male mice. Gene expression data were calculated relative to CD-data and normalized to the house keeping gene GAPDH. The error bar represents a 95 % confidence interval. (CD= control diet, HFD= high fat diet, CD+E= control diet plus vitamin E, HFD+E= high fat diet plus vitamin E, *p-value ≤ 0.05, **p-value ≤ 0.01, ***p-value ≤ 0.001)

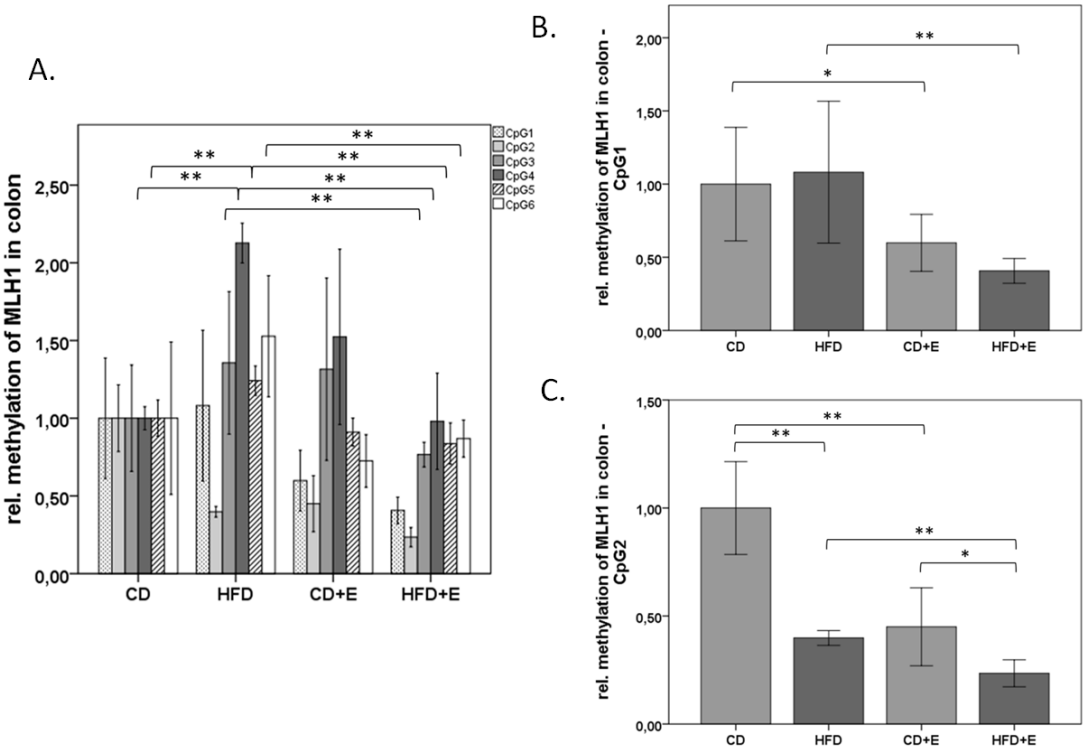

Figure 6: Relative CpG methylation status in promoter region of MLH1 in colon of C57BL/6J male mice. Mean methylation status for MLH1 in colon is shown as an overview in Figure 6A. In Figure 6B the methylation status of CpG1 and in Figure 6C the methylation status of CpG3 is specified. All methylation data are shown relative to CD. The error bar represents a 95 % confidence interval. (CD= control diet, HFD= high fat diet, CD+E= control diet plus vitamin E, HFD+E= high fat diet plus vitamin E, *p-value ≤ 0.05, **p-value ≤ 0.01, ***p-value ≤ 0.001)

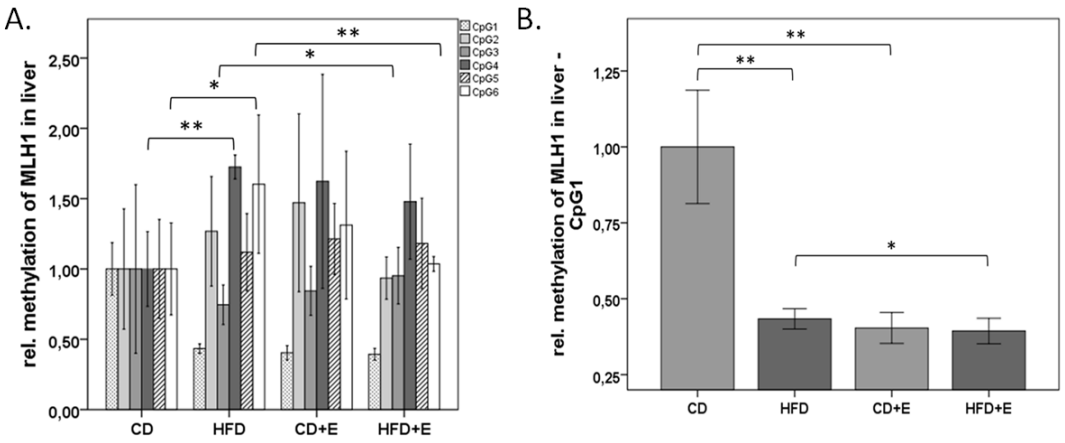

Figure 7: Relative CpG methylation status in promotor region of MLH1 in liver. Mean methylation data are shown for MLH1 in the liver as an overview in Figure 7A and especially for CpG1 in Figure 7B. All methylation data are shown relative to CD. The error bar represents a 95 % confidence interval. (CD= control diet, HFD= high fat diet, CD+E= control diet plus vitamin E, HFD+E= high fat diet plus vitamin E, *p-value ≤ 0.05, **p-value ≤ 0.01, ***p-value ≤ 0.001)